Extending the Realm of SuNS to DNA Nanoarrays and Peptide Features

by

Ozge Akbulut Halatci

B.S. Materials Science & Engineering
Sabanci University, Turkey 2004

SUBMITTED TO THE DEPARTMENT OF MATERIALS SCIENCE AND ENGINEERING IN PARTIAL FULFILLMENT OF THE REQUIREMENT FOR THE DEGREE OF

DOCTOR OF PHILOSOPHY IN MATERIALS SCIENCE AND ENGINEERING

at the

MASSACHUSETTS INSTITUTE OF TECHNOLOGY

February 2010

Signature of Author: _____
Department of Materials Science and Engineering
October 6, 2009

Certified by: _____
Francesco Stellacci
Associate Professor of Materials Science and Engineering
Thesis Supervisor

Accepted by: _____
Christine Ortiz
Associate Professor of Materials Science and Engineering
Chair, Department Committee for Graduate Students

Acknowledgements

I am blessed with such family and friends without whom my life wouldn't have the flavor I enjoy every day.

I would like to start with the past/present members of the Stellacci Group who have been much more than colleagues and made office/lab life a lot fun. More recently, they have proven themselves to be excellent babysitters as well. I have been lucky to work on such a project that everyone involved became close friends; (in the order of appearance) Amy, Sarah, Jin-Mi and Anna, it was great working and spending time with you. And, Amy thanks for passing on what you know; you are a true Master. Kislon, Jeff, Ben,Ying and Randy, I cannot imagine an office without you. Ayse, a former Mayes Group member, thanks for being such a comforting friend, you were there whenever I asked for help.

Prof. Robert E. Cohen, Prof. Micheal F. Rubner and Prof. Darrell J. Irvine, my thesis committee, thank you very much for your support and constructive comments. Special thanks to Ms. Angelita Mireles, who is more than an administrative administrator to me. Prof. Anne M. Mayes, I wish that you were still at MIT and our work had continued throughout my Ph.D, I have always believed I have lot to learn from you. I still remember our first talk and the smile on your face that I hope won't wither away even at harder times. It is my observation that graduate life can be heaven or hell depending on your advisor. I would like thank Prof. Francesco Stellacci for letting me in his heaven; he is and will be a role model for the rest of my life not only due to his scientific achievements but also due to his warm heart.

The Sabanci Community, I think if I took our national university entering exam a million times, I will still choose Sabanci in every single one. It was a place not only shaped my career but also my inner being. Special thanks to Prof. Cleva Ow-Yang, Prof. Yusuf Menceloglu, Prof. Canan Atilgan, Prof. Mehmet Ali Gulgun, Prof. Ali Rana Atilgan and Prof. Alpay Taralp who have done a lot more than teaching/advising.

Oznur and Burak, you are wonderfully unique individuals and I cannot find the words to express my love, respect and gratitude for you, stay together, stay with me. Isil, Evren, Ilker, Elif, Ceren and Erman, your friendship means a lot to me.

Ibrahim, I treasure every moment I am with you. I truly believe you are a gift from God along with Derin.

This thesis is dedicated to Nebile, Ertugrul, Ekin, Ozde, Deniz, Sumer, Sevim, Kutay, Nezaket, Ahmet, Ilknur, Huseyin, Ibrahim, Derin and the rest of Simseks and Seymens who have enveloped me with such a big love. Here or there, I know you are always with me.

Extending the Realm of SuNS to DNA Nanoarrays and Peptide Features

Abstract

Intense research on DNA arrays has been fostered by their applications in the field of biomedicine. DNA microarrays are composed of several different DNA sequences to be analyzed in parallel allowing high throughput information. Current methods to fabricate these arrays are serial in nature resulting in high prices that prevent their extensive utilization. Supramolecular Nanostamping is devised to solve this problem by harnessing the reversible bond formation between complementary DNA strands. This contact based technique is proven to replicate DNA arrays in a three step cycle: 1) Hybridization, 2) Contact and 3) Dehybridization. The overall goal of this thesis is to demonstrate the application of SuNS to DNA nanoarrays, i.e. increase the resolution of the current method, and broaden the printing capability to peptide arrays.

The amount of analyte needed in an array scales with the feature size and spacing i.e. the total array size. The features of a DNA microarray are usually tens of micrometers in size with a spacing on the order of hundred micrometers. Therefore, miniaturization of such arrays is necessary for applications when analyte scarcity is an issue. DNA nanoarrays are promising lower analyte volumes due to their decreased feature size and spacing; namely high resolution. Unfortunately, DNA nanoarrays can only be fabricated by scanning probe microscopy based serial methods which generate each spot individually. To demonstrate SuNS is capable of dealing with the increasing demand to miniaturize DNA arrays, DNA features composed of a few DNA strands is replicated. The faithful printing of feature sizes as small as 14 nm with 70 nm spacing was shown.

Apart from the capability to cope with features of various sizes, the strength of a printing method emerges from its ability to deal with different types of biomolecules. Coiled-coil peptides are treated analogously to complementary DNA strands due to the molecular recognition between two complementary peptide strands. Through Liquid Supramolecular Nanostamping (LiSuNS), the replication of coiled-coil motif peptides was demonstrated. To prove the multiplexing capability of the process, a master made of peptide and DNA features was successfully stamped via LiSuNS as well.

Thesis Supervisor: Francesco Stellacci

Title: Paul M. Cook Career Development Associate Professor of Materials Science and Engineering

Table of Contents

List of Figures

List of Schemes

Chapter 1 Fabrication of Biomolecular Platforms via Contact-Based Methods

This chapter was written in part with 'Fabrication of Biomolecular Devices via Supramolecular Contact-Based Approaches' by Ozge Akbulut, Arum Amy Yu and Francesco Stellacci, accepted for publication in Chemical Society Reviews.

1.1 Introduction

The wider access to micro and nanotechnology fabricated devices will critically depend on their price, which is usually determined in a sizeable fraction by the cost of the fabrication process. Hence, lowering the cost has been a priority for researchers in fields as disparate as information- and bio-technology. For most integrated devices, a master is fabricated through lithography and then replicas of this master are generated through stamping. Contact-based methods are widely used to physically shape or introduce chemical identities to the target substrates in a cost efficient way. *[1]* These methods in general involve a mold or a stamp which carries the 'information' to be transferred in terms of shape or chemistry. For instance, in imprinting based lithography such as Nanoimprint Lithography, a hard mold is pressed onto the appropriate secondary substrate and introduces certain topography, whereas in microcontact printing usually an elastomeric stamp is used to transfer molecules (chemical information) upon contact. *[1]*

Biomolecular platforms such as DNA microarrays have been proven to be indispensable for diagnostics, medical research, toxicology and pharmacology. *[2-4]* Newer type of assays, protein and antibody microarrays, are also expected to be crucial for determining gene function/regulation and wide-screening of protein function.*[5, 6]* However, the possibility of utilizing these platforms more extensively depends on the development of cost efficient

fabrication methods. Nowadays, commercial methods to produce DNA microarrays include spotting (by contact, such as pin based fluid transfer, and by non-contact printing, such as piezo based ink-jet printing) and *in-situ* synthesis. These methods are all serial in nature; hence expensive. *[4, 7]* Protein and antibody microarrays are in their infancy compared to their DNA counterparts. Although, some of the techniques for DNA microarrays are applicable to proteins, such as spotting*[8]* electrospray deposition *[9]* and ink-jet printing *[10]*, there are additional challenges for protein microarrays regarding to protein activity and functionality after fabrication of such arrays.*[5]*

Contact-based methods are suggested to overcome the cost based issues since they potentially allow parallel fabrication. In this review, contact based methods suitable for the fabrication of biomolecular devices or arrays are discussed. All of these methods utilize a stamp (a transfer medium) that is copied onto a target substrate using forces which are suitable to biomolecules. Thus, other types of contact-based techniques which physically shape the target substrate hence need higher forces such as nanoimprint lithography *[11-13]* or step-and-flash imprint lithography *[14, 15]* is not included in this review. The focus is on ink-based stamping techniques; here 'ink' is defined as the molecules to be transferred to the target substrate. The types of stamps and inks, target molecule immobilization methods such as available chemistries as well as the resolution and coverage aspects of each technique are discussed.

1.2 Microcontact Printing

Microcontact printing (μCP) developed by Whitesides' group is the most popular soft-material contact-based printing technique. *[16-18]* In general, an elastomer stamp, typically made of poly (dimethylsiloxane) (PDMS) is used to obtain conformal contact between the stamp and target substrate, and the transfer of ink molecules occurs at the area in contact. This simple and versatile printing technique is good for printing soft molecules since it doesn't require either expensive equipments or harsh chemical treatments.

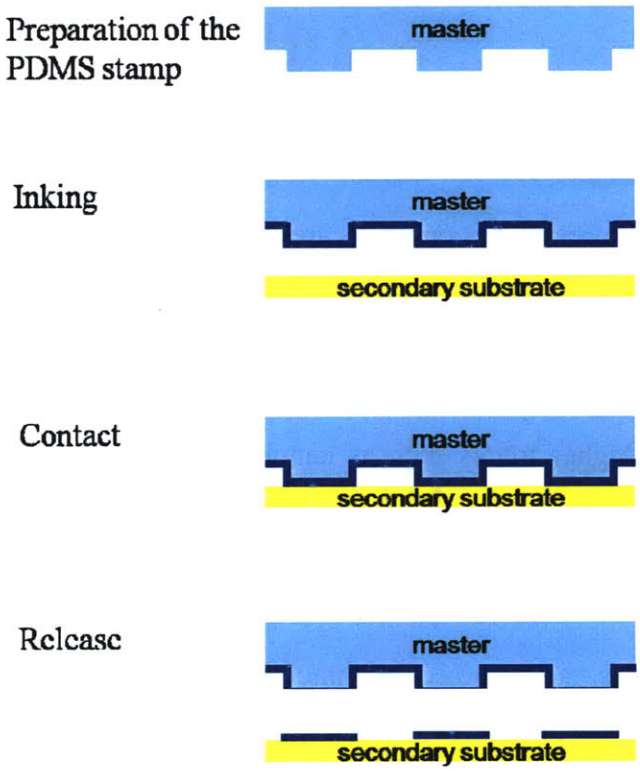

Figure 1.1: Schematic illustration of the microcontact printing process: preparation of the template, inking of the template, contact with the secondary substrate and releasing the template; the ink is patterned on the secondary substrate.

The printing cycle of μCP is composed of three steps: Inking – Contact – Release. For Inking, a solution of ink molecules is dropped onto a stamp (i.e. a substrate with a three dimensionally patterned surface) followed by drying and ink molecules are physisorbed on the surface of the stamp. Subsequently, the stamp is placed onto another substrate (Contact), so that portions of its surface are in contact with it. The ink molecules in contact with this substrate diffuse onto it. Finally, the stamp is removed from the secondary substrate leaving the desired pattern on it (Release). *[19]*

The elastomeric stamp used in μCP is prepared by casting a polymer (or a pre-polymer) onto a mold. The mold contains 3-D patterns fabricated on relatively hard substrates such as SiO_2, Si_3N_4 or metal, using optical lithography or e-beam lithography; upon curing or hardening the polymer/prepolymer takes the shape of the mold. *[17]* Novalac Resins® (a phenol formaldehyde polymer), *[16]* polyolefin plastomers, *[20]* thermoplastic block copolymers, *[21, 22]* UV-curable urethane-related prepolymers, *[23]* agarose, *[24-26]* hydrophilic composite elastomers, *[27]* high molecular weight acrylate monomers crosslinked by poly(ethylene glycol) diacrylate *[28]* and poly(methylmethacrylate) *[29]* were also suggested as stamp materials. However, among all PDMS is still the mostly used since it offers good conformal contact, large printing area coverage over 100 cm^2, easy release from the template, optical transparency, relative stability against aging, and biocompatibility. *[30]*

Through μCP a number of patterned chemistries can be fabricated on various substrates. The most commonly studied systems are alkanethiol monolayers on gold *[17, 31, 32]*; yet printing silanes onto silicon oxide expanded the possible application areas to semiconductors, organic sensors and bioassays as well. *[18, 33-37]* Other printable materials include palladium

colloids, *[38]* catalysts, *[39]* metallic nanoparticles, *[40]* metal loaded polymers, *[41-43]* and vanadium oxide. *[44]*

The hydrophobic character of unmodified PDMS prevents homogeneous inking of hydrophilic biomolecules such as DNA and proteins. Several modifications were utilized to print hydrophilic biomolecules with PDMS: oxygen plasma treatment, *[45-47]* chemical treatment (most frequently silanes), *[48-52]* adsorption of polar molecules such as positively charged dendrimers *[53]* and adhesion agents for target molecules such as poly(ethylenimine) for bacteria. *[54]* Through these modifications or the above mentioned stamp materials biomolecules including DNA, *[50, 53]* DNA surfactants, *[51]* RNA, *[53]* proteins, *[29, 47, 52, 55-61]*, mucopolysaccharides, *[62]* cells, *[26]* and bacteria *[54]* have been successfully printed via μCP. In addition, μCP generated protein patterns were suggested to serve as an initial platform for further immobilization of other biomolecules; for instance fibronectin for bovine capillary endothelial cells *[55]* and laminin for neuronal cells. *[63]*

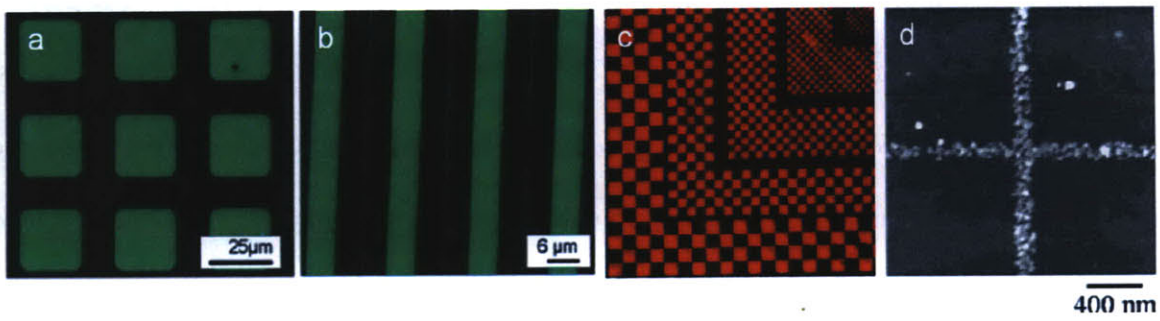

Figure 1.2: Fluorescence micrographs of printed biomolecules, DNA in a) and b); *[50]* protein in c) *[57]* and d) *[60]*

The printing resolution of μCP depends mainly on two factors: i) the mechanical property of the stamp and ii) the diffusion of ink molecules after printing. *[17, 19, 64]* Since PDMS is the mostly used stamp material, further research has been carried out in comparison to PDMS. Although the flexibility of PDMS (Young's modulus ~3 MPa) is essential for conformal contact (large printing area), it also leads to the deformation of the original high definition features on the template under pressure applied for conformal contact. *[65, 66]* Since the whole surface of PDMS template is covered with the ink-molecules and the ink transfer occurs on physical contact area, the deformed features are printed as well. *[19, 66]* As a result, the possible patterns to be printed and the geometry of the stamp are restricted due to the deformation of PDMS. Swelling of PDMS during inking is yet another challenge, Pompe *et al.* suggested an alternative way to ink the stamps by using a stamp pad. *[34]* The PDMS master is brought into contact with a structureless silicon rubber block which was previously inked with the desired molecules. Therefore, the swelling of PDMS stamp is minimized and the excess deposition of ink molecules due to capillary condensation in the wedges of the stamp was avoided.

The resolution of μCP can also change after printing due to the degree of molecular diffusion which is mainly determined by the molecular weight of ink molecules. *[19, 64]* It has been shown that the alkanethiol patterns which are smaller than 500 nm are problematic *[19]* Due to the higher molecular weights of the biomolecules; there is no significant diffusion. μCP gives clear printing results with high resolution as far as the biomolecules are inked homogeneously on the template, which is also a challenging task. Delamarche and coworkers reported 40 nm protein lines using a stiffer PDMS stamp. *[60]*

Efforts for simultaneous increase in the resolution and pattern fidelity posed a significant dilemma to the researchers. *[65, 67]* Although employing stiffer molds seemed to be a sound alternative to elastomeric softer molds, conformal contact remained as an issue to be solved in those cases. Schmid and Michel suggested the use of hybrid stamps (a patterned thin film assisted by a flexible pad) achieving 100 nm resolution over large areas. *[30]* Building upon this knowledge, Odom *et al.* employed a composite stamp composed of thick and soft PDMS to hold hard PDMS and obtained features with 50 nm linewidths. *[68]* Stiffer molds, such as block copolymer thermoplastic elastomers were also shown to print micron sized high aspect ratio relief structures which are harder to print with PDMS due to the collapse of the mold. *[21]* PMMA stamps coupled with a nanoimprint apparatus to apply pressure were also demonstrated to work well with high aspect ratio relief structures. *[29]*

In general, the literature on μCP involves printing of one kind of molecule. However, for μCP to be applicable to multicomponent bio-devices, the process should be redesigned to involve more than one kind of molecule. Bernard *et al.* suggested i) sequential inking and ii) parallel inking to generate multiple protein substrates. Sequential inking involves using stamps inked with different molecules to print onto the same surface. In the same report, the authors also inked a flat PDMS stamp with a microfluidic network and demonstrated the spontaneous printing of 16 proteins.*[57]* However, printing multiple molecules still stands as a challenge for μCP since the re-inking is necessary after a couple of cycles. More recently, Duan *et al.* showed the sequential immobilization of two different silanes through local oxidation on a flat PDMS stamp and printing of polar inks; the authors speculated that once different chemistries are available in the stamp, further modification will be possible to immobilize different molecules. *[69]* Another method includes using a stamp with different levels of topography and sequential inking of those

levels; through adjusting the pressure on the stamp Chalmeau *et al.* was able control the touch of different topographical levels with the target secondary substrate and demonstrated immobilization of two proteins in one step. *[70]*

1.3 Affinity Contact Printing

Affinity Contact Printing (αCP) stems from μCP but it involves additional supramolecular interactions during the inking. The term is coined by Bernard *et al.* reporting the capture of target molecules through their corresponding ligands decorated onto a stamp and consequent μCP. *[71]* In this review, we would like to extend this definition and also categorize other printing methods which involve supramolecular interactions under αCP although their 'affinities' are during 'Contact' or after 'Release'. To give a general idea, supramolecular interaction utilized printing methods are depicted in Figure 1.3.

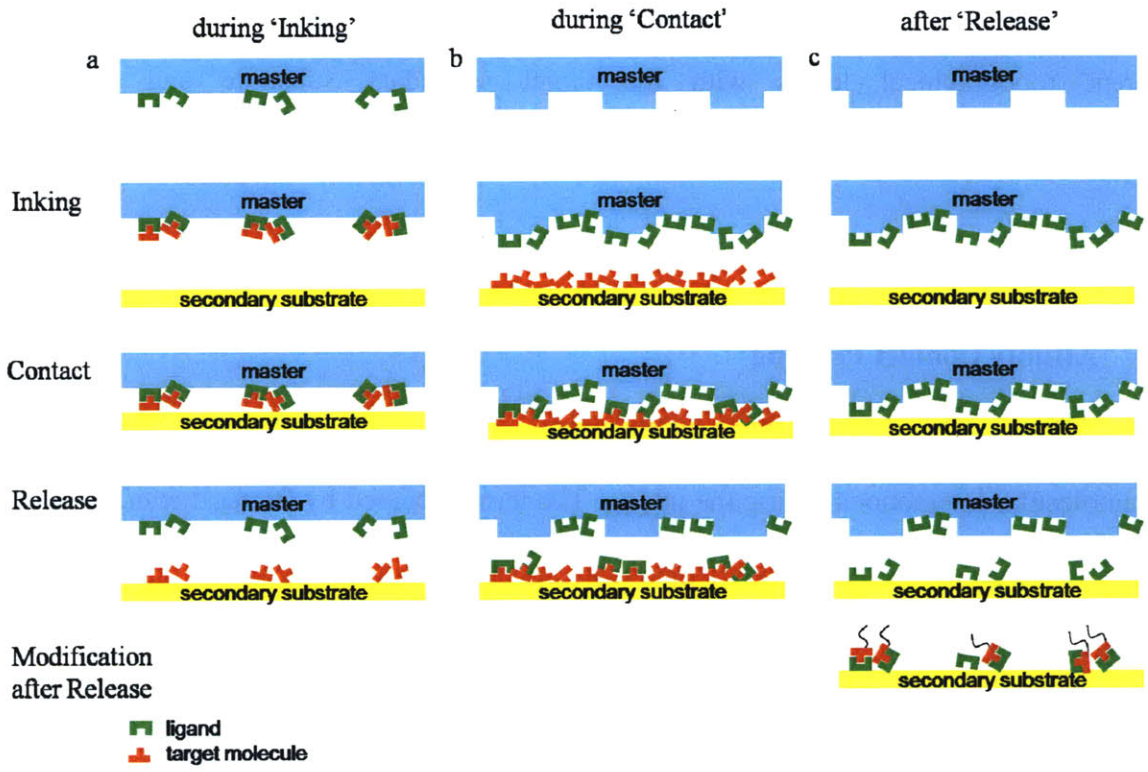

Figure 1.3: Schematic illustration of supramolecular interactions that take place a) during inking, b) during contact, and c) after release. The common steps of contact-based methods are indicated on the left.

1.3.1 Supramolecular Interactions during Inking

Supramolecular interactions during inking refer to the capture of molecules (ink) from inking solution through their complementary molecules which are already immobilized on the stamp. Here, as opposed to stamps defined by physical shape in μCP; the stamps inked through supramolecular forces transfer complementary molecules onto the secondary substrate. The key point of this approach is patterning the corresponding ligand molecules first as precursors, followed by the assembly of final molecules. Since ligand molecules are more robust and simpler

than the target biomolecules, the printing process will be more reliable and the biomolecules will be less damaged. It can also be expected that the biomolecules connected to the printed ligand will have more conformational freedom inducing higher activity compared to directly deposited biomolecules on surface since the ligand can act as a linker molecule. In addition, since the printed molecules also have the same recognition power, the printed substrate is open to further supramolecular modifications and can be used as a template as well.

In order to enable this approach, two main conditions should be satisfied as following: i) the interaction between the complementary units should be reversible by changing the given conditions such as temperature, electric field and pH, and ii) the bonding between the substrate and bound molecules should be stronger than the supramolecular interaction between two complementary molecules during release.

For the first time, the basics of affinity contact printing were demonstrated for the capture of proteins from solution and consequent μCP. Using mouse IgG, anti-mouse IgG was inked on a PDMS stamp and anti-mouse IgG was stamped onto a glass slide. The authors demonstrated the reuse of the stamp and high yields. *[71]* Renault *et al.* utilized micro-wells and micro-fluidic network to decorate an amino-derivatized PDMS stamp with different proteins and fabricated high resolution protein arrays (10^4 in 1 mm^2) in parallel. *[72]* In those works, the dissociation of captured antibodies was achieved by mechanical force. During the release step, the force stabilizing printed molecules on the secondary substrate is Van der Waals adhesion force; since the printed molecules are big and the contact area is large enough, the force required for detaching them is larger than the supramolecular interaction between the antigen and antibody. Recently, Abbott group suggested the possibility of orienting proteins during the printing step

and employing liquid crystals as means to investigate the orientation of the printed proteins. *[73, 74]*

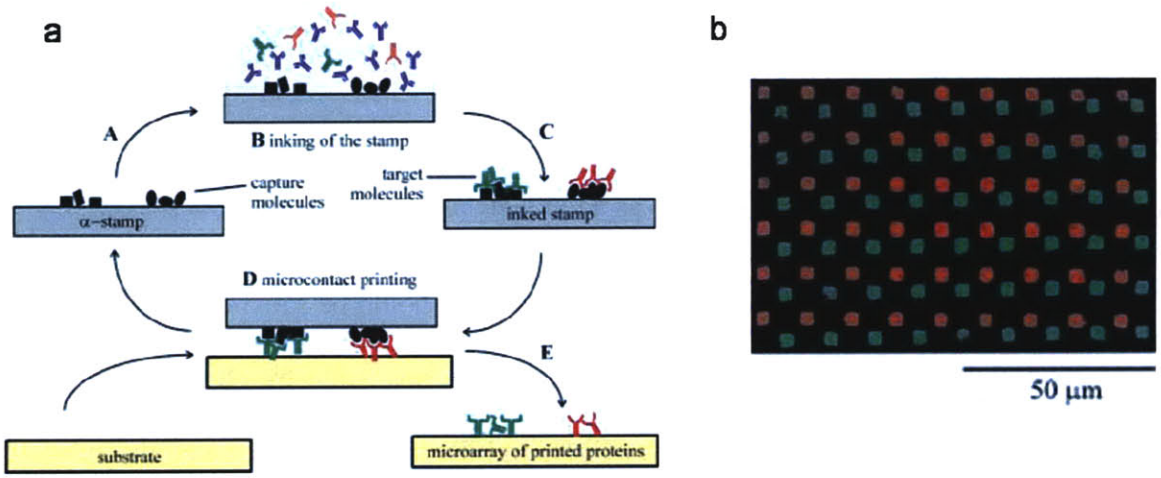

Figure 1.4: a) Schematic illustration of the αCP procedure for printing two different proteins b) the fluorescence micrograph of the printed pattern. The antigens immobilized on a template selectively capture the corresponding antibodies in solution (supramolecular inking) and the antibodies were transferred to another substrate. *[72]*

Using DNA as ink in affinity contact printing offers several advantages due to stability of DNA compared to proteins. Short DNA molecules (oligonucleotides shorter than 100-mer and commonly used for lithography) are smaller, simpler and better understood than proteins. This gives better printing resolution and less non-specific binding due to smaller Van der Waals forces; thus the overall printing process is more reliable. Also, many chemical modifications can be introduced to DNA molecules hence various chemistries and substrate systems can be utilized. The printed platforms can be used as a template for other purposes, for instance protein arrays can be fabricated by *in-situ* transcription on/by the printed DNA microarrays.*[75, 76]*

Recently, Crook's *[77]* and our *[78]* group independently developed a truly parallel soft-material stamping technique to replicate DNA features from one surface onto another. Supramolecular Nanostamping (SuNS), as referred by our group, is a printing technique based on the supramolecular interaction between complementary DNA (cDNA) strands for selective inking. Once a template containing single stranded DNA (ssDNA) features is fabricated, the printing procedure of SuNS is composed of three steps: (1) Hybridization with cDNA modified with a chemical binding group toward a secondary substrate , (2) Contact with the secondary substrate, and (3) Release after dehybridization assisted by increased temperature or mechanical forces. A comprehensive summary on SuNS explaining the technique, master fabrication, substrates utilized and its resolution can be found in Chapter 2. There is also a section describing Crook's work.

Yang and coworkers printed unmodified cDNA using a similar procedure.*[79]* The ssDNA molecules are immobilized on aminated PDMS stamp through electrostatic interaction between the negatively charged backbone of DNA and NH^{3+} groups on aminated PDMS. This stamp is hybridized with cDNA molecules and thereafter printed onto an amine-terminated glass slide. In this work, electrostatic interaction was employed to break the hydrogen bonds between complementary DNA molecules. The negatively charged backbone of the cDNA strands is attached to the amine groups exist as NH^{3+} (after protonation in neutral condition) on the glass slide and cDNA strands got transferred. At this time, the electrostatic attraction between cDNA and positively charged SAM on glass is stronger than the hydrogen bond between complementary DNA strands. More recently, poly(ethyleneimine) functionalized poly(methyl methacrylate) was used to transfer cDNA to aminated glass surface and features as small as 250 nm were successfully printed. *[80]*

Recently, Taussig *et al.* suggested a method for *in-situ* protein synthesis, harnessing the supramolecular interaction between DNA and proteins.*[81]* The authors demonstrated the printing of protein arrays from DNA microarray templates using cell-free protein synthesis. In this technique, a DNA template microarray, a filter-membrane containing required materials for cell-free protein expression and a protein capture slide, which form a sandwich (DNA array – membrane – protein capture slide) are incubated under protein expression conditions. Thereafter, the synthesized proteins are transferred through the membrane from the template array to the target slide via diffusion. This method allows a single DNA microarray to produce at least 20 protein arrays without individual protein expression, purification and spotting.

1.3.2 Supramolecular Interactions during Contact

In order to harness the supramolecular interactions during contact, the secondary substrate is modified to attract the ink molecules. These interactions usually in the forms of electrostatic or Van der Waals are proposed to increase the stability, *[82-85]* function, *[86]* and control the printing area. *[87]* Immobilizing corresponding ligands on the secondary substrate is a common approach in printing biomolecules such as printing avidin onto a polymeric substrate containing biotin moiety *[86]* or vice versa *[77, 88-90]* and horseradish peroxide onto bovine serum albumin precursor layer on quartz. *[87]*

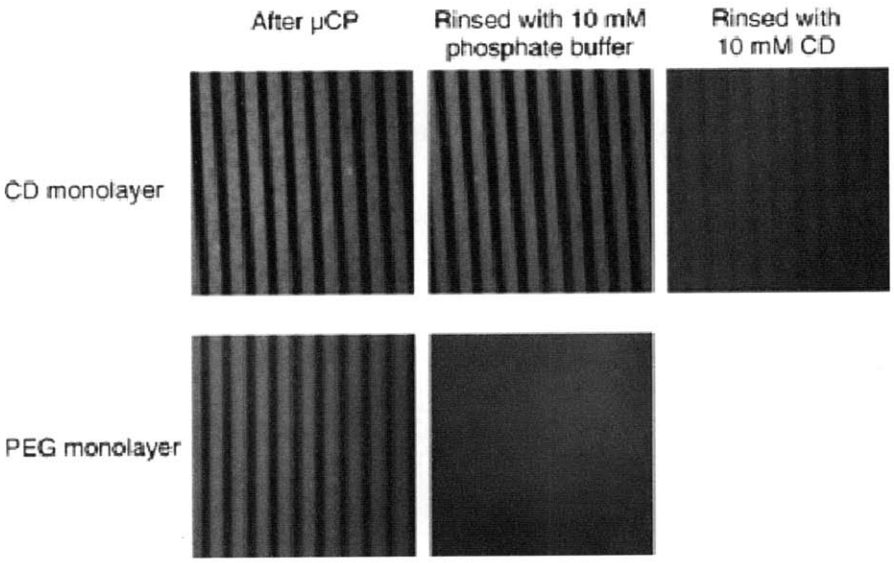

Figure 1.5: Fluorescence micrographs of printed "guests" (150 × 150 μm^2), showing the stability difference between printing on "printboard" containing "host" molecules (β-cyclodextrin) by supramolecular lithography (top) and printing on poly(ethylene glycol) monolayer (bottom). *[85]*

Reinhoudt group utilizes supromolecular affinity by using an artificial host-guest system. *[82-85]* The method is referred as supramolecular microcontact printing and employs 'printboards' which are substrates containing self-assembled monolayer (SAM) of molecules that have specific recognition sites for the target ink molecules. These printboards are composed of an invented host molecule, β-cyclodextrin (β-CD), which exhibits affinity to small hydrophobic molecules and is modified with heptathioether chains to form SAMs on gold surfaces. In general, SAMs of β-CD are prepared on gold-on-silica substrates, and ink molecules containing hybrophobic guest moiety such as adamantly group or p-tert-butylphenyl group are printed on the boards through μCP or other lithographic techniques. These printed patterns remained stable for longer time or even after rinsing with buffer solutions compared to patterns on non-'printboard' substrates such as –OH terminated SAM or poly(ethylene glycol) coated substrates.

[85] This result implies higher stability of printed patterns due to the strong interaction between the designed host-guest molecules. Moreover, through attaching small linkers by microcontact printing, streptavidin and biotinylated protein were sequentially immobilized on β-CD and this structure was shown to specifically adsorb Fc fragment of human immunoglobin G (IgG-Fc). *[91]* In the same work, instead of IgG-Fc whole antibodies were used as well and utilized for counting lympocytes. *[91]* Recently, they have also demonstrated the reversible adsorption of nanoparticles through electrochemically active dendrimers and suggested the same principle may be applicable to biomolecules. *[92]*

1.3.3 Supramolecular Interactions after Release

The most common use of supramolecular interaction is employing supramolecular modification on the printed pattern after release. This approach involves patterning the corresponding ligand molecules first as precursors through μCP and consecutively assembling final molecules on the same substrate. In general, the ligand molecules are more robust and simpler than the target biomolecules; therefore the printing process is potentially more reliable and the biomolecules are less damaged. It can also be expected that the biomolecules connected to the printed ligand will have more conformational freedom resulting in higher activity compared to directly deposited biomolecules on surface due the ligand molecule acting as a linker.

The most broadly studied example is making avidin/streptavidin pattern by exploiting the specific interaction between biotin – avidin/streptavidin. *[52, 93-96]* One strategy is to first print SAMs containing reactive functional groups and decorate these features with biotin. *[52]*

Chilkoti group introduced microstamping on an activated polymer surfaces (MAPS) which involves introducing carboxylic acid groups on polymeric surfaces (poly(ethylene), poly(styrene), poly(methyl methacrylate), and poly(ethylene terephthalate)) and react those with aminated biotin. *[93, 95]* Other groups have also employed similar strategies to have reactive groups on the surface such as surface hydrolysis of poly(glycolic acid) to have carboxylic acid. *[97]* Another method is to use chemical vapor deposition polymerization of functionalized polymers to react with biotin.*[96]*

1.4 Conclusion

Contact-based methods are expected to be more widespread due to the potential solution of the cost issues. In this review, we aimed to give background information on contact based techniques applicable to biomaterials. Supramolecular interactions are likely to improve current printing techniques; thus we believe the direction of the research will be more towards harnessing and investing on biomolecular systems which can form reversible interactions among them as well as synthesis of these biomolecules on the spot before printing.

1.5 References

[1] B. D. Gates, Q. Xu, M. Stewart, D. Ryan, C. G. Willson, G. M. Whitesides, *Chemical Reviews* **2005**, *105*, 1171.
[2] B. Lemieux, A. Aharoni, M. Schena, *Molecular Breeding* **1998**, *4*, 277.
[3] A. Brazma, A. Robinson, G. Cameron, M. Ashburner, *Nature* **2000**, *403*.
[4] M. J. Heller, *Annual Reviews of Biomedical Engineering* **2002**, *4*, 129.
[5] H. Zhu, M. Snyder, *Current Opinion in Chemical Biology* **2003**, *7*, 55.
[6] J. Glokler, P. Angenendt, *Journal of Chromatography B* **2003**, *797*, 229.
[7] M. Dufva, *Biomolecular Engineering* **2005**, *22*, 173.
[8] G. MacBeath, S. L. Schreiber, *Science* **2000**, *289*, 1760.

[9] V. N. Morozov, T. Y. Morozova, *Analytical Chemistry* **1999**, *71*, 3110.
[10] L. Pardo, W. C. Wilson, T. Boland, *Langmuir* **2003**, *19*, 1462.
[11] S. Y. Chou, P. R. Krauss, P. J. Renstrom, *Science* **1996**, *272*, 85.
[12] S. Y. Chou, C. Keimel, J. Gu, *Nature* **2002**, *417*, 835.
[13] L. J. Guo, *Journal of Physics D-Applied Physics* **2004**, *37*, R123.
[14] T. Bailey, B. J. Choi, M. Colburn, M. Meissl, S. Shaya, J. G. Ekerdt, S. V. Sreenivasan, C. G. Willson, *Journal of Vacuum Science & Technology B* **2000**, *18*, 3572.
[15] D. J. Resnick, W. J. Dauksher, D. Mancini, K. J. Nordquist, T. C. Bailey, S. Johnson, N. Stacey, J. G. Ekerdt, C. G. Willson, S. V. Sreenivasan, N. Schumaker, *Journal of Vacuum Science & Technology B* **2003**, *21*, 2624.
[16] A. Kumar, G. M. Whitesides, *Applied Physics Letters* **1993**, *63*, 2002.
[17] Y. Xia, G. M. Whitesides, *Annual Reviews of Materials Science* **1998**, *28*, 153.
[18] A. P. Quist, E. Pavlovic, S. Oscarsson, *Analytical and Bioanalytical Chemistry* **2005**, *381*, 591.
[19] E. Delamarche, H. Schmid, A. Bietsch, N. B. Larsen, H. Rothuizen, B. Michel, H. Biebuyck, *The Journal of Physical Chemistry B* **1998**, *102*, 3324.
[20] G. Csucs, T. Knzler, K. Feldman, F. Robin, N. D. Spencer, *Langmuir* **2003**, *19*, 6104.
[21] D. Trimbach, K. Feldman, N. D. Spencer, D. J. Broer, C. W. M. Bastiaansen, *Langmuir* **2003**, *19*, 10957.
[22] D. C. Trimbach, M. Al-Hussein, W. H. d. Jeu, M. Decr, D. J. Broer, C. W. M. Bastiaansen, *Langmuir* **2004**, *20*, 4738.
[23] P. J. Yoo, S.-J. Choi, J. H. Kim, D. Suh, S. J. Baek, T. W. Kim, H. H. Lee, *Chemistry of Materials* **2004**, *16*, 5000.
[24] M. Mayer, J. Yang, I. Gitlin, D. H. Gracias, G. M. Whitesides, *Proteomics* **2004**, *4*, 2366.
[25] D. B. Weibel, A. Lee, M. Mayer, Sean F. Brady, D. Bruzewicz, J. Yang, W. R. DiLuzio, J. Clardy, G. M. Whitesides, *Langmuir* **2005**, *21*, 6436.
[26] M. M. Stevens, M. Mayer, D. G. Anderson, D. B. Weibel, G. M. Whitesides, R. Langer, *Biomaterials* **2005**, *26*, 7636.
[27] N. Y. Lee, J. R. Lim, M. J. Lee, J. B. Kim, S. J. Jo, H. K. Baik, Y. S. Kim, *Langmuir* **2006**, *22*, 9018.
[28] N. Coq, T. v. Bommel, R. A. Hikmet, Hendrik R. Stapert, W. U. Dittmer, *Langmuir* **2007**, *23*, 5154.
[29] M. Pla-Roca, J. G. Fernandez, C. A. Mills, E. Martnez, J. Samitier, *Langmuir* **2007**, *23*, 8614.
[30] H. Schmid, B. Michel, *Macromolecules* **2000**, *33*, 3042.
[31] R. S. Kane, S. Takayama, E. Ostuni, D. E. Ingber, G. M. Whitesides, *Biomaterials* **1999**, 2363.
[32] G. M. Whitesides, E. Ostuni, S. Takayama, X. Jiang, D. E. Ingber, *Annual Reviews of Biomedical Engineering* **2001**, *3*, 335.
[33] Y. Xia, M. Mrksich, E. Kim, G. M. Whitesides, *Journal of American Chemical Society* **1995**, *117*, 9576.
[34] T. Pompe, A. Fery, S. Herminghaus, A. Kriele, H. Lorenz, J. P. Kotthaus, *Langmuir* **1999**, *15*, 2398.
[35] N. L. Jeon, K. Finnie, K. Branshaw, R. G. Nuzzo, *Langmuir* **1997**, *13*, 3382.
[36] P. M. S. John, H. G. Craighead, *Applied Physics Letters* **1996**, *68*, 1022.

[37] D. Wang, S. G. Thomas, K. L. Wang, Y. Xia, G. M. Whitesides, *Applied Physics Letters* **1997**, *70*, 1593.
[38] P. C. Hidber, W. Helbig, E. Kim, G. M. Whitesides, *Langmuir* **1996**, *12*, 1375.
[39] E. Delamarche, J. Vichiconti, S. A. Hall, M. Geissler, W. Graham, B. Michel, R. Nunes, *Langmuir* **2003**, *19*, 6567.
[40] V. Santhanam, R. P. Andres, *Nano Letters* **2004**, *4*, 41.
[41] Y. Cong, J. Fu, Z. Zhang, Z. Cheng, R. Xing, J. Li, Y. Han, *Journal of Applied Polymer Science B* **2005**, *100*, 2737.
[42] S.-H. Yun, B.-H. Sohn, J. C. Jung, W.-C. Zin, M. Ree, J. W. Park, *Nanotechnology* **2006**, *17*, 450.
[43] R. D. Bennett, A. J. Hart, Andrew C. Miller, P. T. Hammond, D. J. Irvine, R. E. Cohen, *Langmuir* **2006**, *22*, 8273.
[44] Y.-K. Kim, S. J. Park, J. P. Koo, D.-J. Oh, G. T. Kim, S. Hong, J. S. Ha, *Nanotechnology* **2006**, *17*, 1375.
[45] A. F. Runge, S. S. Saavedra, *Langmuir* **2003**, *19*, 9418.
[46] B. A. Langowski, K. E. Uhrich, *Langmuir* **2005**, *21*, 6366.
[47] C. D. James, R. C. Davis, L. Kam, H. G. Craighead, M. Isaacson, J. N. Turner, W. Shain, *Langmuir* **1998**, *14*, 741.
[48] C. Donzel, M. Geissler, A. Bernard, H. Wolf, B. Michel, J. Hilborn, E. Delamarche, *Advanced Materials* **2001**, *13*, 1164.
[49] E. Delamarche, C. Donzel, F. S. Kamounah, H. Wolf, M. Geissler, R. Stutz, P. Schmidt-Winkel, B. Michel, H. J. Mathieu, K. Schaumburg, *Langmuir* **2003**, *19*, 8749.
[50] S. A. Lange, V. Benes, D. P. Kern, J. K. H. Horber, A. Bernard, *Analytical Chemistry* **2004**, *76*, 1641.
[51] C. Xu, P. Taylor, M. Ersoz, P. D. I. Fletcher, V. N. Paunov, *Journal of Materials Chemistry* **2003**, *13*, 3044.
[52] J. Lahiri, E. Ostuni, G. M. Whitesides, *Langmuir* **1999**, *15*, 2055.
[53] D. I. Rozkiewicz, W. Brugman, R. M. Kerkhoven, B. J. Ravoo, D. N. Reinhoudt, *Journal of American Chemical Society* **2007**, *129*, 11593.
[54] L. Xu, L. Robert, Q. Ouyang, F. Taddei, Y. Chen, A. B. Lindner, D. Baigl, *Nano Letters* **2007**, *7*, 2068.
[55] M. Mrksich, L. E. Dike, J. Tien, D. E. Ingber, G. M. Whitesides, *Experimental Cell Research* **1997**, *235*, 305.
[56] A. Bernard, E. Delamarche, H. Schmid, B. Michel, H. R. Bosshard, H. Biebuyck, *Langmuir* **1998**, *14*, 2225.
[57] A. Bernard, J. P. Renault, B. Michel, H. R. Bosshard, E. Delamarche, *Advanced Materials* **2000**, *12*, 1067.
[58] J. L. Tan, J. Tien, C. S. Chen, *Langmuir* **2002**, *18*, 519.
[59] H. D. Inerowicz, S. Howell, F. E. Regnier, R. Reifenberger, *Langmuir* **2002**, *18*, 5263.
[60] J. P. Renault, A. Bernard, A. Bietsch, B. Michel, H. R. Bosshard, E. Delamarche, M. Kreiter, B. Hecht, U. P. Wild, *Journal of Physical Chemistry B* **2003**, *107*, 703.
[61] D. I. Rozkiewicz, Y. Kraan, M. W. T. Werten, F. A. d. Wolf, V. Subramaniam, B. J. Ravoo, D. N. Reinhoudt, *Chemistry European Journal* **2006**, *12*, 6290.
[62] A. Peramo, A. Albritton, G. Matthews, *Langmuir* **2006**, *22*, 3228.
[63] L. Lauer, S. Ingebrandt, M. Scholl, A. Offenhäusser, *IEEE Transactions on Biomedical Engineering* **2001**, *48*, 838.

[64] L. Libioulle, A. Bietsch, H. Schmid, B. Michel, E. Delamarche, *Langmuir* **1999**, *15*, 300.
[65] A. Bietsch, B. Michel, *Journal of Applied Physics* **2000**, *88*, 4310.
[66] K. G. Sharp, G. S. Blackman, N. J. Glassmaker, A. Jagota, C.-Y. Hui, *Langmuir* **2004**, *20*, 6430.
[67] B. Michel, A. Bernard, A. Bietsch, E. Delamarche, M. Geissler, D. Juncker, H. Kind, J. P. Renault, H. Rothuizen, H. Schmid, P. Schmidt-Winkel, R. Stutz, H. Wolf, *IBM Journal of Research and Development* **2001**, *45*, 697.
[68] T. W. Odom, J. C. Love, D. B. Wolfe, K. E. Paul, G. M. Whitesides, *Langmuir* **2002**, *18*, 5314.
[69] X. Duan, V. B. Sadhu, A. Perl, M. Pter, D. N. Reinhoudt, J. Huskens, *Langmuir* **2008**, *24*, 3621.
[70] J. Chalmeau, C. Thibault, F. Carcenac, C. Vieu, *Applied Physics Letters* **2008**, *93*, 133901.
[71] A. Bernard, D. Fitzli, P. Sonderegger, E. Delamarche, B. Michel, H. R. Bosshard, H. Biebuyck, *Nature Biotechnology* **2001**, *19*, 866.
[72] J. P. Renault, A. Bernard, D. Juncker, B. Michel, H. R. Bosshard, E. Delamarche, *Angewandte Chemical International Edition* **2002**, *41*, 2320.
[73] M. L. Tingey, S. Wilyana, E. J. Snodgrass, N. L. Abbott, *Langmuir* **2004**, *20*, 6818.
[74] M. L. Tingey, E. J. Snodgrass, N. L. Abbott, *Advanced Materials* **2004**, *16*, 1331.
[75] M. He, O. Stoevesandt, M. J. Taussig, *Current Opinion in Biotechnology* **2008**, *19*, 4.
[76] M. He, O. Stoevesandt, E. A. Palmer, F. Khan, O. Ericsson, M. J. Taussig, *Nature Methods* **2008**, *5*, 175.
[77] H. Lin, L. Sun, R. M. Crooks, *Journal of American Chemical Society* **2005**, *127*, 11210.
[78] A. A. Yu, T. A. Savas, G. S. Taylor, A. Guiseppe-Elie, H. I. Smith, F. Stellacci, *Nano Letters* **2005**, *5*, 1061.
[79] H. Tan, S. Huang, K.-L. Yang, *Langmuir* **2007**, *23*, 8607.
[80] Y. Wang, S. H. Goh, X. Bi, K.-L. Yang, *Journal of Colloid and Interface Science* **2009**, *333*, 188.
[81] M. He, O. Stoevesandt, E. A. Palmer, F. Khan, O. Ericsson, M. J. Taussig, *Nature Methods* **2008**, *5*, 175.
[82] T. Auletta, B. Dordi, A. Mulder, A. Sartori, S. Onclin, C. M. Bruinink, M. Peter, C. A. Nijhuis, H. Beijleveld, H. Schonherr, G. JuliusVancso, A. Casnati, R. Ungaro, B. J. Ravoo, J. Huskens, D. N. Reinhoudt, *Angewandte Chemical International Edition* **2004**, *43*, 369.
[83] C. M. Bruinink, C. A. Nijhuis, M. Peter, B. Dordi, O. Crespo-Biel, T. Auletta, A. Mulder, H. Schonherr, G. J. Vancso, J. Huskens, D. N. Reinhoudt, *Chemistry A European Journal* **2005**, *11*, 3988.
[84] O. Crespo-Biel, M. Peter, C. M. Bruinink, Bart Jan Ravoo, D. N. Reinhoudt, J. Huskens, *Chemistry A European Journal* **2005**, *11*, 2426.
[85] A. Mulder, S. Onclin, M. Peter, J. P. Hoogenboom, H. Beijleveld, J. t. Maat, M. F. Garcia-Parajo, B. J. Ravoo, J. Huskens, N. F. v. Hulst, D. N. Reinhoudt, *Small* **2005**, *1*, 242.
[86] N. Patel, R. Bhandari, K. M. Shakesheff, S. M. Caninizzaro, M. C. Davies, R. Langer, C. J. Roberts, S. J. B. Tendler, P. M. Williams, *Journal of Biomaterials Science Polymer Edition* **2000**, *11*, 319.
[87] B. Wang, J. Feng, C. Y. Gao, *Macromolecular Bioscience* **2005**, *5*, 767.
[88] H. Lin, J. Kim, L. Sun, R. M. Crooks, *Journal of American Chemical Society* **2006**, *128*, 3268.

[89] J. Kim, R. M. Crooks, *Journal of American Chemical Society* **2006**, *128*, 12076.
[90] J. Kim, R. M. Crooks, *Analytical Chemistry* **2007**, *79*, 7267.
[91] M. J. W. Ludden, X. Li, J. Greve, A. v. Amerongen, M. Escalante, V. Subramaniam, D. N. Reinhoudt, J. Huskens, *Journal of American Chemical Society* **2008**, *130*, 6964.
[92] X. Y. Ling, D. N. Reinhoudt, J. Huskens, *Chemistry of Materials* **2008**, *20*, 3574.
[93] J. Hyun, Y. Zhu, A. Liebmann-Vinson, J. Thomas P. Beebe, A. Chilkoti, *Langmuir* **2001**, *17*, 6358.
[94] L. Iversen, N. Cherouati, T. Berthing, D. Stamou, K. L. Martinez, *Langmuir* **2008**, *24*, 6375.
[95] Z. Yang, A. M. Belu, A. Liebmann-Vinson, H. Sugg, A. Chilkoti, *Langmuir* **2000**, *16*, 7482.
[96] J. Lahann, M. Balcells, T. Rodon, J. Lee, I. S. Choi, K. F. Jensen, R. Langer, *Langmuir* **2002**, *18*, 3632.
[97] K.-B. Lee, D. J. Kim, Z.-W. Lee, S. I. Woo, I. S. Choi, *Langmuir* **2004**, *20*, 2531.

Chapter 2 Supramolecular Nanostamping (SuNS)

2.1 Introduction

Biomolecular platforms, such as DNA microarrays, which now proved to be indispensible for medical and diagnostic applications, have became one of the major areas of research since their invention. As described in the previous chapter, the main limitation of wide utilization of such platforms is their costly fabrication processes; hence their price. The methods to fabricate DNA microarrays can be grouped under two headlines: 1) Printing (Contact and Non-contact and 2) *In situ* synthesis. *[1]* Contact printing involves pins carrying the desired DNA solutions; namely spotting. When brought in contact with the target substrate (mostly chemically modified glass), these pins deposit the DNA solutions onto the target substrate. Piezo and ink-jet devices are examples for non-contact printing systems in which the DNA solution is dispensed without touching the target substrate. *[2]* Contact-based fabrication of nanoarrays by scaning probe microscopy will be mentioned in the following chapter. In *in situ* synthesis, usually a glass slide is patterned with sites that are ready to bind to oligonucleotides. *[1]* Each site has a photo-active cap which is a light sensitive chemical. Synthesis is carried on by directing light to the corresponding site and treating the whole substrate with the desired and capped base. (Figure 2.1) This process requires various masks to activate specific sites on the substrate. The utilization of mirrors instead of masks was suggested to cut down the cost associated with the mask fabrication as well. *[3]* However, the length of the *in situ* synthesized DNA is limited by the efficiency of the process (77% of 25 base pair long oligonucleotides were synthesized correctly). *[4]*

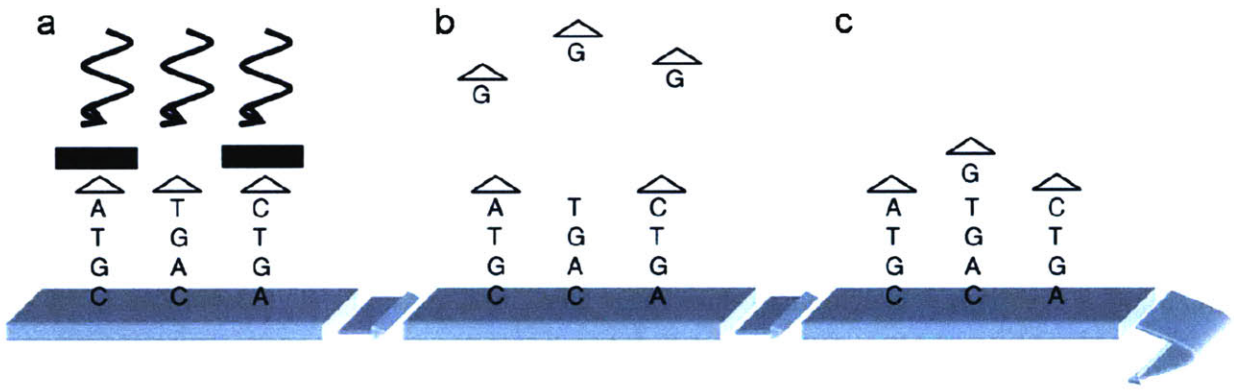

Figure 2.1: Schematic illustration of in situ synthesis by using masks a) a specific site is activated by destroying the photolabile group, b) the substrate is washed with a capped base, c) the substrate is ready for the further extension. *[1]*

All above mentioned commercially available methods are serial in nature and apart from the cost have inherent problems associated with it. For instance, although pin-based spotting systems can deposit a reasonable number of DNA (<100) in one cycle, to replicate a whole microarray, this deposition has to be repeated several times resulting in heterogeneity on the product surface. Therefore, in terms of cost and product quality new methods should be developed to handle the complexity of the DNA-based devices. As described in the previous chapter contact based methods seem promising in fabricating such platforms in a cheaper way. It is important to note that although spotting is also contact based, from now on by 'contact based' I am referring to methods which can fabricate rather larger areas than a pin generated spot. Supramolecular Nanostamping (SuNS) was developed in our group *[5]* and Crook's group *[6]* to solve the main hurdle, the cost of fabrication, by suggesting a parallel fabrication process. The idea is to capture target (complementary) DNA molecules from solution through a master composed of DNA features and transfer this spatial information as well as chemical information encoded in different DNA sequences onto a secondary substrate. The process, as depicted in

Scheme 2.1, is composed of three steps: 1) Hybridization, 2) Contact and 3) Dehybridization. In the first step (Hybridization), a master bearing DNA features (i.e. patterned single strand DNA) is hybridized with its complementary molecules by exploiting the molecular recognition between two complementary DNA strands. These complementary DNA strands contain a chemical group which can react with the secondary substrate. Thus in the second step (Contact), when the hybridized master is brought into contact with the secondary substrate, these complementary strands covalently attach to the secondary substrate and bond two surfaces together. In the last step, two surfaces are detached from each other by breaking the hydrogen bonds holding DNA strands together either by heat or mechanical forces leaving the complementary replica of the master on the secondary substrate.

Scheme 2.1. Schematic illustration of the SuNS procedure

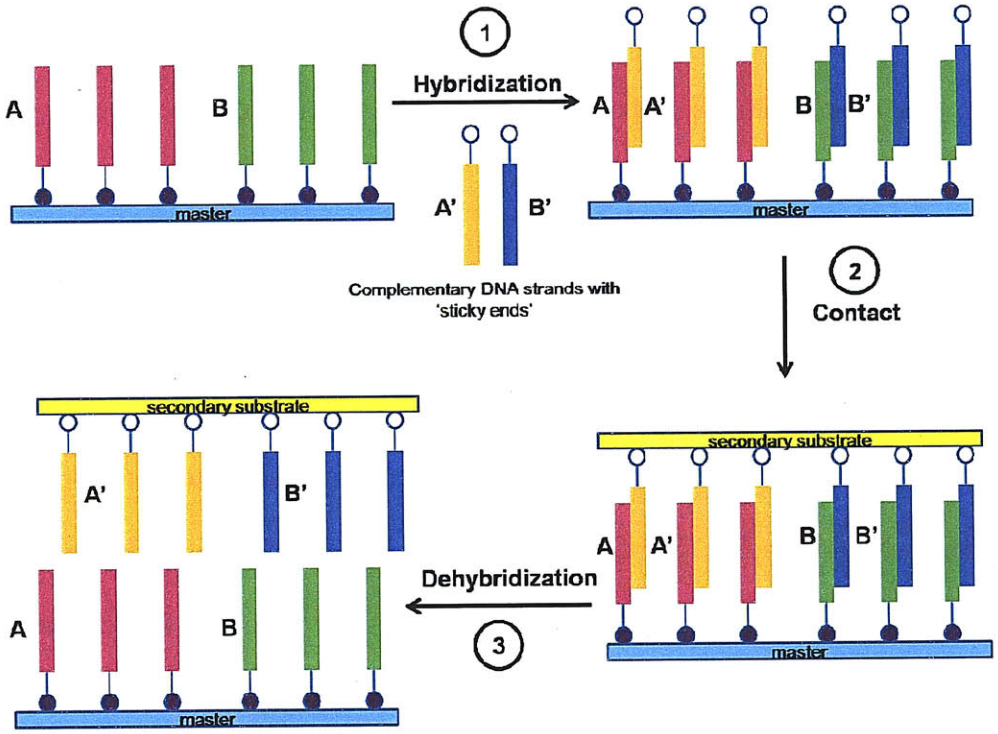

The strength of SuNS comes from spontaneous printing of chemical and spatial information. DNA strands carry the chemical information through their sequence formed by four DNA bases (adenine, guanine, cytosine and thymine); differing combination of these bases results in different chemical information. The spatial information is registered on the master and preserved during printing; thus distinct sequences with distinct locations can be replicated in a single SuNS cycle.

2.2 Variety of Masters

SuNS process starts with hybridization of the master, which can be defined as single strand DNA (ssDNA) immobilized substrate. The immobilization of ssDNA on the master surface is also assured by the chemical moieties attached to the ends of ssDNA. Here, it is important to note that SuNS is a technique which can replicate the master features in a parallel fashion. However the master can be prepared by serial techniques as well; thus SuNS is complementary to current fabrication techniques which can immobilize DNA on suitable substrates. Several different types of methods have been employed to fabricate masters such as dip-pen nanolithography, *[5]* achromatic interference lithography, *[5, 7]* optical lithography, *[8]* electron-beam lithography, *[9]* microfluidic techniques, *[8]* spotting *[10]* and simply self-assembly. *[11]*

Although expensive, thiol-gold chemistry is widely used in our group to prepare the masters since gold features are easy to obtain using lithography. Desired patterns such as squares or lines are coated with gold through thermally evaporating gold onto these features (sometimes followed by lift-off, if the initial pattern was negative)

The very first master replicated through SuNS was DNA monolayer on gold.*[5]* In the same report, gold coated 50 nm silicon oxide wires fabricated with achromatic interference lithography were used as a master as well. Another approach is to backfill a surface with DNA. A square made of octadecanethiol was fabricated through dip-pen nanolithography on gold and ssDNA was assembled on the rest of the surface. Consequently, the printed substrate was composed of a DNA monolayer and a clean square.*[5]*

Microfluidic techniques *[8]* and spotting *[10]* were also employed to immobilize different DNA strands onto the same substrate as well. Microfluidic channels made of poly(dimethyl siloxane) (PDMS) brought into contact with gold-on-glass substrate and different DNA solutions (with thiol ends) were injected into different channels. Once the microfluidic network was removed, the surface was treated with mercaptohexanol to minimize the unspecific binding of complementary DNA strands during the 'Hybridization' step. *[8]* In spotting, the same approach was followed; different DNA solutions were immobilized using a micropipette. *[10]*

More recently, as will be described in the following chapter in order to increase the printing resolution of SuNS, gold nanoparticles on silicon were used as a template to assemble ssDNA. Through employing a well-studied approach, metal salt loaded block-copolymer micelles were immobilized on a silicon substrate with a chromium adhesion layer. The gold nanoparticles were obtained after the removal of the polymer with oxygen plasma cleaning. *[11]*

Although, for the convenience, gold surfaces are used as initial masters, the secondary substrate after printing (replica) bearing the complementary DNA strands can be used as a master (2^{nd} generation master). Thus, the materials which is described in the next section such as

PMMA *[9]* and poly(4-formyl-*p*-xylylene-*co*-*p*-xylylene) *[7]* coated substrates should also be considered as master materials.

2.3 Variety of Secondary Substrates

The evolution of SuNS in our group revolves around increasing printing resolution and coverage. Starting from replication of a DNA monolayer on gold surface to another gold substrate, we aimed to go down in feature size. In general, to obtain high resolution one should use hard secondary substrates (such as gold-on-glass); yet it is intrinsically hard to obtain perfect contact between two solid substrates; hence the printing coverage is low. Therefore, the alternative materials were sought to comply the goal: high resolution and coverage.

Poly(methyl methacrylate) (PMMA), being optically transparent, cheap and durable was the first candidate. PMMA is hard enough to sustain sub-100nm features and it is possible to soften PMMA by slightly increasing the temperature during the 'Contact' step so that better contact is assured between the master and secondary substrate (PMMA). To print onto PMMA, complementary amine-end DNA was used and the PMMA surface was aldehyde functionalized. After contact, coupled substrates (master and secondary PMMA surface) were kept in an oven at 75 °C for 20 minutes. This way, gold lines as thin as 50 nm were successfully printed and area coverage over 100 μm^2 was achieved. In addition, the printed PMMA substrate was used as a master itself. This substrate was treated with thiol-end DNA (that of the original sequence on the master) and used to print on gold-on-glass. *[9]*

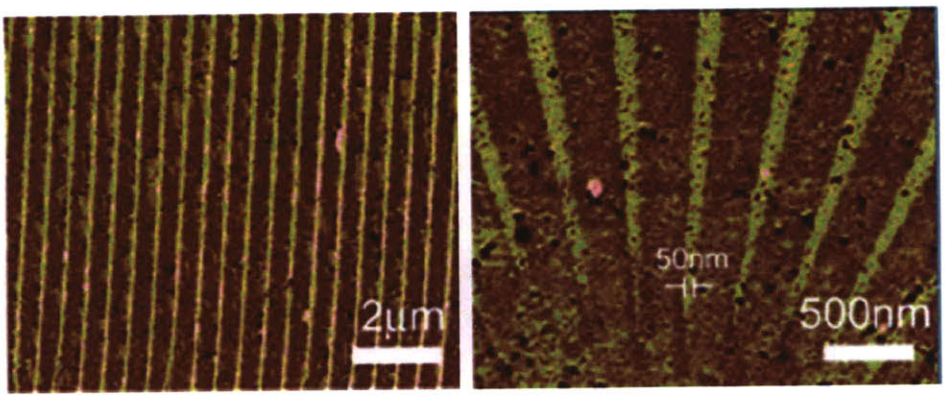

Figure 2.2: AFM micrographs of DNA lines on a PMMA substrate.*[9]*

To further increase the coverage, the solid secondary substrate in the process was replaced with a liquid prepolymer. This method is called Liquid Supramolecular Nanostamping (LiSuNS), as illustrated in Scheme 2.2, and truly ensures the utmost large area printing. *[8]* Onto the hybridized master, a liquid PDMS prepolymer was poured and subsequently cured. The complementary DNA in this process is vinyl terminated so that it can join the crosslinking of the PDMS prepolymer during curing. The PDMS prepolymer perfectly takes the shape of the master and bond to the DNA with vinyl terminal during curing. After curing, 'Dehybridization' takes place by a combination of thermal and mechanical forces i.e the complementary copy of the master is separated from the master by lifting the cured polymer. Although, LiSuNS adds an extra step (Curing) to the process, it does not require any surface modification of the secondary substrate or any contact equipment.

Scheme 2.2. Schematic illustration of the LiSuNS procedure*[8]*

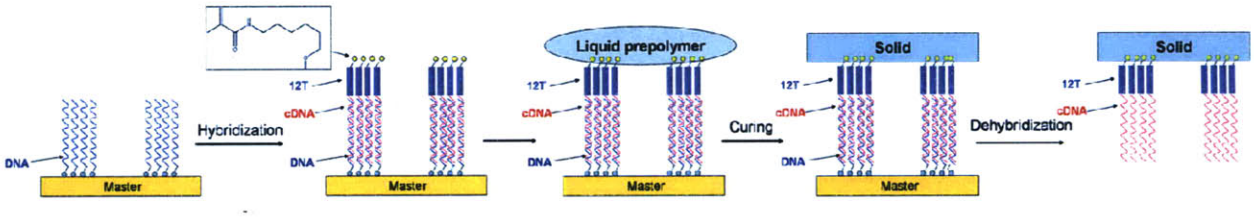

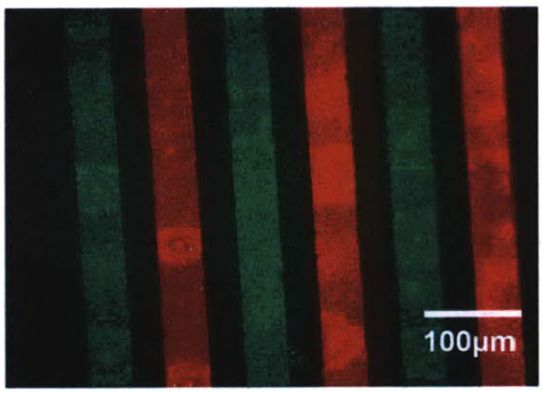

Figure 2.3: Simultaneous printing of two different DNA sequences via LiSuNS (false color overlay).

SuNS uses DNA with 'sticky ends' thus a reactive chemistry must be present between the terminal group of DNA and the secondary substrate. To demonstrate SuNS is applicable to all kinds of surfaces with different mechanical properties, various substrate such as silicon, quartz, glass, PMMA, PDMS and poly(styrene) were coated with poly(4-formyl-*p*-xylylene-*co*-*p*-xylylene) through chemical vapor deposition (CVD). This aldehyde terminated polymer can react with amine-end DNA forming an imine bond. For this report, thiol-end ssDNA was immobilized on gold coated silicon oxide wires fabricated through achromatic interference lithography or interference lithography. This master was hybridized with amine-end DNA and subsequently printed onto poly(4-formyl-*p*-xylylene-*co*-*p*-xylylene) coated substrates.*[7]* The SuNS procedure was the same for each substrate but the method of contact was varied. For

instance, the hard substrates such as silicon and quartz were brought together with a mechanical vise which had adapted PDMS plates whereas for a soft substrate like PDMS a balloon was placed between the plates of the vise to apply uniform pressure.*[12]* The successful printing on all secondary substrate shows that there is no need for a different immobilization procedure every time a different substrate is used.

2.4 Proof of Concept & Detection Techniques

The assessment of biomolecule-based platforms is currently carried out by fluorescence microscopy due to the feature size and spacing of these devices.*[1]* In our experiments, we also use fluorescence microscopy whenever possible. However, due to the efforts to increase resolution, we also use Atomic Force Microscopy (AFM) to assess the SuNS steps and detect printing. There are a few methods we use to validate the successful replication of the master as depicted:

1) After printing, 'Hybridization' of the secondary substrate with its complementary fluorescent DNA (that of original sequence on the master) and imaging this hybridized secondary substrate with fluorescence microscopy. (Scheme 2.3)

Scheme 2.3. Schematic illustration of Method 1

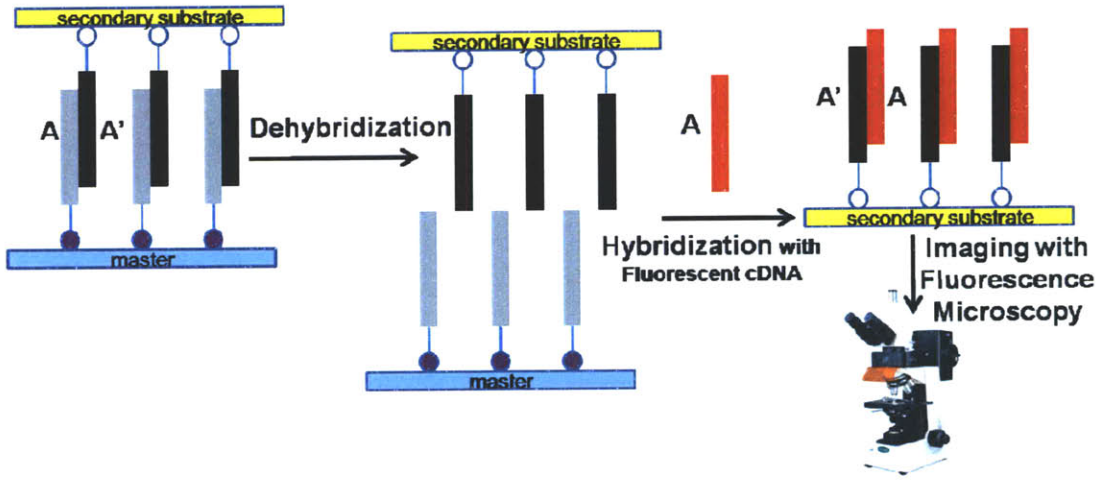

2) Although availability of the chemistry is limited (for instance if one would like to have thiol-modified and fluorescent DNA, the only dye that can be attached to thiol-modified DNA is FITC) there is also a library of fluorescent DNAs bearing a chemical group (sticky end) which can immediately used as complementary DNA to hybridize the master. Through this method, immediate assessment with fluorescence microscopy is possible right after printing. (Scheme 2.4)

Scheme 2.4. Schematic illustration of Method 2

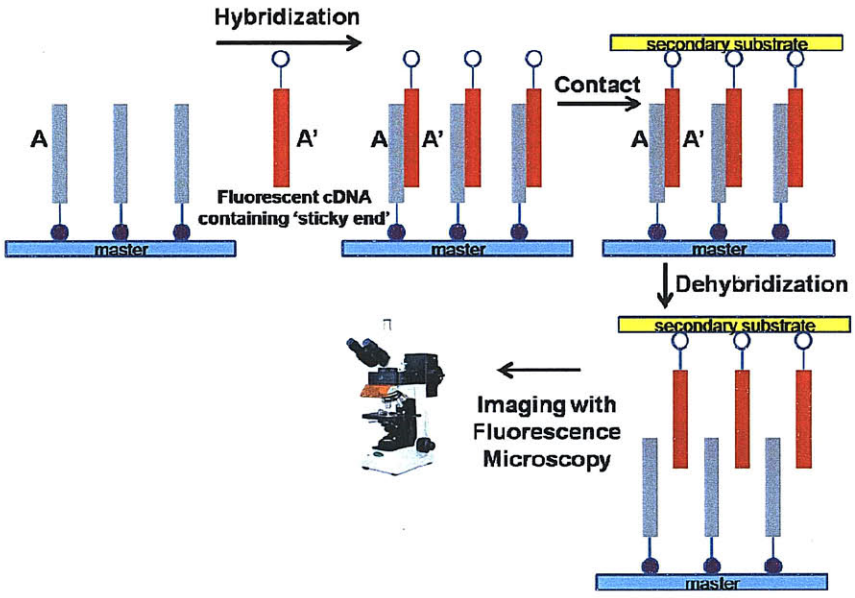

3) After printing, 'Hybridization' of the secondary substrate (now containing cDNA strands) with the original sequence that on the master and using this substrate as a 'new master' (2^{nd} generation master). Printing from this 'new master' to a 'new secondary substrate' and detecting printing on this 'new secondary substrate' by hybridizing with fluorescent complementary DNA and subsequent fluorescence microscopy. (Scheme 2.5)

Scheme 2.5. Schematic illustration of Method 3

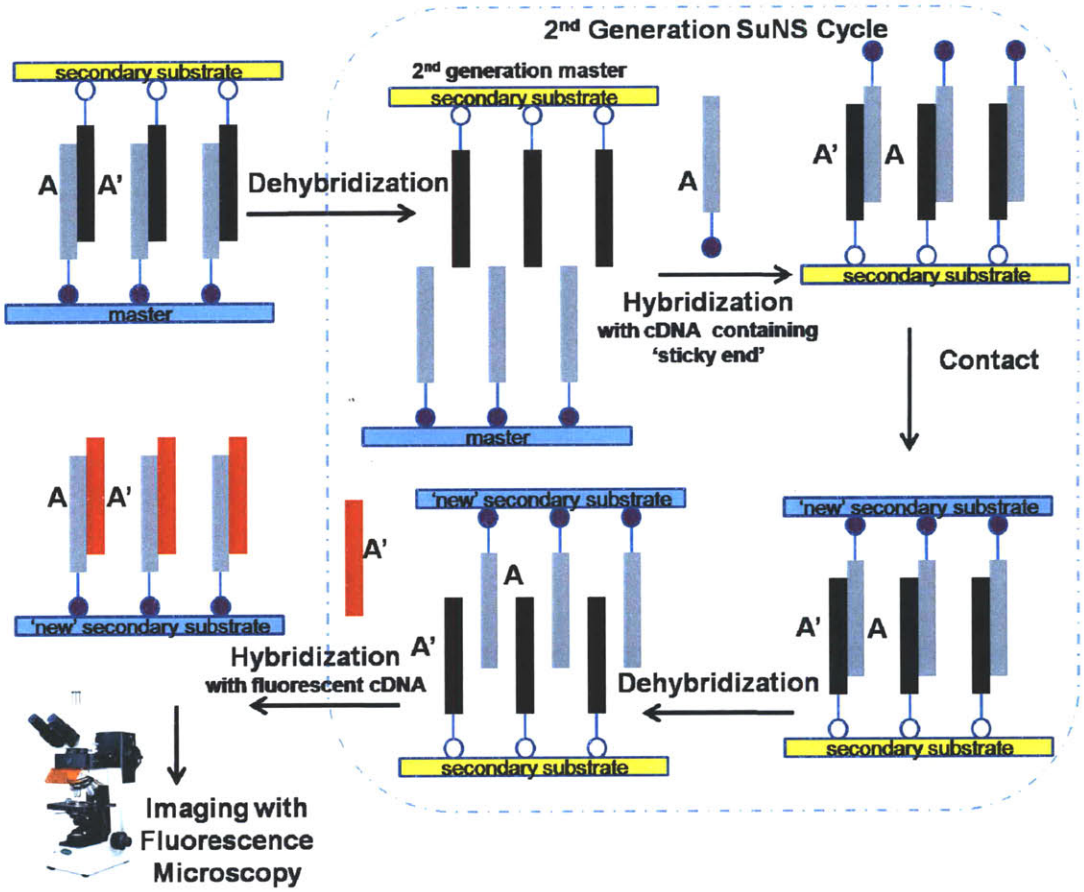

4) If master has high resolution, after printing, imaging the printed substrate with AFM by looking at the height and phase difference between the printed DNA and the substrate. (Scheme 2.6)

Scheme 2.6. Schematic illustration of Method 4

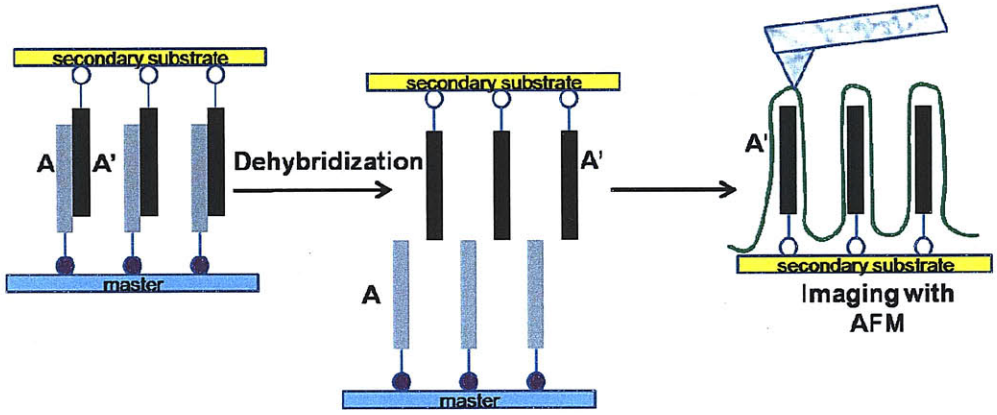

5) If master has high resolution, same as 'Method 3', but instead of 'Hybridization' with fluorescent complementary DNA to detect second generation printing, instead imaging the printed substrate with AFM. (Scheme 2.7)

Scheme 2.7. Schematic illustration of Method 7

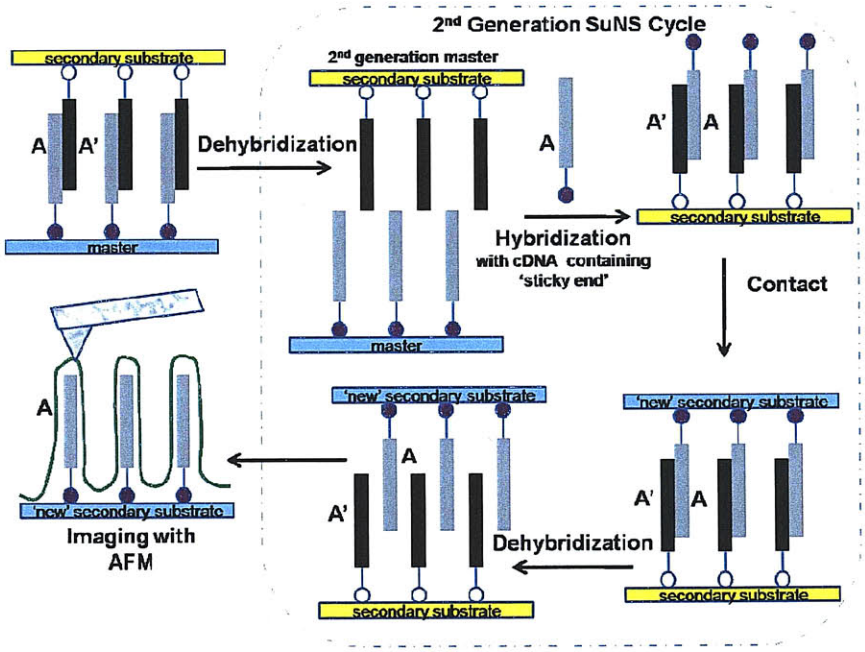

6) Reprinting from the same master several times through rehybridizing the same master after each SuNS cycle to prove the intactness of the master; consequently imaging with AFM or hybridizing the printed substrate with fluorescent cDNA and imaging with fluorescence microscopy. (Scheme 2.8) Here, the master can each time be hybridized with 'fluorescent cDNA with chemical modification'; then immediate fluorescence microscopy can be carried out without hybridizing the printed substrates.

Scheme 2.8. Schematic illustration of Method 6

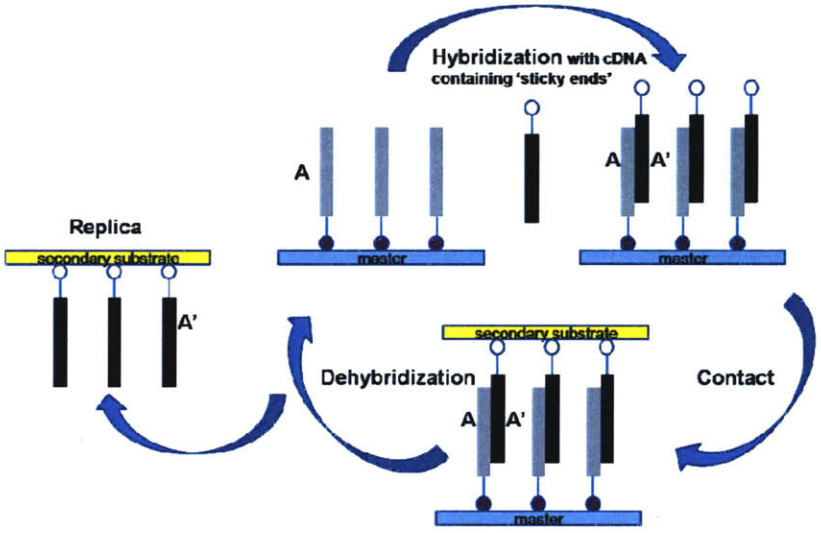

Using the replica as a master not only ensures the printing is successful but also guarantees a cheaper process by exponentially increasing the number of master considering the master is usually fabricated by a serial process. In addition, as described in Method 6, being able to use the same master several times also cuts down the cost associated with master preparation. Overall, we believe the cost reduction and fidelity of SuNS (transfer of chemical and spatial information spontaneously) will result in ultimate printing platform for DNA.

2.5 Crook's Approach

Crook's method differs from our procedure in terms of master and secondary substrate materials, the end groups of DNA and resolution. *[6, 13-16]* Their master is fabricated by reacting amine-end DNA with an *N*-hydroxysuccinimide-functionalized polymer on a glass slide. The complementary DNA has biotin moiety as an end group and the secondary substrate is prepared by reacting maleimide modified streptavidin with thiol-modified (PDMS); the printing is assured through biotin-streptavidin reaction. A small amount of buffer or water is introduced before the template is placed on a secondary substrate. *[6]* Additionally, the secondary substrate, streptavidin coated PDMS, has 10 μm deep trenches which are believed to help to drain the solution away from the interface to facilitate contact. *[6]* For dehybridization, two substrates are separated with mechanical forces as opposed to our mainly thermal approach.

Crook's group invented a general method called 'zip-code' approach to facilitate a single master for various sequences. (Scheme 2.9) *[13]* The 'zip code' master is generated by spotting the short 'zip code' sequences onto the initial substrate. These 'zip code' sequences can hybridize to any sequence which bears a complementary sequence to them (complementary 'code sequence'). The DNA to be hybridized to this code sequences also contains a 'functional sequence' as well as a biotin end group attached to the 'functional sequence'. 'Functional sequence' can be of any sequence and the 'zip code' master captures these functional DNA through their complementary 'code sequences'. Thus, the 'zip code' master can be used several times to hybridize with different 'functional sequences' thus eliminating the need for new master preparation each time a different array is needed.

Scheme 2.9. Schematic illustration of the 'zip code' approach *[13]*

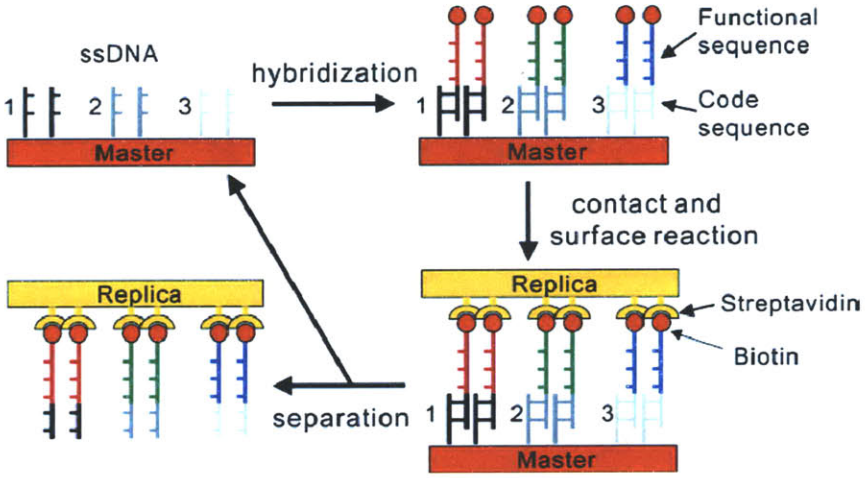

As stated above the strength of SuNS comes from stamping different DNA sequences in a single step. Recently, Crook's group demonstrated the enzymatic growth of complementary DNA on the initial DNA master and transfer of these products to a secondary substrate. (Scheme 2.10) *[16]* This eliminates the need for presynthesized complementary DNA. After spotting of DNA as to prepare master, this surface is hybridized with biotinylated primer oligonucleotides. These oligonucleotides thereafter were extended with T4 polymerase reaction. This surface was then brought in contact with a streptavidin coated secondary PDMS substrate. Upon dehybridization, the extended product stays on the secondary substrate. This result demonstrates the small amounts of reaction products can be transferred preserving their spatial information. Most importantly, in-situ synthesis of complementary DNA and subsequent transfer of the reaction products makes the initial goal of SuNS, reproducing DNA arrays in parallel, possible.

Scheme 2. 10. Schematic illustration of enzymatic growth of complementary DNA strands and subsequent transfer of the reaction products onto a secondary substrate *[16]*

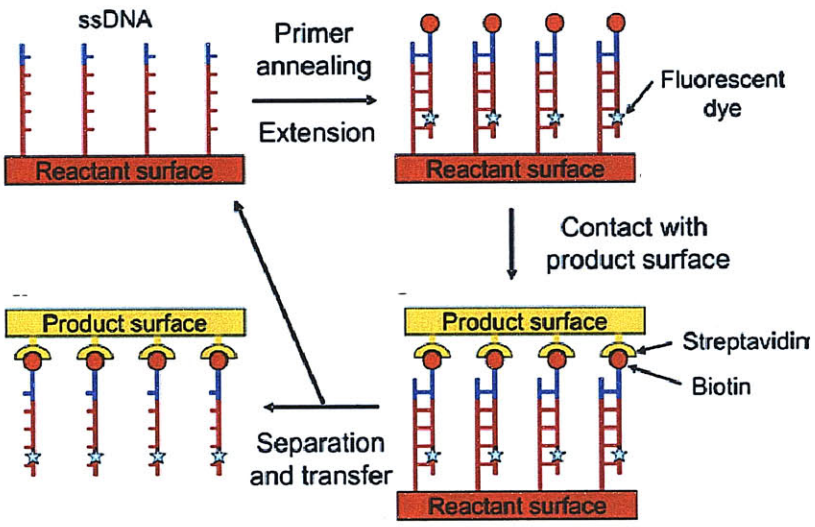

Crook's group also showed the replication of RNA arrays from DNA templates using a similar strategy. Instead of complementary DNA strands, complementary RNA strands are hybridized with ssDNA on the master surface and consequently transferred to the secondary substrate through biotin/streptavidin reaction. *[15]*

2.6 References

[1] M. Dufva, *Biomolecular Engineering* **2005**, *22*, 173.
[2] S. K. Moore, *IEEE Spectrum* **2001**, *38*, 54.
[3] S. Singh-Gasson, R. D. Green, Y. Yue, C. Nelson, F. Blattner, M. R. Sussman, F. Cerrina, *Nature Biotechnology* **1999**, *17*, 974.
[4] E. F. Nuwaysir, W. Huang, T. J. Albert, J. Singh, K. Nuwaysir, A. Pitas, T. Richmond, T. Gorski, J. P. Berg, J. Ballin, M. McCormick, J. Norton, T. Pollock, T. Sumwalt, L. Butcher, D. Porter, M. Molla, C. Hall, F. Blattner, M. R. Sussman, R. L. Wallace, F. Cerrina, R. D. Green, *Genome Research* **2002**, *12*, 1749.
[5] A. A. Yu, T. A. Savas, G. S. Taylor, A. Guiseppe-Elie, H. I. Smith, F. Stellacci, *Nano Letters* **2005**, *5*, 1061.
[6] H. Lin, L. Sun, R. M. Crooks, *Journal of American Chemical Society* **2005**, *127*, 11210.
[7] S. Thévenet, H.-Y. Chen, J. Lahann, F. Stellacci, *Advanced Materials* **2007**, *19*, 4333.
[8] A. A. Yu, F. Stellacci, *Advanced Materials* **2007**, *19*, 4338.

[9] A. A. Yu, T. Savas, S. Cabrini, E. diFabrizio, H. I. Smith, F. Stellacci, *Journal of American Chemical Society* **2005**, *127*, 16774.
[10] A. A. Yu, in *Department of Materials Science and Engineering*, Vol. Ph.D, MIT, Cambridge **2006**.
[11] O. Akbulut, J.-M. Jung, R. D. Bennett, Y. Hu, H.-T. Jung, R. E. Cohen, A. M. Mayes, F. Stellacci, *Nano Letters* **2007**, *7*, 3493.
[12] S. Thévenet, in *Department of Materials Science and Engineering*, MIT, Cambridge **2007**.
[13] H. Lin, J. Kim, L. Sun, R. M. Crooks, *Journal of American Chemical Society* **2006**, *128*, 3268.
[14] J. Kim, R. M. Crooks, *Analytical Chemistry* **2007**, *79*, 7267.
[15] J. Kim, R. M. Crooks, *Analytical Chemistry* **2007**, *79*, 8994.
[16] J. Kim, R. M. Crooks, *Journal of American Chemical Society* **2006**, *128*, 12076.

Chapter 3 Application of Supramolecular Nanostamping (SuNS) to the Replication of DNA Nanoarrays

The basis of this chapter was a letter, Application of Supramolecular Nanostamping (SuNS) to the Replication of DNA Nanoarrays, by Ozge Akbulut, Jin-Mi Jung, Ryan D. Bennett, Ying Hu, Hee-Tae Jung, Robert E. Cohen, Anne M. Mayes, and Francesco Stellacci in Nano Letters, 2007, 7 (11), 3493-3498.

3.1 Introduction

As stated in Chapter 2, in our group we have focused on increasing the printing resolution of Supramolecular Nanostamping to demonstrate it is compatible with feature sizes well below 100 nm and can cope with further miniaturization of DNA arrays. Currently, commercially available DNA arrays have 10 to 500 μm feature size. *[1]* However, the amount of analyte scales with the area of the assay; hence it has been speculated that the arrays with smaller feature sizes and spacing will have higher sensitivity due to smaller analyte volumes. *[2]* We claim that SuNS can also be the cost efficient replication method for nanoscale arrays such that previously, 50 nm resolution on PMMA substrates was reported. *[3]* In this chapter, further investigation on increasing SuNS' resolution and detection of hybridization on this level will be presented. First, fabrication of a single-component DNA nano-array is explained. This array is then replicated via SuNS. It is also important to note that there is an additional challenge at the nano-level apart from fabricating or replicating the array: one should devise a detecting strategy as well. Here an AFM based statistical analysis is suggested to assess hybridization. *[4]*

At present, the techniques to fabricate nanoarrays rely on scanning probe microscopy (SPM) which can deliver molecules on specific locations. Dip-pen nanolithography (DPN) has

become the most popular method to immobilize biomolecules or biomolecule-reacting agents (such as mercaptohexadecanoic acid).*[2]* This SPM-based technique, although promising and easy for proof-of-concept studies, is serial in nature and commercially it will be very costly to fabricate each nanoarray platform with it. Nevertheless, I would like to introduce two studies which use DPN to underline the prospect of nanoarrays. Mirkin and coworkers immobilized 16-mercaptohexadecanoic acid through DPN, and reacted those features with HIV antibodies. This antibody array was used to capture HIV-1 p24 antigens. The antibody-antigen binding was tracked through the height increase via AFM. Further verification was carried out with antibody coated gold nanoparticles by attaching them to the antibody-antigen complex already present on the array and again monitoring the height increase. The authors reported more then 1000-fold increase in sensitivity compared to conventional enzyme-linked immunosorbent assay based immunoassays (ELISA). *[5]*

Scheme 3.1. Schematic representation of fabricating the anti-p24 array and subsequent detection of p24 (HIV) *[5]*

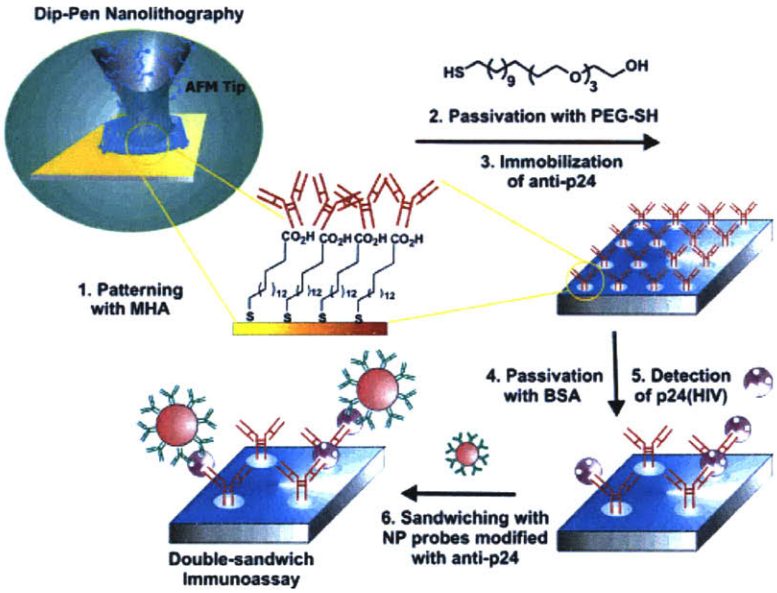

Sinensky and Belcher proposed the use of Kelvin Probe Force Microscopy (KPFM) which can measure the local variations in charge density to detect the complex formation between biomolecules. This technique relies on biomolecules being on their charged states under physiological conditions and change in this charge density upon complex formation. Using DPN two types of bioarrays are fabricated: MHA was immobilized on a gold surface to capture biotin (protein array) and thiol-end single strand DNA was patterned on a gold surface (DNA array). Through KPFM, avidin-biotin complex formation and DNA hybridization were detected. The authors reported high resolution (<10 nm), sensitivity (<50 nM) and speed (>1,100 μm/s). Further investigation was carried out to detect the mismatch between the DNA strands; mismatch down to three base pairs was successfully monitored. *[6]*

3.2 Fabrication of a Single Component DNA Array

To fabricate a single component high resolution array with sub-20 nm feature size and sub-100 spacing, we have employed block copolymer (BCP) micelles.*[7-9]* As described in Scheme 3.2, an amphiphilic block copolymer, poly(styrene)-*block*-poly(2-vinylpyridine) (PS-*b*-P2VP), dissolved in toluene (toluene selectively dissolves the poly(styrene) block), with a metal precursor salt forms micelles (core-shell structures). The metal precursor salt also forms a complex with the poly(2-vinylpyridine) block. When this solution was spin cast onto a substrate, a micelle monolayer was formed. Through oxygen plasma cleaning, the organic part of this monolayer was removed and semi-hexagonal array of gold nanoparticles was obtained. As detected by transmission electron microscopy (TEM), the obtained gold features were 9± 2 nm in diameter and spaced by 77± 9 nm. (Figure 1) The versatility of this method, i.e. control over the

spacing and partial control over particle size, and large area coverage make it an ideal candidate for single-component arrays.

Scheme 3.2. Schematic illustration of gold nanoparticle array fabrication

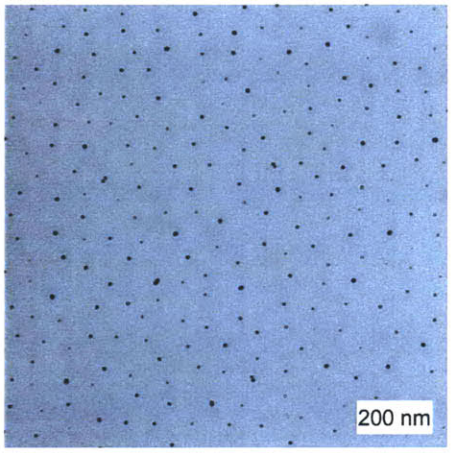

Figure 3.1: TEM image of gold nanoparticles obtained from PS_{780}-*b*-$P2VP_{200}$ block copolymer. (Courtesy of Dr. Ryan D. Bennett)

3.3 SuNS Cycle on Gold Nanoparticle Template

Once the gold nanoparticle template is ready, as described in Scheme 3.3, the DNA immobilization was carried out by modifying the method reported by Herne and Tarlov*[10]* and thereafter regular SuNS cycle, as described in the previous chapter, was followed. In brief, the gold nanoparticle substrate was placed in hexyl-thiol 5' modified 5 μM single stranded (50-mer) DNA (HS-ssDNA) solution. After cleaning with deionized (DI) water, the substrate (here on I will refer this ssDNA immobilized substrate as 'master') was treated with 6-mercapto-1-hexanol

(MH) to minimize the nonspecific adsorption during the hybridization step (this step is not depicted in the Scheme 3.3). The master was then placed in 5 μM 5' hexyl-thiol modified complementary DNA (HS-cDNA) solution for 12 h. The hybridized master was brought into contact with a gold-on-glass substrate in a mechanical vise and a light pressure was applied (<2 atm as determined by Pressurex films by Sensor Products LLC.) for 1 day in a desiccator. The dehybridization was carried out in a 90° C oven, after 30 minutes, the vise was loosened and several drops of the dehybridization buffer was placed onto the sandwiched substrates and the two were gently separated.

Scheme 3.3. SuNS cycle on gold nanoparticle template

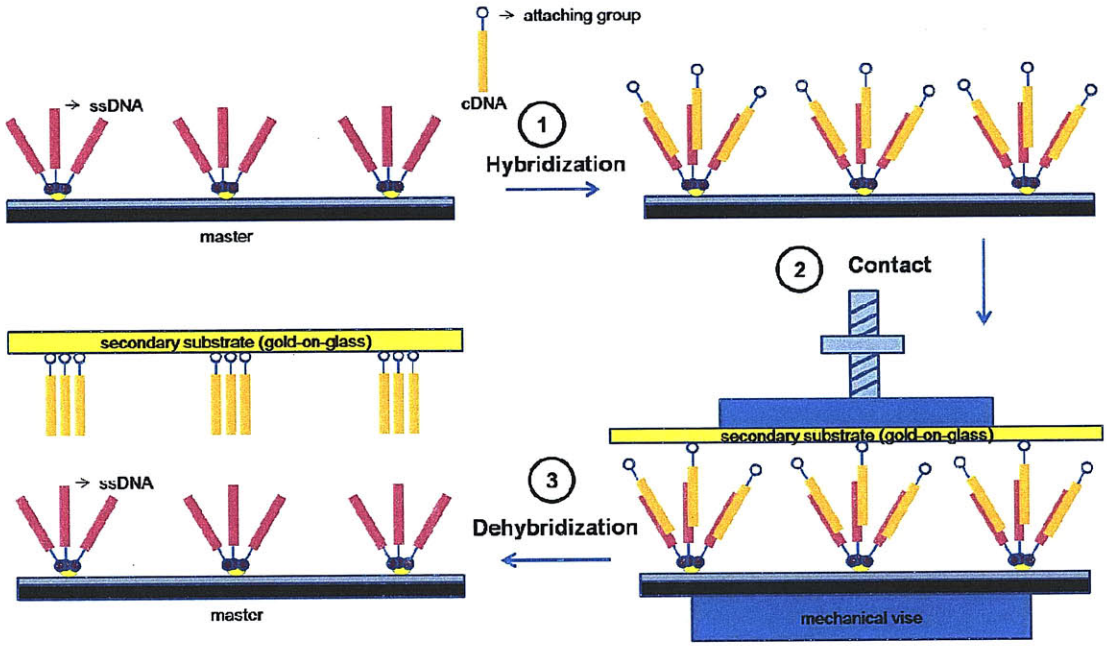

The steps of this process were tracked down via x-ray photoelectron spectroscopy (XPS) to determine the chemical composition on the gold nanoparticles by monitoring the phosphorus to gold ratio (P/Au) (Figure 3.2). The ratio was almost doubled from the ssDNA immobilized

state (master) (P/Au: 0.85), to the hybridized state (hybridized master) (P/Au: 1.47). The MH treatment in between those steps didn't seem to affect this ratio (P/Au: 0.77). After dehybridization, the master exhibited a return to the unhybridized state (P/Au: 0.68). The gold nanoparticle template was also imaged with AFM throughout the mentioned steps and no significant change was observed in particle spacing as well.

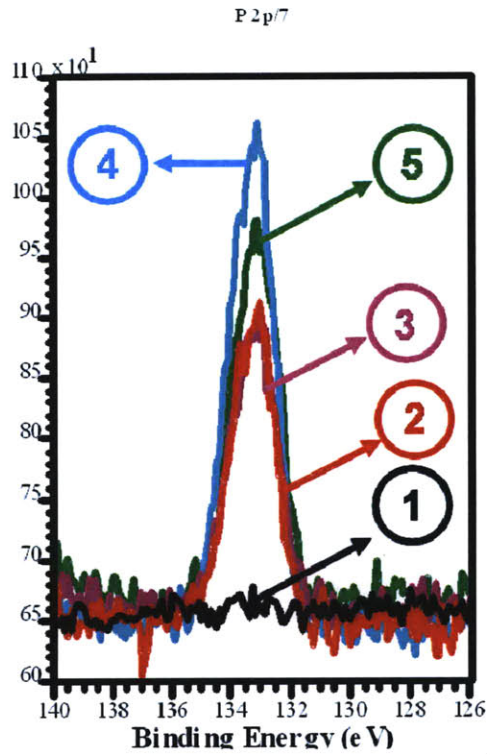

Figure 3.2: XPS measurements on (1) pristine gold nanoparticles (P/Au: 0), (2) ssDNA-immobilized gold nanoparticles (P/Au: 0.85), (3) MH treatment (P/Au: 0.77), (4) DNA-hybridized gold nanoparticles (P/Au: 1.47), and (5) master after printing/dehybridization (P/Au: 0.68).

3.4 Proof of Printing

The printed substrate was imaged with AFM; the presence of nanoscale dots and the close match between the particle spacing between the master (77± 9 nm) and the printed substrate (77± 10 nm) indicated successful printing. We also observed, although infrequently, (<5% of the printed area of the substrate) transfer of individual nanoparticles to the secondary substrate. A typical printed pattern is demonstrated in Figure 3.3b. To underline the close match of the patterns, radial distribution functions were calculated for both the master and the printed substrate patterns using an image analysis software (ImageJ, National Institute of Health) and a custom written code in MatLab (The MathWorks, Inc.). As shown in Figure 3.3c, the radial distribution functions for both substrates are in close agreement, indicating that the feature arrangement of the printed substrate was derived from the one present on the master.

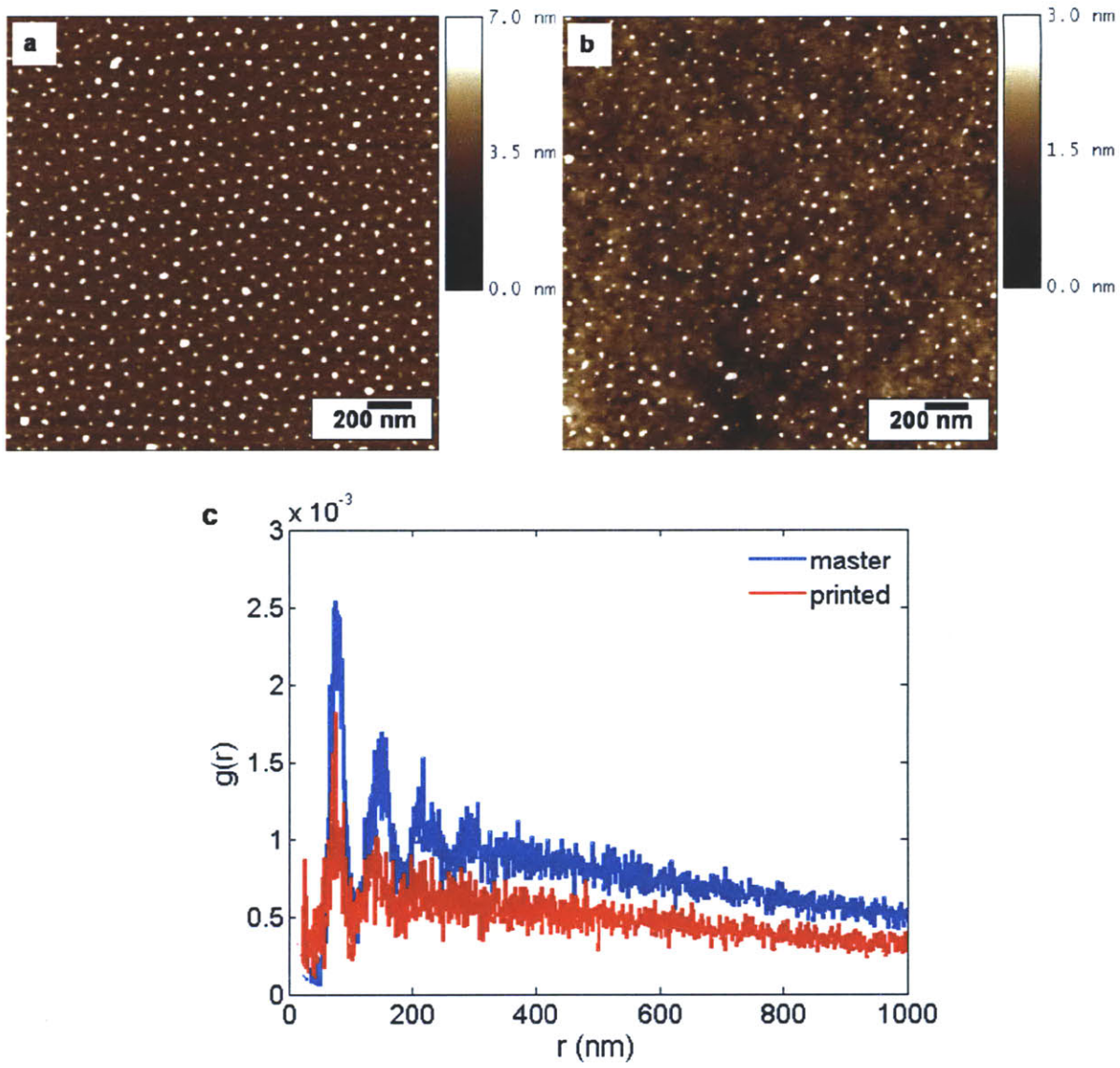

Figure 3.3: AFM height images of a) gold nanoparticle master, b) printed pattern, c) RDF comparison of 'a' and 'b'.

Although AFM can detect the printed DNA features and their spacing, it cannot give the true size of the DNA dots since the feature shape in an AFM image is a convolution of the AFM tip and feature shape itself. We have used scanning tunneling microscopy (STM) on printed DNA patterns to realistically assess their size. (Figure 3.4) However, it should also be noted that STM images suffer from 'combing' effects which is the rough alignment of DNA molecules in

the fast scanning direction of the STM tip; hence the feature size was estimated from the direction that is perpendicular to the scanning direction. As demonstrated in Figure 3.4, we have printed 14± 2 nm sized features. A rough calculation was carried out to estimate the number of DNA strands in those features: the diameter of the DNA helix was taken as 1 nm; *[11]* and the maximum number of DNA strands per feature was calculated as ~50 (ratio of r^2s).This calculation was made under the assumption that the DNA is close-packed hence should be fully extended; however in fully extended length the DNA features should be ~17 nm for a 50-mer DNA *[12]* as opposed to 1-2 nm height of our printed features. We suggest that the printed DNA is lying flat on the secondary substrate and is not closed packed; thus the number of DNA strands should be much less than 50. This result, to the best of our knowledge is the best soft-material-printing resolution and comparable to the best hard material results. *[13]*

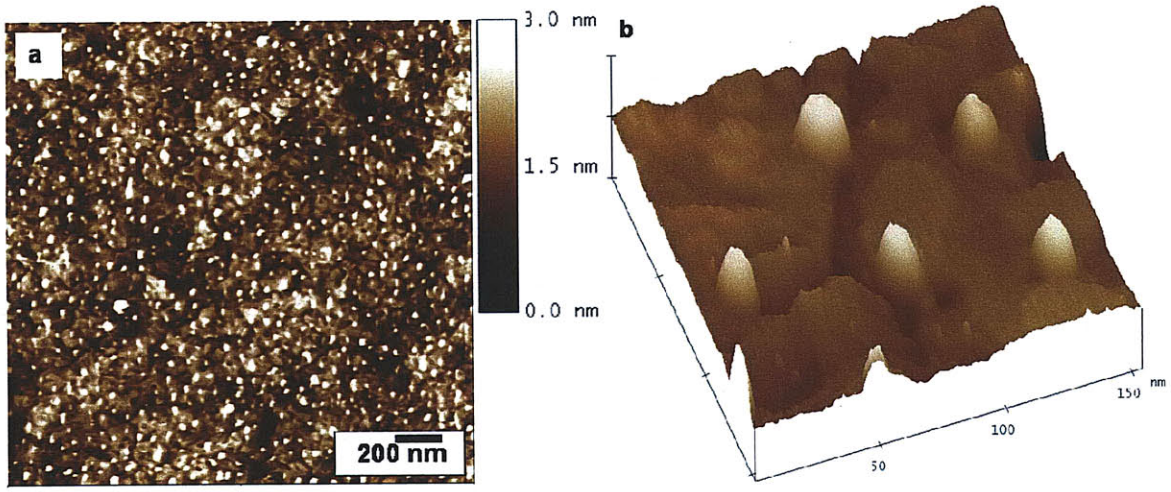

Figure 3.4: STM height image of the printed pattern a) 2μm × 2μm, b) 150 nm × 150 nm.

3.5 Detection of Hybridization

As pointed out earlier, apart from the challenge to fabricate dense arrays, one should devise a detection scheme to monitor hybridization on such an array. To achieve this, we first treated the printed substrate with MH; the AFM images did not exhibit a height increase (1.09± 0.33 to 0.99± 0.24) due to this passivation. Thereafter, printed 50-mer DNA features were hybridized with their complementary 50-mer DNA and 0.36 nm height increase was detected (1.09 ± 0.33 to 1.46± 0.40 nm). (Figure 3.5a) A t-test analysis showed that this result was significant at the 0.01 level. When the substrate was treated with a noncomplementary 50-mer DNA solution, the height increase was not statistically significant at the 0.01 level (significant at only 0.7 level, the height averages were 1.65±0.38 and 1.69±0.39 nm for printed pattern and "hybridized" pattern respectively). (Figure 3.5b)

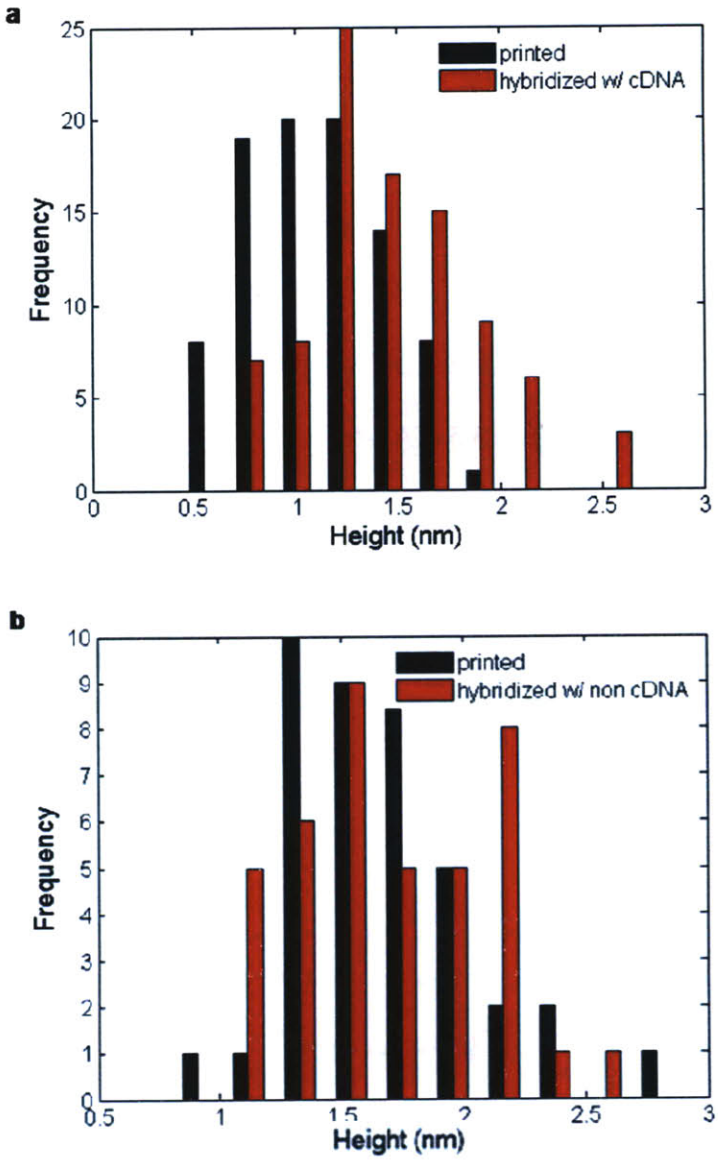

Figure 3.5: Height histogram of a) printed pattern and hybridized pattern with complementary 50-mer DNA, b) printed pattern and 'hybridized' pattern with non-complementary 50-mer DNA.

To have a more pronounced height increase, the printed DNA features was exposed to a solution of a 100-mer DNA having the first half of its sequence complementary to the one on the array. The average height of the printed DNA was 2.08± 0.57 nm and the average height of the hybridized pattern was 4.17± 0.82 nm. The comparative histogram is demonstrated in Figure 3.6a; a t-test reveals the heights are significantly different at the 0.01 level. By contrast, there

was no statistical height increase when the 'hybridization' was carried out with 100-mer noncomplementary DNA as demonstrated in Figure 3.6b (the average heights were 1.98± 0.36 and 1.98± 0.40 nm for the printed pattern and hybridized pattern, respectively).

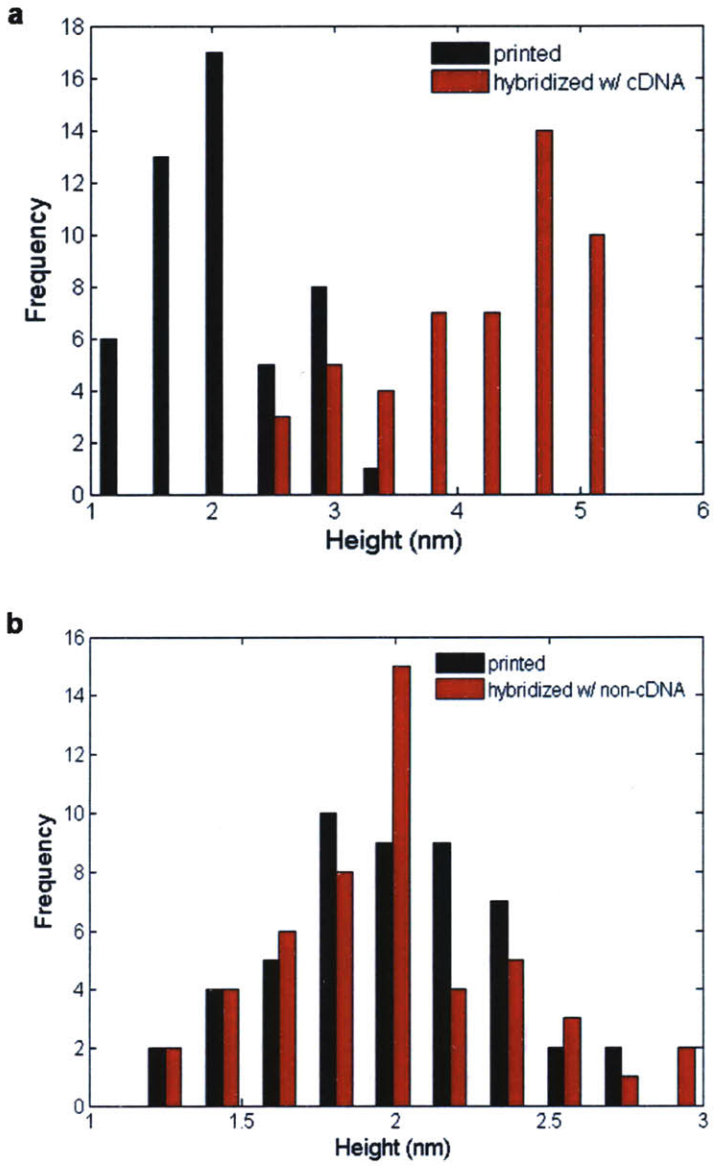

Figure 3.6: Height histogram of a) printed pattern and hybridized pattern with complementary 100-mer DNA, b) printed pattern and 'hybridized' pattern with non-complementary 100-mer DNA.

In addition to detect hybridization at nanoscale, using AFM has the advantage of being label free. However, we speculate that using DNA with a bulky end group such as streptavidin can further enhance the height increase resulting in easier detection. Here, we proposed AFM as a detection tool for nanoarrays and proved our hypothesis with a statistical method. Considering statistical analysis should involve several measurements and for the sake of argument if we should have 25 dots to carry the analysis on, currently the resolution of our approach is on the order of 400 nm. A better resolution can be achieved if one can find a system without the overlap of height distributions of the printed pattern and the hybridized pattern or exactly track the same dot during the process.

3.6 References

[1] M. J. Heller, *Annual Reviews of Biomedical Engineering* **2002**, *4*, 129.
[2] K. Salaita, Y. Wang, C. A. Mirkin, *Nature Nanotechnology* **2007**, *2*, 145.
[3] A. A. Yu, T. Savas, S. Cabrini, E. diFabrizio, H. I. Smith, F. Stellacci, *Journal of American Chemical Society* **2005**, *127*, 16774.
[4] O. Akbulut, J.-M. Jung, R. D. Bennett, Y. Hu, H.-T. Jung, R. E. Cohen, A. M. Mayes, F. Stellacci, *Nano Letters* **2007**, *7*, 3493.
[5] K.-B. Lee, E.-Y. Kim, C. A. Mirkin, S. M. Wolinsky, *Nano Letters* **2004**, *4*, 1869.
[6] A. K. Sinensky, A. M. Belcher, *Nature Nanotechnology* **2007**, *2*, 653.
[7] J. P. Spatz, S. Mossmer, C. Hartmann, M. Moller, T. Herzog, M. Krieger, H. G. Boyen, P. Ziemann, B. Kabius, *Langmuir* **2000**, *16*, 407.
[8] R. D. Bennett, A. C. Miller, N. T. Kohen, P.T.Hammond, D. J. Irvine, R. E. Cohen, *Macromolecules* **2005**, *38*, 10728.
[9] J. Q. Lu, S. Yu, *Langmuir* **2006**, *22*, 3951.
[10] T. M. Herne, M. J. Tarlov, *Journal of American Chemical Society* **1997**, *119*, 8916.
[11] L. Stryer, *Biochemistry*, W.H. Freeman & Company, New York **1995**.
[12] A. A. Yu, T. A. Savas, G. S. Taylor, A. Guiseppe-Elie, H. I. Smith, F. Stellacci, *Nano Letters* **2005**, *5*, 1061.
[13] B. D. Gates, Q. Xu, M. Stewart, D. Ryan, C. G. Willson, G. M. Whitesides, *Chemical Reviews* **2005**, *105*, 1171.

Chapter 4 Application of Liquid Supramolecular Nanostamping (LiSuNS) to Peptide and DNA/Peptide Features

This chapter was written in part with 'Supramolecular Replication of Peptide and DNA Patterned Arrays' by Anna Laromaine, Ozge Akbulut*, Francesco Stellacci and Molly M. Stevens, accepted for publication in Journal of Materials Chemistry.*

** marks equal contribution*

4.1 Introduction

As described earlier, DNA arrays have been proven to be indispensible for biomedicine. *[1]* Recently, protein arrays have also been under focus due to promising applications in biomarker detection, and elucidation of genomic and proteomic pathways and networks. *[2-4]* Proteins by their nature are more fragile than DNA; hence fabrication of protein arrays is more challenging, namely immobilizing proteins on specific locations on a substrate does not guarantee their activity (folding and function) will be preserved. *[4-6]* Nevertheless, protein arrays can be produced by a subset of DNA array fabrication methods such as spotting. *[6, 7]* DNA array fabrication methods based on new approaches (mostly based on *in-situ* synthesis) are emerging, whereas alternative approaches for the fabrication of protein arrays or mixed arrays are in their infancy. The most promising studies to synthesize proteins *in-situ* utilize pre-arrayed DNA or messenger RNA (mRNA). *[5]* Recently, by means of pre-arrayed DNA Taussig group presented printing proteins repeatedly. *[8]* The method is named, DAPA (DNA Array to Protein Array), and involves a slide bearing DNA features which can encode the desired proteins. (Figure 4.1) This slide is brought into contact with a secondary slide with a permeable membrane incorporating cell extracts (lysates) containing all the essential elements for transcription and

translation. Lysates performs the transcription and translation and the newly synthesized proteins diffuse through the membrane and are immobilized on the secondary slide. The authors reported fabrication of a protein array with 500 μm feature size and 1 mm spacing.

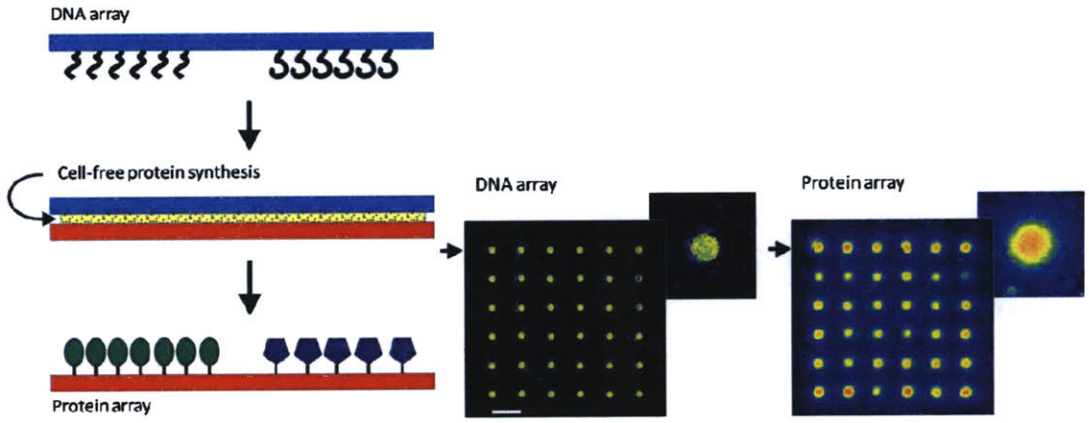

Figure 4.1: Schematic illustration of the DAPA method, (middle) DNA array, template for the protein synthesis, (right) protein array synthesized from the DNA array in the middle. (scale bar 1 mm)

Another newly suggested *in-situ* synthesis method for peptides involves the use of an elastomeric stamp inked with a single aminoacid to force the bond formation between the Boc-protected aminoacid and the reactive (with an amine group) self assembled monolayers. *[9]* This amide bond formation doesn't require any catalyst, long reaction times or high temperatures but only depend on the nanoscale confinement of molecules. The authors also reported the synthesis of a tripeptide (RGD, arginine-glycine-aspartate) on a reactive surface by consequentially printing the Boc-protected peptides. The proof of synthesis was carried out by cell attachment studies. (Figure 4.2)

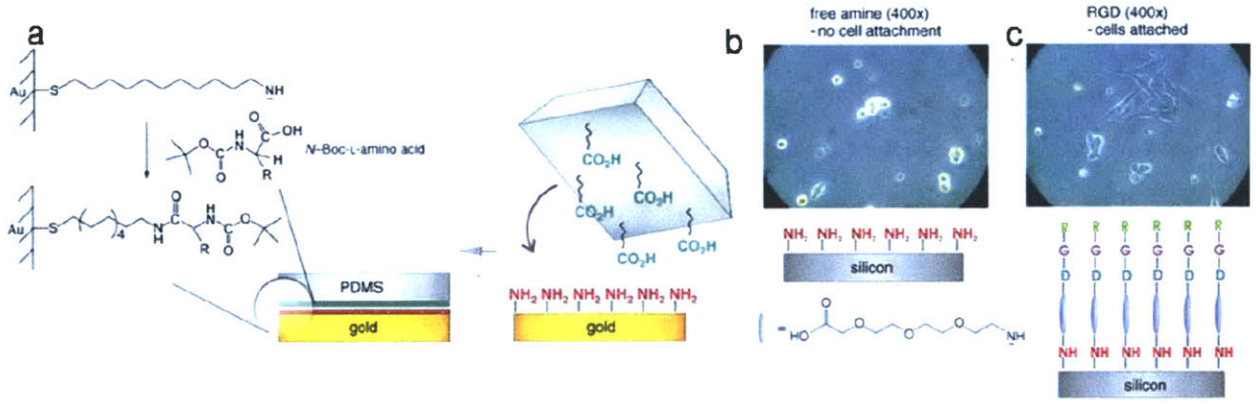

Figure 4.2: a) Schematic illustration of printing a Boc-protected amino acid onto a reactive amine SAM. A plasma-oxidized flat PDMS stamp inked with an N-Boc-l-amino acid is pressed into contact with an amine monolayer on gold. After the stamp is released, the surface is washed to remove non-covalently bound molecules. Optical micrograms demonstrating cell growth on an RGD surface: b) On amine surfaces, the cells are still round and not stretched indicating the absence of proteins; c) cells are attached and stretched in the presence of the tripeptide RGD on the surface. *[9]*

I believe that recent *in-situ* synthesis methods are pivotal in protein array research; yet since they are synthesized by DNA-fragments the inital pre-arraying of DNA is still an issue and multiplexing is another challange as well. Supramolecular Nanostamping (SuNS), as described in Chapter 2, is a modified αcp technique (Chapter 1) which depends on the reversible bond formation between two complementary DNA strands. In this respect, we have long believed that any biomolecule-couple exhibiting this type of bond formation is printable through SuNS. In this chapter, I will present the supramolecular replication of peptide and DNA/peptide features through Liquid Supramolecular Nanostamping (LiSuNS). (Scheme 4.1)

Scheme 4.1. Schematic illustration of Liquid Supramolecular Nanostamping (LiSuNS)

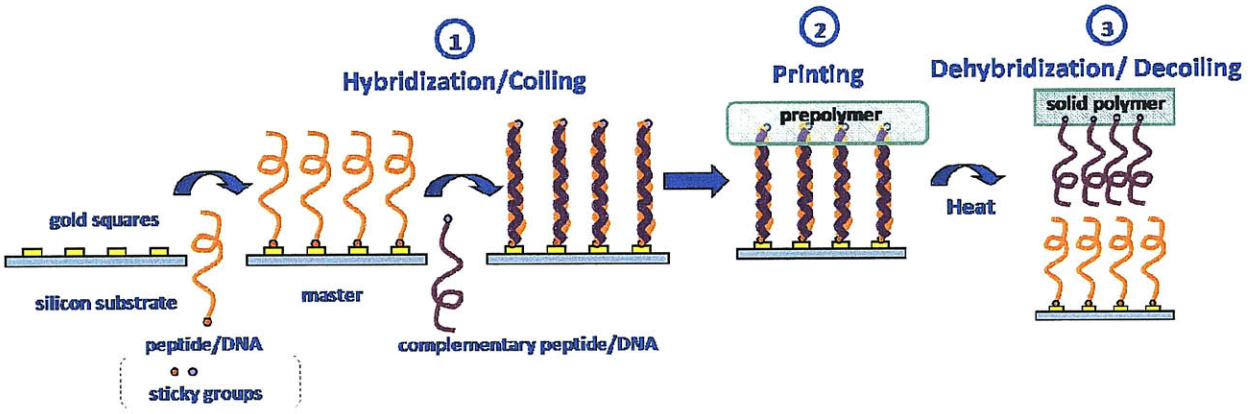

4.2 Background Information on Coiled-coil Peptides

We have employed coiled-coil peptides which is a common and well-studied folding motif in proteins and it is treated analogously to DNA structure. *[10-15]* The α-helical coiled-coil motif is an oligomerization domain present in many cytoskeletal proteins, transcription factors, motor proteins, or viral proteins, amongst others. *[16-18]* The α-helical peptides are wrapped together like the strands of a rope to structure the coiled-coil motif. This secondary structure is formed due to a series of heptads amino acids repeats $(a\text{-}b\text{-}c\text{-}d\text{-}e\text{-}f\text{-}g)_n$ in each helix. Hydrophobic amino acids (a/d) stabilize the motif and polar residues at e/g positions give specificity between the two helices through electrostatic interactions. This molecular recognition does not involve formation or rearranging of a peptide bond thus allowing the system to be reversible. The applications of coiled-coil motifs include biosensors, *[19-21]* directed assembly of extracellular receptor domains, *[22]* stabilization of antibody fragments, *[23]*; the use of coiled-coil peptides in drug delivery was also suggested. *[24]* The sequence of the heterodimeric coiled-coil used here was initially reported by Hodges *et al.[25]* and has been slightly modified to introduce a terminal thiol group and a

tri-glycine spacer to each of the complementary peptides **E** and **K** (Figure 4.3a). **E** and **K** heterodimerisation was assessed using Circular Dichroism (CD), Figure 1b. Solid line in CD spectra shows an α-helical structure with characteristic minima at 208 and 222nm for **K+E**, whereas homopeptides (**E** or **K**) exhibit a random coil structure (dashed and circle line in Figure 4.3b).

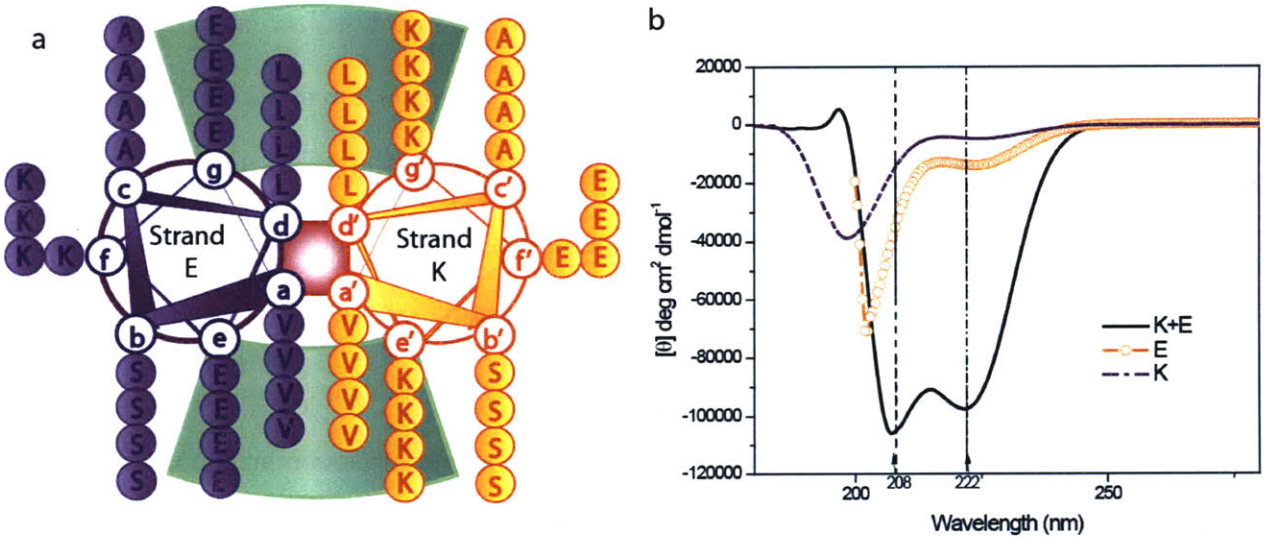

Figure 4.3: a) Helical wheel projection, looking down the axes of the helices of the dimerization domain of the coiled-coil peptides used in this work. Heptad positions are labelled *a* to *g* for Strand **E** and *a'* to *g'* for Strand **K**. Residues *e/g'(-1)* and *g(-1)/e'* participate in the interhelical electrostatic interactions, residues a/a' and *d/d'* contribute in the stabilization by hydrophobic interactions. b) Circular dichroism spectra of single stranded peptides **K** and **E** and the heterodimeric coiled coil peptide **K/E**.

4.3 Printing Coiled-coil Peptides via LiSuNS

The LiSuNS steps were applied to a coiled-coil peptide master as outlined in Scheme 4.1. As explained in the introduction, a challenging issue for peptide arrays is to preserve the functionality of the printed peptides. Therefore, the first step to prove successful printing was to show the printed peptide only form coiled-coil structure with its complementary sequence. An array of 10 μm × 10 μm gold squares on a silicon wafer were utilized and immersed in a solution of peptide **K** in phosphate buffered saline (PBS) to allow the peptides to bond on the gold features through their terminal thiol groups. After thorough washing in PBS and deionized (DI) water, this substrate was treated with 6-mercapto-1-hexanol (MH) solution to minimize non-specific adsorption. Hereafter, the **K**-functionalized and passivated substrate is referred to as the 'master'. For complementary peptide coiling, analogous to DNA-hybridization, the master was incubated in a solution of the complementary peptide **E** for 12 hours. A poly(dimethyl siloxane) (PDMS) prepolymer solution was prepared by mixing the silicon elastomer and curing agent with a weight ratio of 10:1. This mixture and the coiled master were allowed to settle for 1 h in an environmental chamber with 35% humidity to spontaneously remove any trapped air bubbles. *[26]* Thereafter, the prepolymer mixture was poured into the Petri dish containing the coiled master and cured for 1.5 hours at 60 °C. The cured and hardened PDMS (i.e. the secondary substrate) was separated from the master by mechanical force and treated with a solution of fluorescent complementary printed peptide **K** sequence in PBS for 3 hours as depicted in Figure 4.4a. After washing with DI water, fluorescence microscopy of the substrate revealed that the peptide **K** array had been accurately replicated by LiSuNS (Figure 4.4b). When the same experiment was carried out with a fluorescent non-complementary sequence, no pattern was observed.

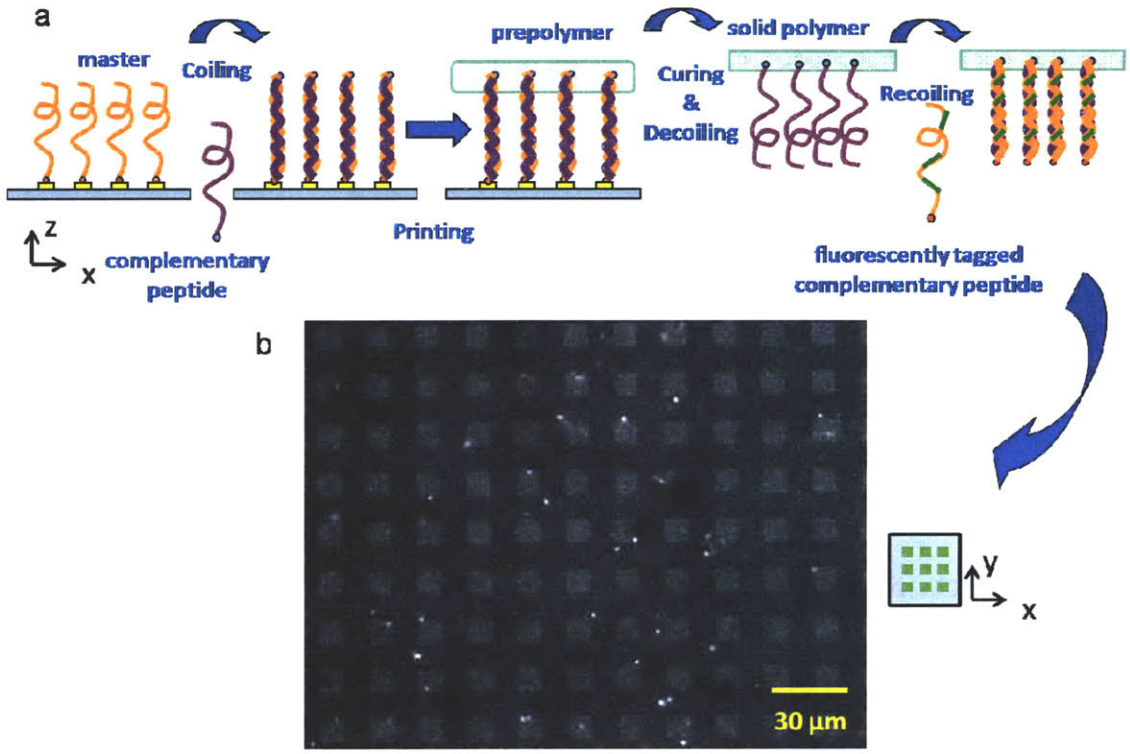

Figure 4.4: a) Schematic illustration of LiSuNS and subsequent hybridization of the printed pattern with the complementary fluorescent peptide b) Fluorescence micrograph of the PDMS secondary substrate with the peptide sequence **K** printed and labelled with the complementary fluorescent peptide **E**.

To ensure the integrity of the master after printing, we repeated the printing cycle with the same master as illustrated in Figure 4.5a. The peptide **K** functionalized master was incubated with complementary fluorescent peptide **E** and this peptide was transferred to the PDMS secondary substrate enabling immediate assessment by fluorescence microscopy. (similar to Method 2 of DNA-SuNS in Chapter 2) Fluorescence microscopy of printed arrays generated from a first printing cycle and repeated printing cycles (where the same master was re-incubated in peptide **E**) is shown in Figure 4.5b and 4.5c. No significant loss in fluorescence intensity was observed confirming the functional robustness of the master for multiple printing cycles (e.g. 5 print runs) Figure 4.6.

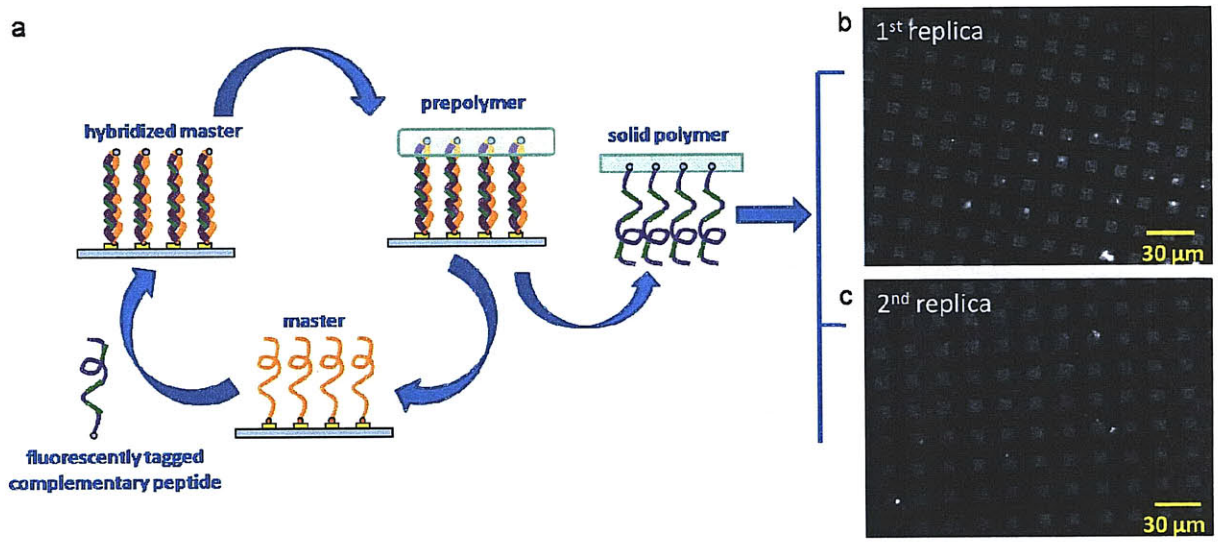

Figure 4.5: a) Schematic illustration of repeated printing cycles, b) The printed pattern from the 1st printing cycle, c) The printed pattern from the 2nd printing cycle.

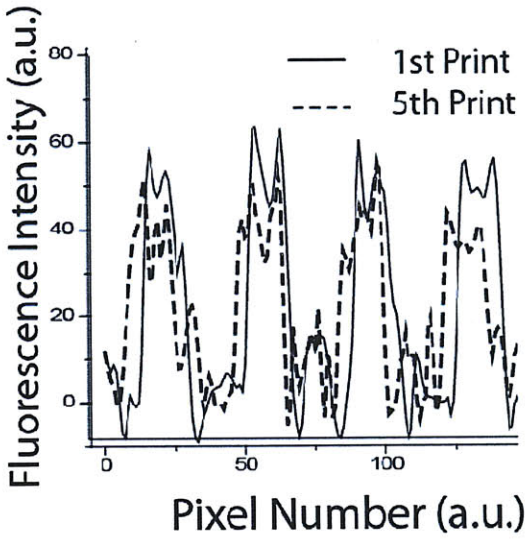

Figure 4.6: Comparison of fluorescence intensities of the printed patterns after the 1st and 5th printing cycles.

The integrity of the master also depends on the intactness of the initial sequence; namely the initial sequence shouldn't transfer to the secondary substrate. To prove the initial sequence stays on the master during printing, the gold square array was immersed in a solution of

fluorescently tagged initial sequence and without being treated with the complementary sequence; it was printed onto the PDMS substrate. After hardening and lift off, no pattern was observed on the PDMS substrate proving the initial sequence stays on the gold pattern during printing.

4.4 Printing Coiled-coil Peptide/DNA Features

As explained earlier, LiSuNS has the ability to print spatial as well as chemical information: that is this technique not only transfers the shape, size and the position of the features on the master (spatial information), but also their chemical nature (chemical information). The potential use in the transfer of multiplexed nucleic acid and protein based chemical information in one cycle is a tantalizing goal. Thus, the multiplexing capability to print a substrate containing DNA and peptide features in one cycle was also explored. A master was fabricated by using a microfluidic approach and peptide **K** and a single stranded thiolated DNA were immobilized on a gold slide as illustrated in Figure 4.7a. The master was passivated with mercaptohexanol (MH) and was treated with its complementary peptide **E** and complementary DNA sequence terminated with an acryl group sequentially. The PDMS prepolymer was poured into the Petri dish containing this coiled/hybridized master. After curing, the hardened PDMS polymer was mechanically separated from the master. The printed secondary substrate was then incubated in complementary fluorescent DNA and NHS-Fluorescein, which is a marker for primary amines, and imaged with fluorescence microscopy. Figure 4.7b shows a successful replication of the original patterns of DNA and peptide. When the hybridization step was carried out with a fluorescent non-complementary DNA sequence, no pattern was observed.

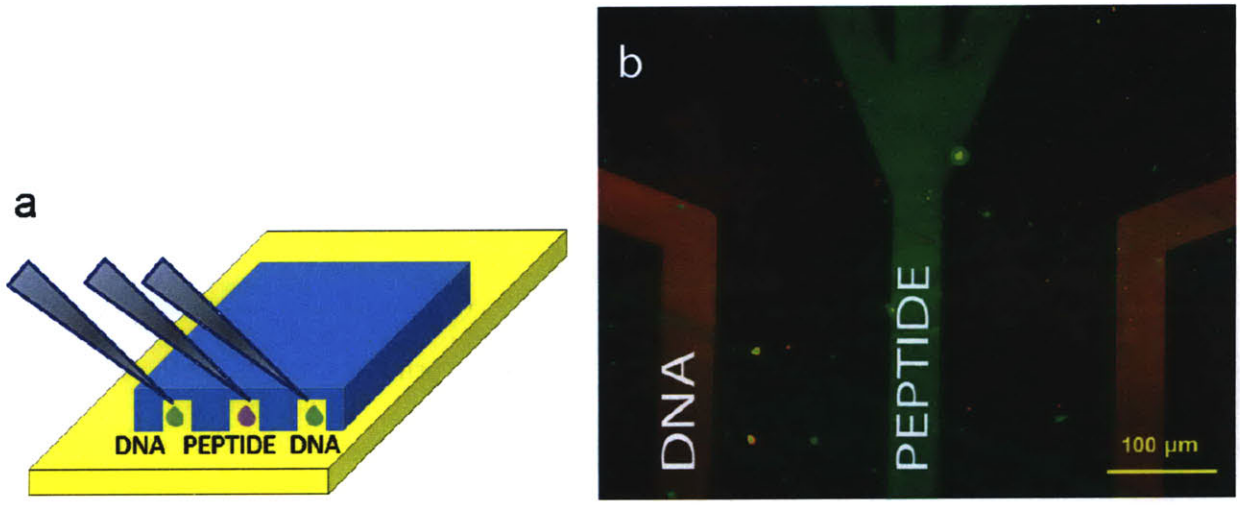

Figure 4.7: Multiplexed LiSuNS of peptide and DNA patterned array. a) Schematic illustration the micro fluidic channels used for master preparation, b) Fluorescence micrograph of printed peptide and DNA lines with false colour overlay.

This result, to the best of my knowledge, is the first time demonstration of DNA/peptide printing in a single step underlining the multiplexing capability of LiSuNS. Additionally, we believe that this work lays the foundation for the use of SuNS and LiSuNS with complex biomolecules leading to the fabrication of surfaces and devices that go beyond microarrays.

4.5 References

[1] M. Dufva, *Biomolecular Engineering* **2005**, *22*, 173.
[2] S. F. Kingsmore, *Nature Reviews Drug Discovery* **2006**, *5*, 310.
[3] C. Wingren, C. A. K. Borrebaeck, *Drug Discovery Today* **2007**, *112*, 813.
[4] M. J. Taussig, *Comperative and Functional Genomics* **2001**, *2*, 298.
[5] M. He, O. Stoevesandt, M. J. Taussig, *Current Opinion in Biotechnology* **2008**, *19*, 4.
[6] F. G. Zaugg, P. Wagner, *MRS Bulletin* **2003**, *28*, 837.
[7] G. MacBeath, S. L. Schreiber, *Science* **2000**, *289*, 1760.
[8] M. He, O. Stoevesandt, E. A. Palmer, F. Khan, O. Ericsson, M. J. Taussig, *Nature Methods* **2008**, *5*, 175.

[9] T. P. Sullivan, M. L. v. Poll, P. Y. W. Dankers, W. T. S. Huck, *Angewandte Chemie International Edition* **2004**, *43*, 4190.
[10] A. Lupas, *Trends in Biochemical Sciences* **1996**, *21*, 375.
[11] W. D. Kohn, R. S. Hodges, *Trends in Biotechnology* **1998**, *16*, 379.
[12] E. H. C. Bromley, R. B. Sessions, A. R. Thomson, D. N. Woolfson, *Journal of American Chemical Society* **2009**, *131*, 928.
[13] R. Y. Sweeney, E. Y. Park, B. L. Iverson, G. Georgiou, *Biotechnology and Bioengineering* **2006**, *95*, 539.
[14] J. M. Mason, K. M. Muller, K. M. Arndt, *Biochemistry* **2007**, *46*, 4804.
[15] M. O. Steinmetz, I. Jelesarov, W. M. Matousek, S. Honnappa, W. Jahnke, J. H. Missimer, S. Frank, A. T. Alexandrescu, R. A. Kammerer, *Proceedings of National Academy and Sciences* **2007**, *104*, 7062.
[16] P. Burkhard, J. Stetefeld, S. V. Strelkov, *Trends in Cell Biology* **2002**, *11*, 82.
[17] J. R. Beasley, M. H. Hecht, *Journal of Biological Chemistry* **1997**, *272*, 2031.
[18] D. A. D. Parry, R. D. B. Fraser, J. M. Squire, *Journal of Structural Biology* **2008**, *163*, 258.
[19] S. M. Lu, R. S. Hodges, *Journal of Biological Chemistry* **2002**, *277*, 23515.
[20] B. Catimel, M. C. Faux, M. Nerrie, J.Rothacker, L. J. Otvos, J. D. Wade, E. C. Nice, A. W. Burgess, *Journal of Peptide Research* **2001**, *58*, 493.
[21] B. Tripet, L. Yu, D. L.vBautista, W. Y. Wong, R. T. Irvin, R. S. Hodges, *Protein Engineering* **1996**, *9*, 1029.
[22] S. N. Behncken, N. Billestrup, R. Brown, J. Amstrup, B. Conway-Campbell, M. J. Waters, *Journal of Biological Chemistry* **2000**, *275*, 17000.
[23] K. M. Arndt, K. M. Muller, A. Pluckthun, *Journal of Molecular Biology* **2001**, *312*, 221.
[24] Y. B. Yu, *Advanced Drug Delivery Reviews* **2002**, *54*, 1113.
[25] J. R. Litowski, R. S. Hodges, *Journal of Peptide Research* **2001**, *58*, 477.
[26] A. A. Yu, F. Stellacci, *Advanced Materials* **2007**, *19*, 4338.

Chapter 5 Utilizing Polyelectrolyte Multilayers (PEMs) as Secondary Substrates

5.1 Introduction

Since their introduction by Decher and coworkers, *[1]* there has been extensive research on polyelectrolyte multilayers (PEMs) *[2, 3]* due to their potential applications in biomedicine, *[4, 5]* fuel cells/electrochemistry, *[6-8]* and coatings of various properties. *[9, 10]* PEMs are fabricated by layer-by-layer (LbL) assembly which relies on alternative electrostatic adsorption of polymers with opposite charges as shown in Scheme 5.1. The fabrication process is rather tunable; by varying the pH of the deposition solution, the interpenetration between the layers, bilayer composition, surface charge and layer thickness can be varied. *[11-13]* This ease and versatility of fabrication which gives a wide room for control over the structure, as well as compatibility with biomolecules, make PEMs target substrates for biomedical applications*[4]* such as drug delivery*[14]* and bioactive coatings. *[15]* DNA *[16, 17]* and peptides *[18, 19]* can also be utilized as layers in these multilayer systems due to their charged nature. In addition, controlled release of DNA layer can also be achieved in physiological conditions *[20]* or enzymatically. *[21]* The interaction, in terms of adsorption, between biomolecules such as proteins *[22, 23]* and PEMs is widely studied as well.

Scheme 5.1. Fabrication of Polyelectrolyte Multilayers *[5]*

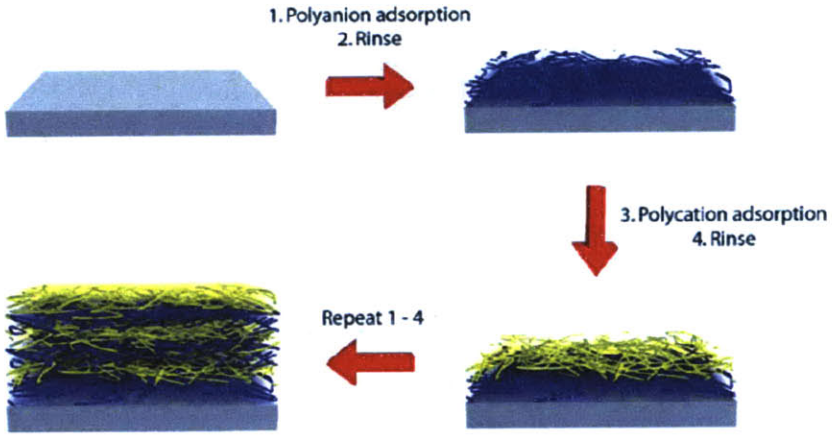

PEMs are also utilized as biomolecule immobilization platforms. Zhou *et al.* spotted DNA onto anionic poly(sodium styrene sulfonate) (PSS) and cationic poly(allylamine hydrochloride) (PAAH) bilayers (positively charged PAAH being the outermost layer). *[24]* The authors compared their results with commercially available aldehyde-modified slides and poly(L-lysine) (PLL)-coated slides and reported higher binding capacity and better hybridization efficiency than those. The same group also carried out a similar study with proteins, by using anionic poly(vinylsulfonic acid, sodium salt) solution (PVS) and PAAH (the outermost layer), they demonstrated PEMs has higher sensitivity compared to aldehyde-modified slides and PLL-coated slides. *[25]* To my knowledge, the confirmation of DNA on negatively charged surfaces and its hybridization behavior have not been studied. However, there is one report on covalently attaching proteins to the carboxylic acid groups of poly(acrylic acid) (PAA) in a PEM system of polyacrylic acid and protonated poly(allyl amine) (PAH). *[26]* The authors found these films to be extremely resistant to non-specific protein adsorption, such that even a blocking step is not necessary.

Current DNA immobilization platforms include silanized glass (amine or aldehyde terminated) and polymeric substrates. *[27]* Through SuNS, we have successfully print DNA onto gold, *[28]* PDMS, *[29]* PMMA *[15]* and poly(4-formyl-*p*-xylylene-*co*-*p*-xylylene). *[30]* However, we believe that there is an ample room for improvement regarding to the secondary substrates; for instance, in theory by tuning the charge density of a secondary substrate the hybridization efficiency hence the signal strength can be increased. In general, positively charged surfaces are utilized to immobilize DNA (for non-covalent interactions) with the assumption that negatively charged DNA will be better attached to these surfaces. However, if DNA can be immobilized on a negatively charged substrate, the molecular backbone won't be sticking to the substrate thus preferring a more 'stand up' confirmation and DNA in this position should be more accessible by its complementary DNA molecule. In addition, during the hybridization step, there is a possibility that the complementary DNA would not be attracted to the negatively charged substrate resulting in less non-specific binding. Therefore, there is a possibility that negatively charged surfaces in fact should serve as better immobilizing platforms than their positively charged counterparts.

In this chapter, I will report our efforts to utilize PEMs as a secondary substrate, namely printing DNA onto PEMs and assessing the hybridization efficiency and printing coverage. We tested the hypothesis above by using PAA/PAH films on glass, with both PAA on top (negatively charged) and PAH on top (positively charged).

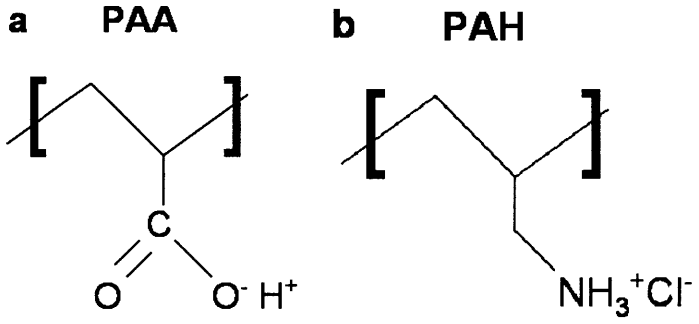

Figure 5.1: Chemical structures of PAA and PAH.

5.2 Printing onto PAA-on-top PEMs

The PEMs, PAA (7.5)/PAH (3.5) (20 bilayers) on glass, were supplied by the Rubner Group (courtesy of Dr. Jennifer Lichter). This combination was selected due to the large number of carboxylic acid groups available on the surface determined by visually assessing the methylene blue adsorption; namely dipping the PEMs into 10^{-3} M pH 7 aqueous methylene blue solution and choosing the combination with darkest shade of blue. I have used 5' hexyl thiol modified single strand DNA (HS-ssDNA) immobilized gold square pattern (10 μm × 10 μm) as the master. This optical lithography fabricated pattern was on silicon with a 5 nm titanium adhesion layer. The master was treated with mercaptohexanol for 1 hour prior to hybridization. I have used 5' amine modified complementary DNA which also had Rhodamine Green (Excitation:504, Emission:531) modification on 3' end (to enable immediate assessment of the printed pattern, described as 'Method 2' in Chapter 2), I will refer this DNA as NH_2-cDNA-RhoG.

Immediately before contact, PAA (7.5)/PAH (3.5) film was dipped into pH 7 DI water (pH adjusted by dilute NaOH solution) for 30 seconds to ionize the carboxylic acid groups and blow dried. The hybridized master and the PEMs was brought into contact and placed into a

home-built stamping machine. (Figure 5.2) The upper chunk of the machine was lowered to supply a pressure around 10 atm. The printing was carried on for 24 hours; in the first 4 hours the temperature of the chunks were increased to 45-50 °C via circulating warm water in the chunks. I believe rising the temperature leads to a better contact and consequentially larger printed areas; yet it is also possible to print without this treatment though with lower coverage. The chunks of the machine also have holes connected to a vacuum pump which can hold the samples attached to each chunk during dehybridization i.e. separation of chunks. For dehybridization, the temperature of the chunks was brought to 90 °C with circulating water and chunks were separated after 15 minutes. The substrates were washed with DI water before fluorescence microscopy imaging. The typical PAA-on-top printed substrate image is shown in Figure 5.3. Since complementary DNA has a Rhodamine Green modification; it was possible to observe printing prior to hybridization of the secondary substrate. Throughout the experiments, I have used Rhodamine Red (Excitation: 574, Emission: 594) modified complementary DNA and FITC (Excitation: 495, Emission: 520) modified complementary DNA to assess the hybridization efficiency on the secondary substrate. FITC and Rhodamine Green have similar fluorescence intensities; thus the hybridization efficiency can be directly visualized when the printed substrate is hybridized with a FITC modified complementary DNA. To have a background signal before hybridizing with Rhodamine Red-modified DNA, I have taken images under two different filters (FITC filter for Rhodamine Green and Rhodamine filter for Rhodamine Red) upon printing since the Rhodamine Green-modified DNA (the printed sequence) has some fluorescence under Rhodamine filter as well. In addition, I have carried out the same printing procedure by a mechanical vise as described for 'printing from gold nanoparticle template' in Chapter 3 and observed similar results though with lower printing coverage. I believe the pressure distribution

in the stamping machine is more even compared to a mechanical vise; hence resulting in higher coverage.

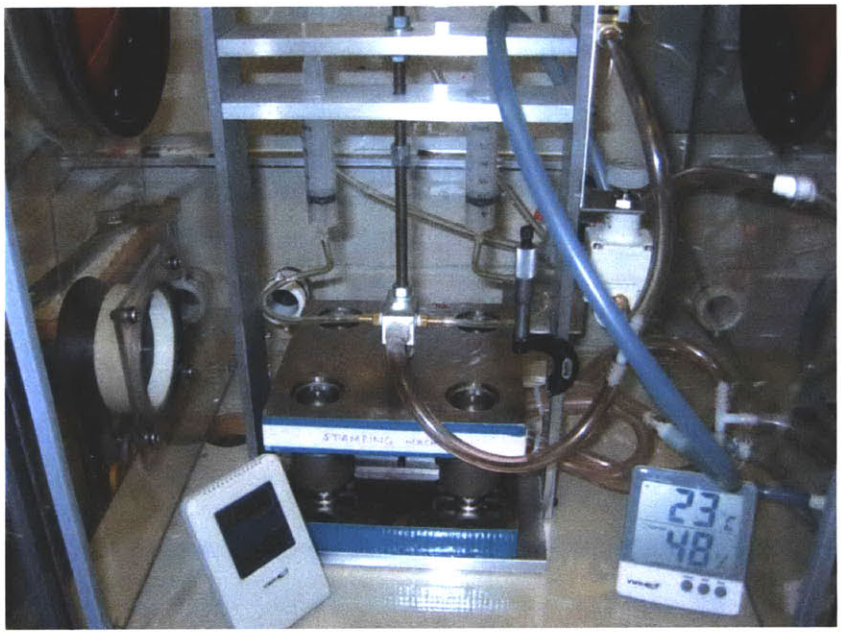

Figure 5.2: Home-built stamping machine.

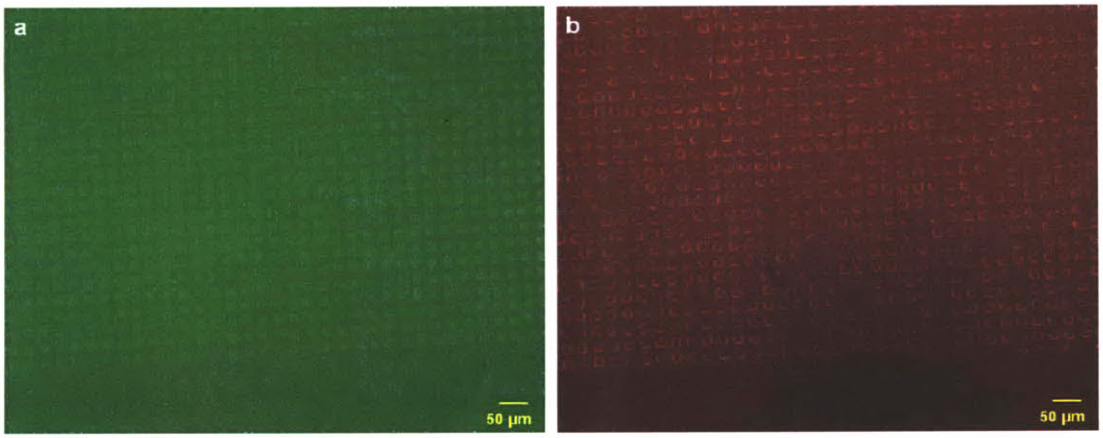

Figure 5.3: Fluorescence images of printed pattern on PAA-on-top PEMs (before hybridization) a) FITC filter, b) Rhodamine Red filter.

5.2.1 Effect of Time on Hybridization

The pieces of the same PAA-on-top sample was treated with 1 µm complementary Rhodamine-Red tagged DNA for 1 h (Figure 5.4a) and 3h (Figure 5.4b) to assess the effect of time on hybridization. The fluorescence intensities of these micrographs are shown in Figure 5.4c, the intensity has increased around 35% in those additional 2 hours.

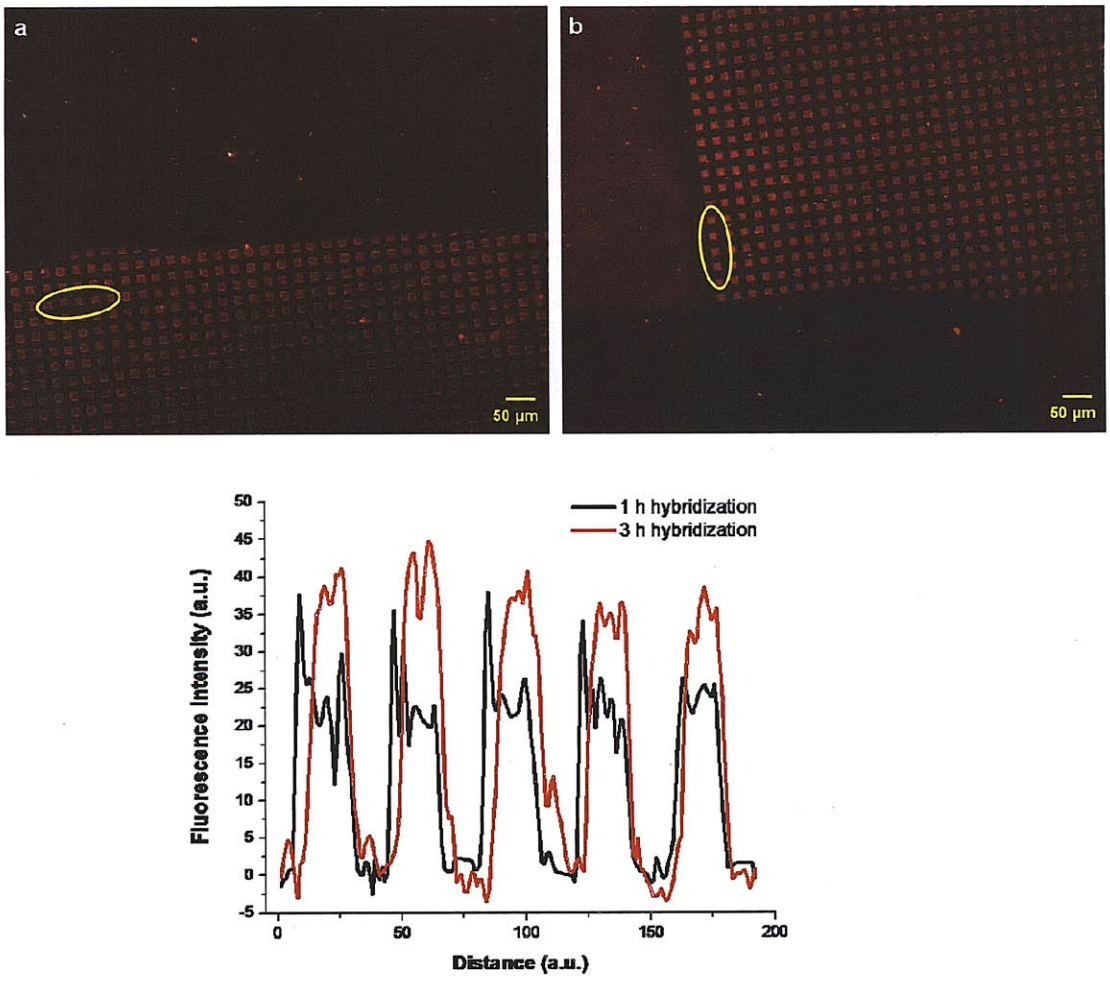

Figure 5.4: Fluorescence images of hybridized pattern on PAA-on-top sample a) 1 hour, b) 3 hours, c) fluorescence intensity measurements across the printed patterns on these samples. The intensities in 'c' are calculated across the squares enclosed by the yellow circles.

5.2.2 Concentration Limit for Detection of Hybridization

To detect the minimum concentration analyzable by fluorescence microscopy on PAA-on-top PEMs, five pieces of the same sample were treated with 1 μM, 500 nM, 100 nM, 10 nM, 5 nM complementary DNA solutions for 3 hours. The smallest concentration detectable was 10 nM and the background signal arising from the Rhodamine Green (printed DNA) has been carefully considered.

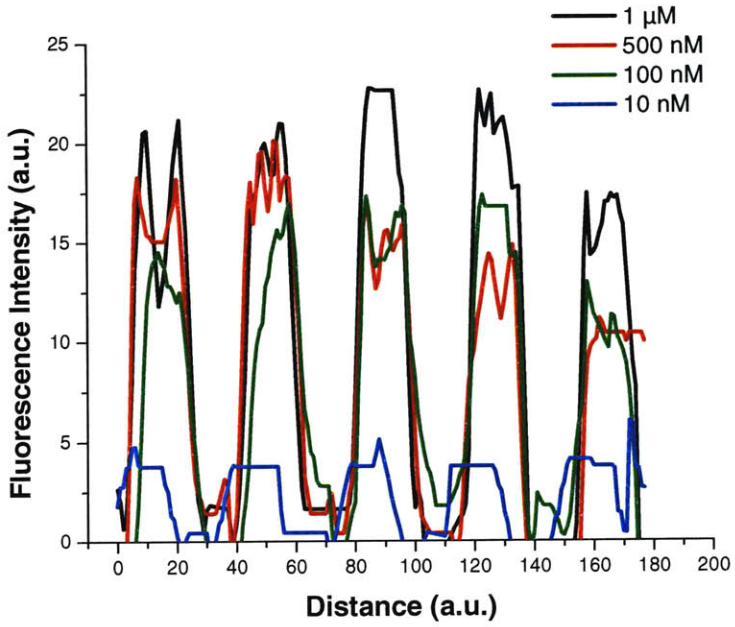

Figure 5.5: Fluorescence signal intensities at different concentrations.

5.3 Printing onto PAH-on-top PEMs

The printing was carried on PAH-on-top samples exactly by following the same procedure of printing to PAA-on-top PEMs; generic images are displayed below.

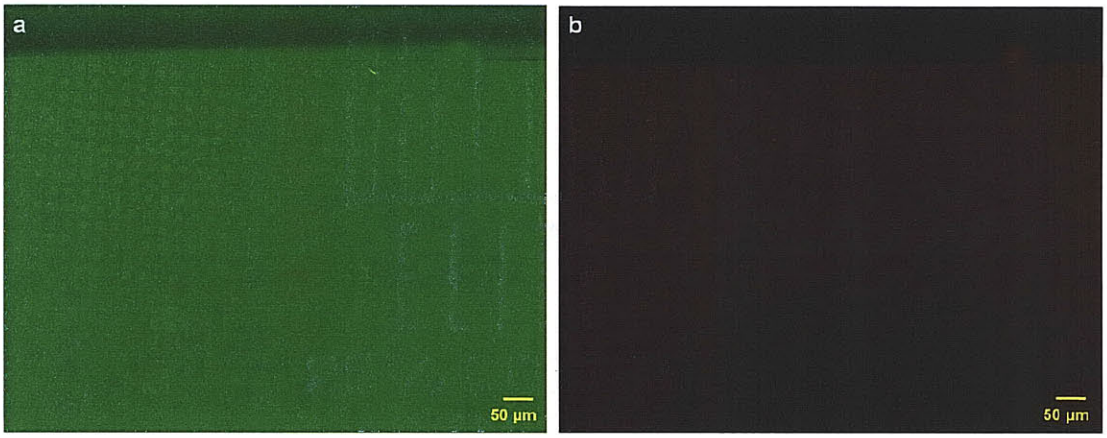

Figure 5.6: Fluorescence images of printed pattern on PAH-on-top PEMs (before hybridization) a) FITC filter, b) Rhodamine Red filter.

5.3.1 Effect of Time on Hybridization:

I treated the pieces of the same PAH-on-top sample with 1 µm complementary Rhodamine-Red tagged DNA for 1 h and 3h to figure out whether the duration of hybridization reaction effects the signal intensity or not. The fluorescence intensity didn't seem to change from 1h to 3h.

5.4 Assessment of Hybridization Efficiency

5.4.1 Hybridizing with a FITC-modified Complementary DNA

After printing onto PEMs (both onto PAA-on-top and PAH-on-top samples), the pieces of the same sample is hybridized with FITC-modified complementary DNA and Rhodamine Red-modified complementary DNA. The results for PAA-on-top and PAH-on-top samples are shown in Figure 5.7 and Figure 5.8 respectively. Figure 5.7a and Figure 5.8a were taken immediately after printing under FITC filter and demonstrate the printed NH_2-cDNA-RhoG. In Figure 5.7b and Figure 5.8b, after hybridization results are shown for PAA-on-top and PAH-on-top samples respectively. The hybridization efficiency comparison is carried out from the plot profiles. The background signal of each image is subtracted from the whole signal. The typical signal intensities are shown in Figure 5.9. Although, the initial printing signals are comparable for both PAA-on-top and PAH-on-top samples, when hybridized, the background signal in PAH-on-top sample is considerably high compared to the PAA-on-top sample.

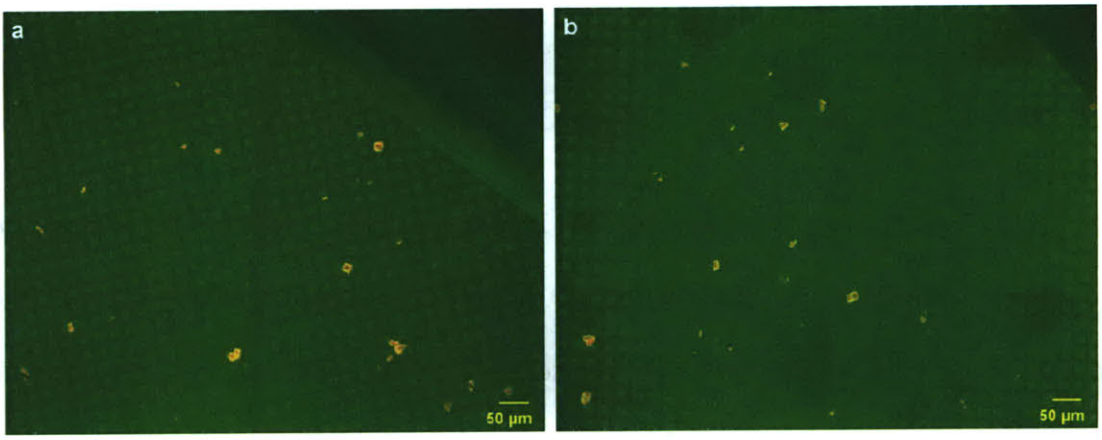

Figure 5.7: Printing and hybridization images for PAA-on-top sample a) after printing, b) after hybridization.

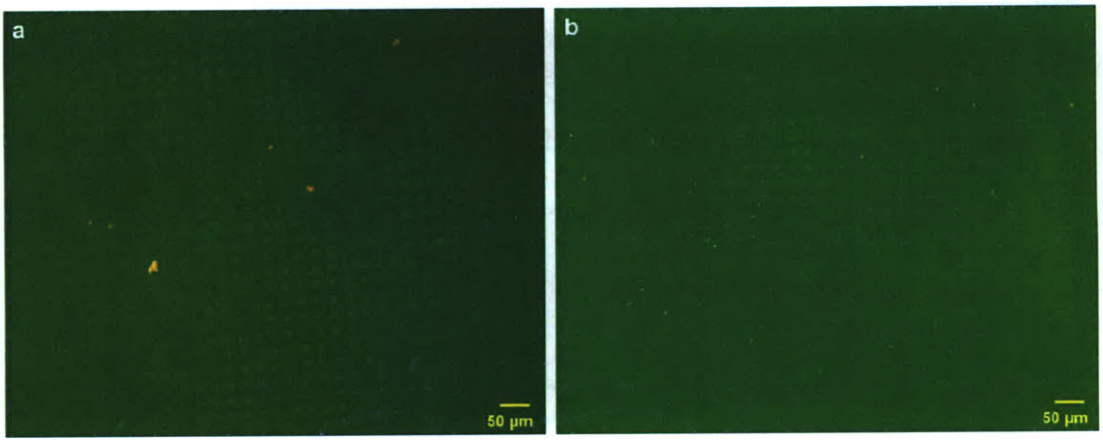

Figure 5.8: Printing and hybridization images for PAH-on-top sample a) after printing, b) after hybridization with FITC-modified complementary DNA.

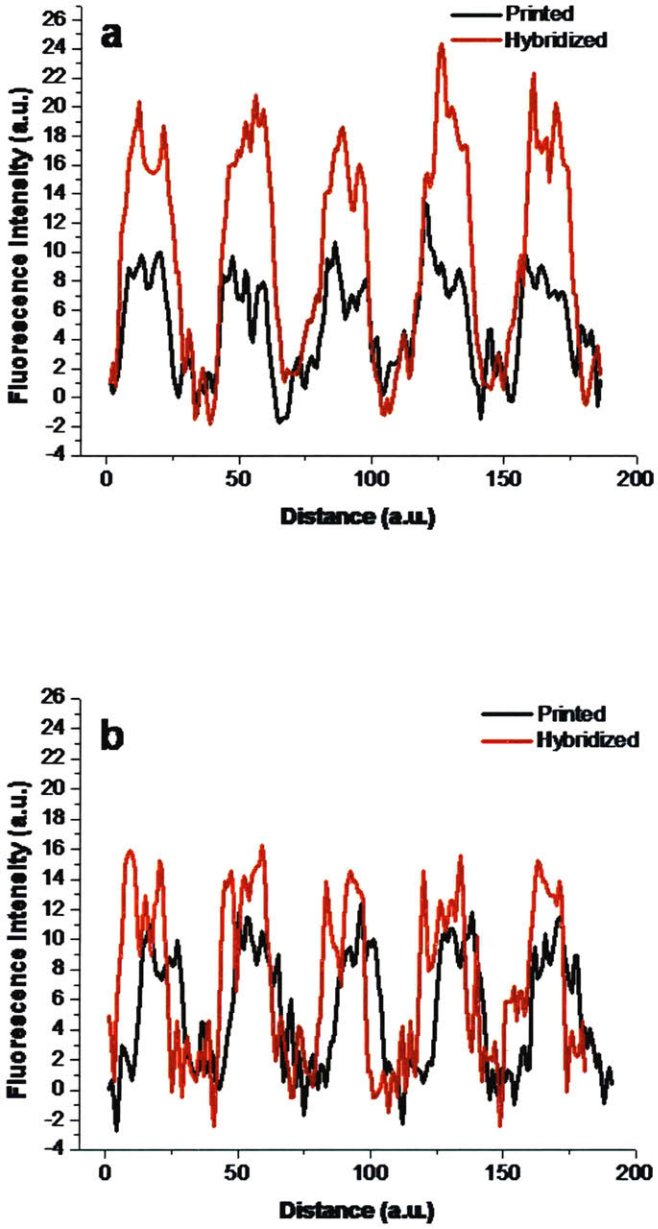

Figure 5.9: Fluorescence intensity comparison for FITC-hybridized samples a) PAA-on-top, b) PAH-on-top.

5.4.2 Hybridizing with a Rhodamine Red-modified Complementary DNA

The same procedure described above was carried out for PAA-on-top and PAH-on-top samples while hybridizing with Rhodamine Red modified complementary DNA. The typical results are shown in Figure 5.10 for PAA-on-top and Figure 5.11 for PAH-on-top samples.

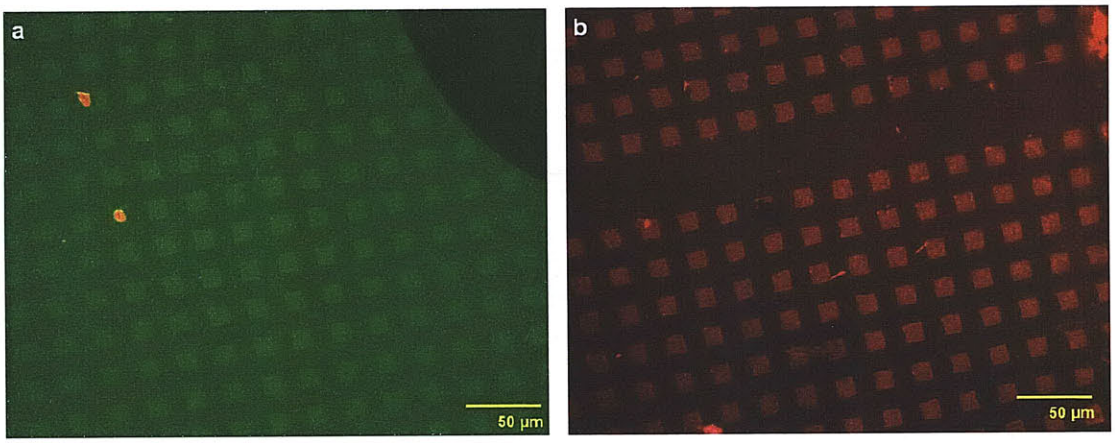

Figure 5.10: Printing and hybridization images for PAA-on-top sample a) after printing, b) after hybridization with Rhodamine Red-modified complementary DNA.

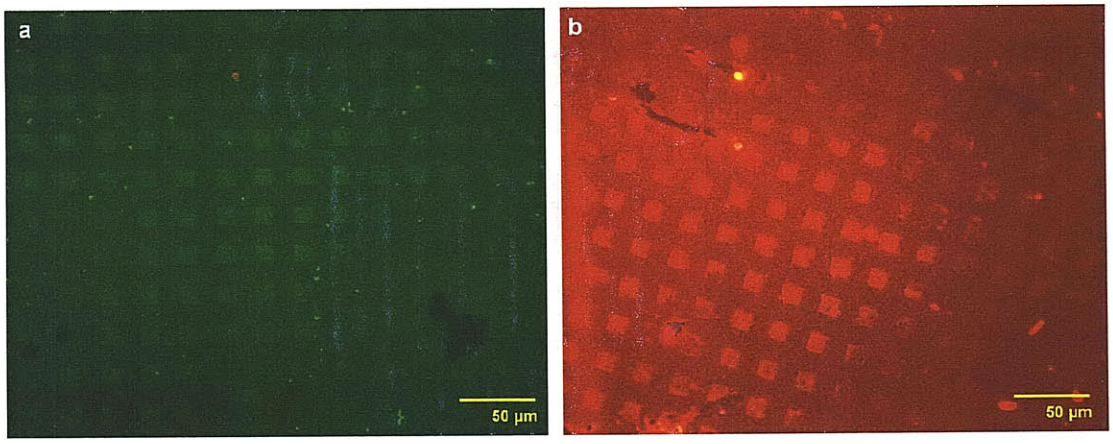

Figure 5.11: Printing and hybridization images for PAH-on-top sample a) after printing, b) after hybridization with Rhodamine Red-modified complementary DNA.

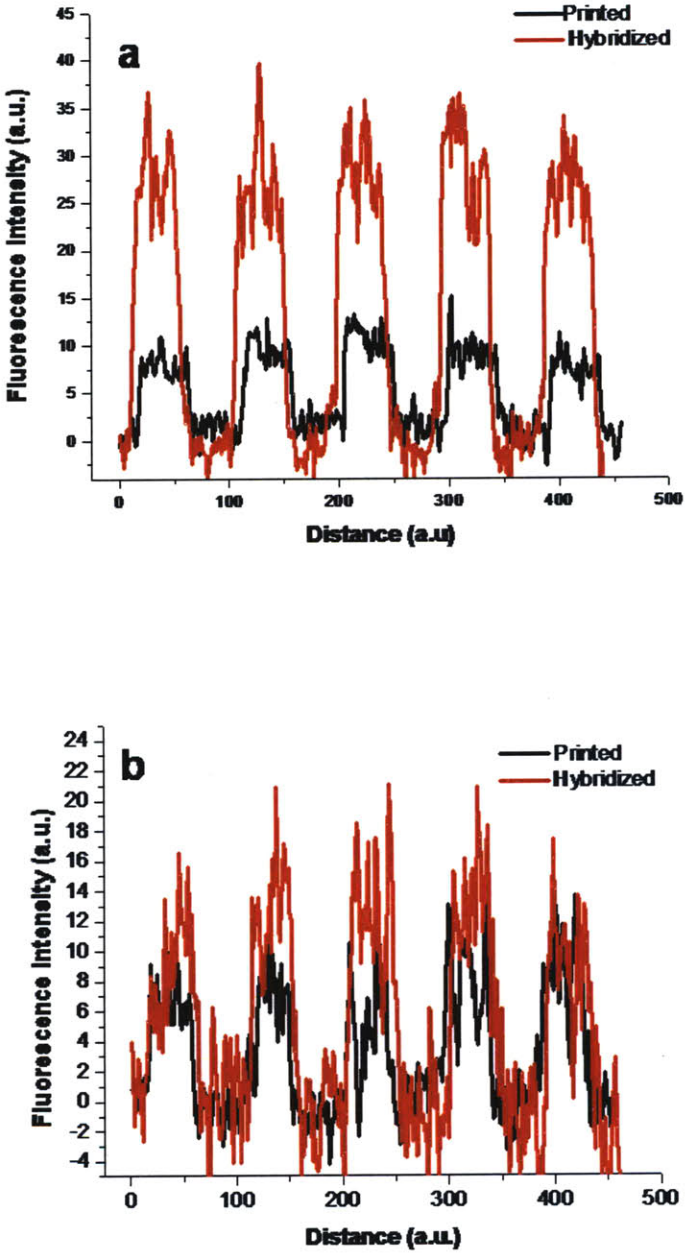

Figure 5.12: Fluorescence intensity comparison for Rhodamine Red-hybridized samples

a) PAA-on-top, b) PAH-on-top.

The similar result was observed for Rhodamine Red-hybridized samples; again although the printing signal is similar, the hybridization efficiency is much higher in PAA-on-top samples due to the high background signal in PAH-on-top samples. (Figure 5.12)

5.5 Transfer of the DNA Helix

In SuNS, we use DNA with 'sticky ends' to ensure that the complementary DNA attaches to the secondary substrate covalently. For PEMs work, we have used amine modified DNA since it can react with the carboxylic acid groups of PAA forming an amide bond. In solution, amine-carboxylic acid reaction is usually carried out with the help of N-hydroxysuccinimide (or N-hydroxysulfosuccinimide) (NHS) and 1-ethyl-3-(3-dimethylaminopropyl) carbodiimide hydrochloride (EDC). However for printing, this reaction should happen by contact in air. I tried to make this reaction possible by placing the stamping machine into an environmental chamber and keep the humidity at minimum (15%) since the by-product of this reaction is water. In an ideal situation as depicted in Scheme 5.2, only the complementary DNA should be transferred to the secondary substrate. However when printing from the gold square template, I have detected significant amount of original sequence (referred as single strand DNA,ssDNA) on the PEMs (both PAA and PAH on top). This transfer was detected by hybridizing the secondary substrate with a fluorescent DNA that is complementary to the original sequence; namely this sequence is the same as the printed sequence on the secondary substrate, typical images are shown in Figure 5.13.

Scheme 5.2. Transfer of double strand DNA from gold surface to PEMs

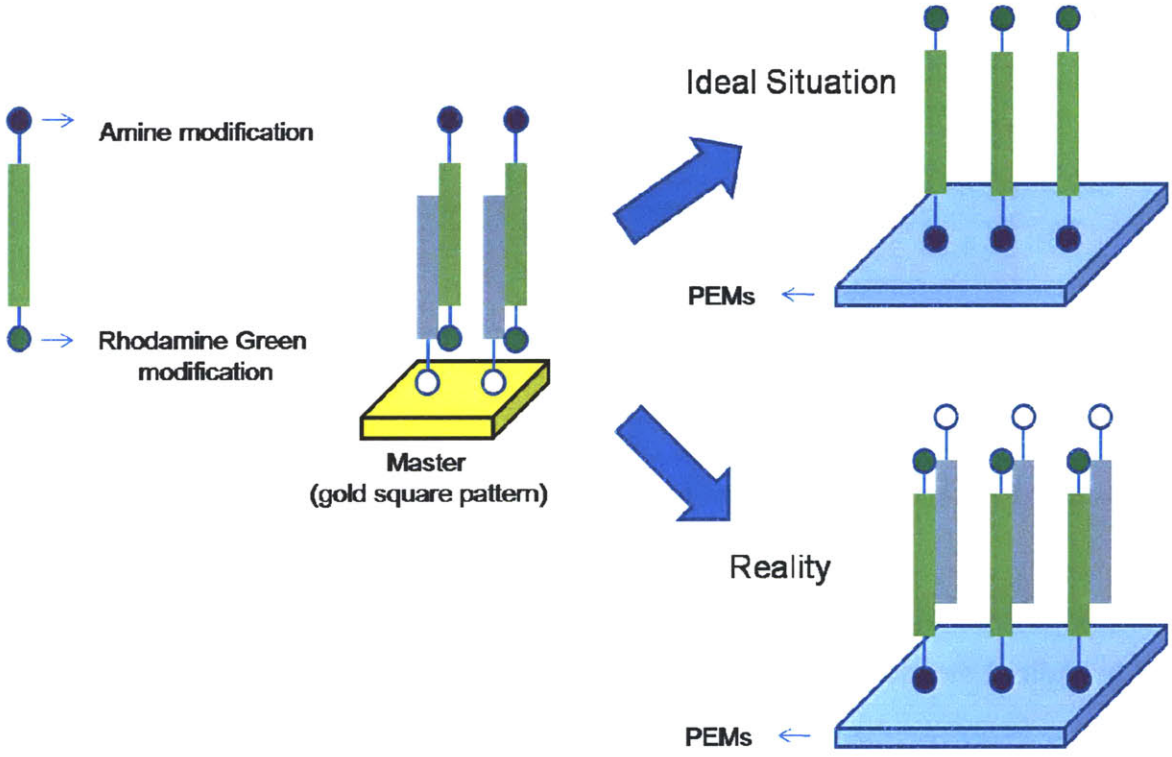

This unusual transfer is striking; the signal is as high as the normal hybridization cases i.e. hybridizing with the sequence complementary to the printed one. This result indicates considerable amount of ssDNA got transferred during the printing process.

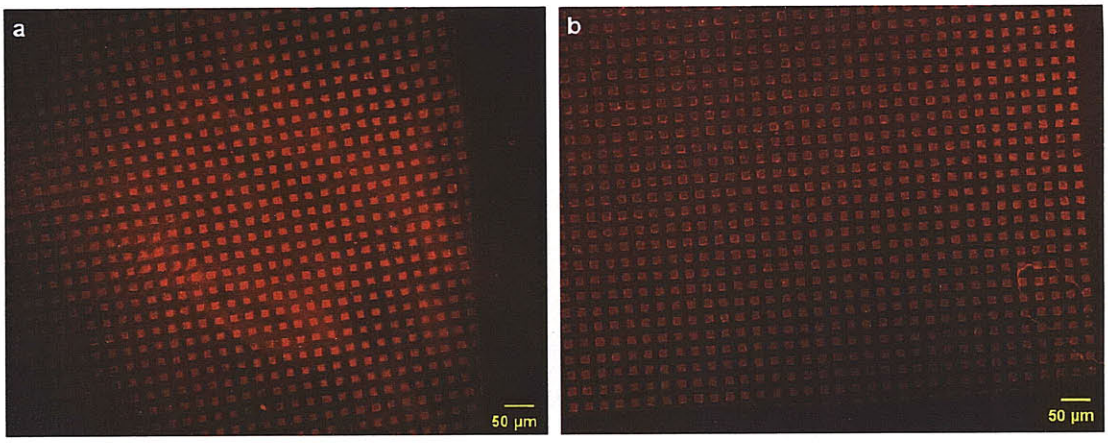

Figure 5.13: Hybridization with DNA that is complementary to the original sequence on the master a) PAA-on-top, b) PAH-on-top.

In order to figure out the possible effects of the amine group of the complementary DNA, I hybridized the master with a complementary fluorescence sequence that does not contain any reactive group. The success of printing (transfer) indicates that the transfer is not arising from the amine-carboxylic acid reaction and even a DNA without a reactive end group can get transferred. (Figure 5.14)

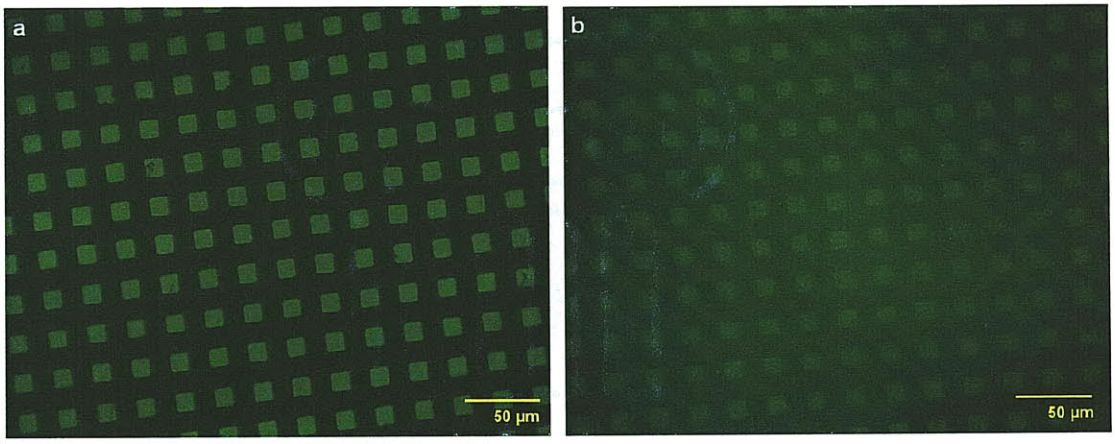

Figure 5.14: Transfer of complementary DNA without amine-end a) PAA-on-top substrate, b) PAH-on-top substrate.

Finally, I printed from an unhybridized master, namely a substrate only containing the single strand DNA, and also observed the transfer of this single strand, the image is shown in Figure 5.15.

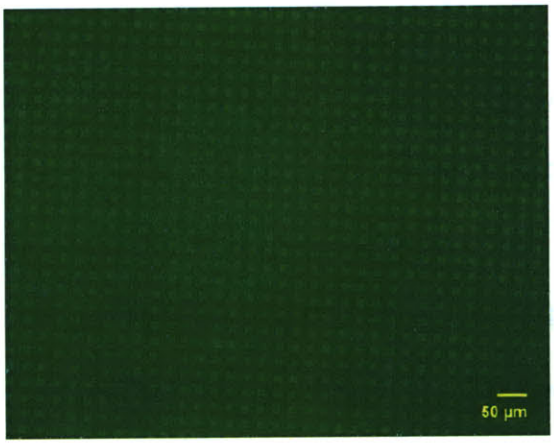

Figure 5.15: Transfer of DNA from an unhybridized master.

To truly assess the hybridization behavior, I tried to carry out the same experiments on different master materials. Spotted DNA microarrays which were fabricated by a pin based system on aldehyde modified glass (Genetixs, Ltd.) were ordered from Whitehead Institute. Unfortunately, I never obtained successful printing from these arrays. I also fabricated 10 µm × 10 µm square pattern on silicon by reactive ion etching, treat this substrate with triethoxysilylbutyraldehyde (TESA) and immobilize amine modified DNA as the original sequence on this substrate through amine-aldehyde reaction. Although, I infrequently managed to get partial printing from these substrates (< 5% of the area of the master, ~0.5 mm^2), the process wasn't reproducible from case to case. Given the fact that DNA gets transferred only when using the gold square template indicates that the 'transfer' has something to do with the surface characteristics of gold. It is also important to note that this transfer of DNA cannot be categorized as 'printing' since it should be covalently attached by our definition. During the

printing step, DNA, being a charged polymer, was attracted to the local charge of the PEMs. However, there are also local charges on aldehyde treated surfaces whereas gold is very inert compared to those two; therefore DNA prefers PEMs to the gold surface but not when on aldehyde.

I believe negatively charged PEMs can be efficient platforms to immobilize DNA since they have higher signal to background ratio if one can find a method to immobilize DNA only on the surface; namely the initial sequence should not diffuse into the layers. I have spotted amine-modified DNA onto EDC/NHS activated PAA and PAH top PEMs and react these surfaces with fluorescent complementary DNA. In those cases, PAH-on-top surfaces have signal strength as good as the PAA-on-top surfaces indicating that DNA diffused through the layers and attached to PAA. Hence, it is important to keep DNA on the surface as much as possible to obtain better signal to noise ratio.

5.6 References

[1] G. Decher, J. D. Hong, *Physical Chemistry Chemical Physics* **1991**, *95*, 1430.
[2] P. T. Hammond, *Advanced Materials* **2004**, *16*, 1271.
[3] K. Ariga, J. P. Hill, Q. Ji, *Physical Chemistry Chemical Physics* **2007**, *9*, 2319.
[4] Z. Tang, Y. Wang, Paul Podsiadlo, N. A. Kotov, *Advanced Materials* **2006**, *18*, 3203.
[5] J. F. Quinn, A. P. R. Johnston, G. K. Such, A. N. Zelikin, F. Caruso, *Chemical Society Reviews* **2007**, *36*, 707.
[6] T. R. Farhat, P. T. Hammond, *Advanced Functional Materials* **2006**, *16*, 433.
[7] A. A. Argun, J. N. Ashcraft, P. T. Hammond, *Advanced Materials* **2008**, *20*, 1539.
[8] D. M. DeLongchamp, M. Kastantin, P. T. Hammond, *Chemistry of Materials* **2003**, *15*, 1575.
[9] L. Zhai, F. C. Cebeci, R. E. Cohen, M. F. Rubner, *Nano Letters* **2004**, *4*, 1349.
[10] J. Hiller, J. D. Mendelsohn, M. F. Rubner, *Nature Materials* **2002**, *1*, 59.
[11] D. Yoo, S. S. Shiratori, M. F. Rubner, *Macromolecules* **1998**, *31*, 4309.
[12] P. T. Hammond, *Current Opinion in Colloid & Interface Science* **2000**, *4*, 430.
[13] S. S. Shiratori, M. F. Rubner, *Macromolecules* **2000**, *33*, 4213.
[14] F. Boulmedais, C. S. Tang, B. Keller, J. Vörös, *Advanced Functional Materials* **2006**, *16*, 63.

[15] B. Thierry, F. M. Winnik, Y. Merhi, J. Silver, M. Tabrizian, *Biomacromolecules* **2003**, *4*, 1564.
[16] Y. Lvov, G. Decher, G. Sukhorukov, *Macromolecules* **1993**, *26*, 5396.
[17] R. Pei, X. Cui, X. Yang, E. Wang, *Biomacromolecules* **2001**, *2*, 463.
[18] F. Caruso, K. Niikura, D. N. Furlong, Y. Okahata, *Langmuir* **1997**, *13*, 3427.
[19] D. T. Haynie, L. Zhang, J. S. Rudra, W. Zhao, Y. Zhong, N. Palath, *Biomacromolecules* **2005**, *6*, 2895.
[20] J. Zhang, L. S. Chua, D. M. Lynn, *Langmuir* **2004**, *20*, 8015.
[21] K. F. Ren, J. Ji, J. C. Shen, *Biomaterials* **2006**, *27*, 1152.
[22] G. Ladam, P. Schaaf, F. J. G. Cuisinier, G. Decher, J.-C. Voegel, *Langmuir* **2001**, *17*.
[23] G. Ladam, C. Gergely, B. Senger, G. Decher, J.-C. Voegel, P. Schaaf, F. J. G. Cuisinier, *Biomacromolecules* **2000**, *1*, 674.
[24] X. Zhou, L. Wu, J. Zhou, *Langmuir* **2004**, *20*, 8877.
[25] X. Zhou, J. Zhou, *Proteomics* **2006**, *6*, 1415.
[26] J. Dai, G. L. Baker, M. L. Bruening, *Analytical Chemistry* **2006**, *78*, 135.
[27] M. Dufva, *Biomolecular Engineering* **2005**, *22*, 173.
[28] A. A. Yu, in *Department of Materials Science and Engineering*, Vol. Ph.D, MIT, Cambridge **2007**.
[29] A. A. Yu, F. Stellacci, *Advanced Materials* **2007**, *19*, 4338.
[30] S. Thévenet, H.-Y. Chen, J. Lahann, F. Stellacci, *Advanced Materials* **2007**, *19*, 4333.

Chapter 6 Conclusion and Future Outlook on Biomolecular Arrays

6.1 Thesis Summary

In this thesis, I have presented two improvements on an already published contact-based printing method (Li)SuNS. First, it has been demonstrated that SuNS is capable of printing discrete DNA features composed of a few DNA strands (14 nm) onto a hard surface (gold-on-glass). Previously, DNA lines of 50 nm was printed onto an acrylic polymer (poly(methyl methacrylate)). Additionally, I have devised a statistical method to assess hybridization at this size scale via monitoring the height increase due to hybridization by AFM.

(Li)SuNS has been shown to transfer chemical and spatial information in a single cycle; namely multi-DNA features can be replicated in one step. However, in theory (Li)SuNS should be applicable to all biomolecular systems that can form reversible bonds. Hence, the second part of my work involves the application of LiSuNS to replicate coiled-coil peptide features. In addition, to exhibit the multiplexing capability of LiSuNS, the replication of a master composed of DNA and peptide features was shown. This result is also the first time demonstration of printing multiple types of biomolecules in a single cycle.

I believe the next step for (Li)SuNS will be adding another dimension to the scheme. As underlined throughout the thesis, every DNA (or peptide strand) carry a unique chemical combination which gets transferred onto a secondary substrate by preserving the spatial registration. The next probable challenge is the transfer of molecules which needs to preserve their shapes for proper functioning such as aptamers and Affibody molecules. In this chapter, I will try to give a basic review on those two types of biomolecules whose functions depend on their confirmation (3-D shape) and discuss their replication by (Li)SuNS.

6.2 Future Outlook on Biomolecular Arrays

Aptamers and Affibody molecules emerged as protein capture agents to serve as an alternative to antibodies mainly due to limitations explained below. Antibodies have been utilized as protein capture agents in an array format long ago due to unique complex formation with their targets. *[1-5]* However, in 2001 Haab *et al.* immobilized 115 antibodies and antigens in array format to assess their specificity and sensitivity. 50% of the arrayed antigens and 20% of the arrayed antibodies exhibited accurate selectivity and specificity to their targets indicating the challenge of multiplexing of an antibody/antigen array. *[6]* In other words, when these assays contain one type of antibody/antigen, they work nicely with dissociation constants on picomolar to nanomolar range; yet once there is more than one type of antibody/antigen, they exhibit unspecific binding to non-target proteins. Although, antibody/antigen assays revolutionized the field of diagnostics there are additional inherent problems emerging from their biophysical properties such as sensitivity to temperature (irreversible denaturation) resulting in limited shelf life. *[7]* There are also a limited number of antibodies to serve as detection agents in a multiplex array. *[3]* Nevertheless, more recently the research on 'engineered antibodies' has been intensified; the term refers to assuring molecular recognition by parts of an antibody instead of the whole protein itself or forging several fragments of an antibody to create multivalent binding domains. *[8]* Aptamer and Affibody molecules are also 'engineered' to bear unique features, I will summarize the efforts to put them into an array format and characterization methods of such arrays. I will also briefly mention the techniques to generate those molecules.

6.2.1 Aptamers

6.2.1a Structure and Synthesis

Aptamers are oligonucletides which are designed to bind specific targets such as peptides, proteins and small ions. *[9]* They have short sequences (10-60 in length) and their basis of affinity with proteins is similar to the antibodies: molecular recognition achieved by folding into a three dimensional shapes. The affinity constants range from 10^{-12} to 10^{-7} M for many protein targets. *[10]* They are smaller than antibodies with higher conformational freedom. More importantly, since they are oligonucleotides instead of proteins, they don't experience the intrinsic problems of antibodies such as limited shelf life and denaturation both on surfaces and in solution. *[10, 11]* Due to their very specific binding capabilities, their possible applications in therapeutics are investigated as well; recently an aptamer-based drug for macular degeneration became available for clinical use. *[12]* A deeper outlook on utilization of aptamers in drug development and gene therapy can be found in the related review by Que-Gewirth and Sullenger. *[13]* Nimjee *et al.* also comprehensively reported the efforts to include aptamers in therapeutics. *[14]*

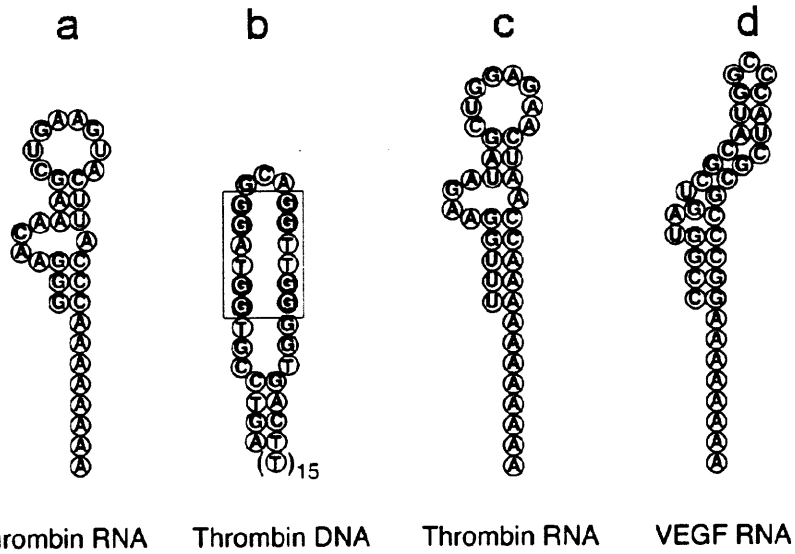

Figure 6.1: Examples of aptamer structures a) an RNA aptamer for human thrombin b) a DNA aptamer for human thrombin, c) an RNA aptamer that was selected for bovine thrombin but can also bind to human thrombin, d) an RNA aptamer for human vascular endothelial growth factor. The boxed guanine bases in 'b' form a G-quadruplex structure (not shown) that is responsible for human thrombin binding. *[15]*

Aptamers are *in vitro* generated through a process called SELEX (Systematic Evolution of Ligands by Exponential Enrichment). *[16-18]* A large pool of oligonucleotides is incubated with the target molecule and the unbound oligonucleotides are eliminated. The bound ones are eluted and amplified via Polymerase Chain Reaction (PCR). This cycle is repeated several times to figure out the best combination. Expectedly, at some point during this iteration oligonucleotides with similar affinities to the target molecule compete for the binding spots on the target leading to an enhancement in the pool. Over years, researchers came up with modifications on the initial process for more specific purposes such as photoSELEX and capillary electrophoresis SELEX, Mairal *et al.* gives comparative information about these techniques in a recent review.*[19]*

Scheme 6.1. Schematic illustration of the SELEX process *[20]*

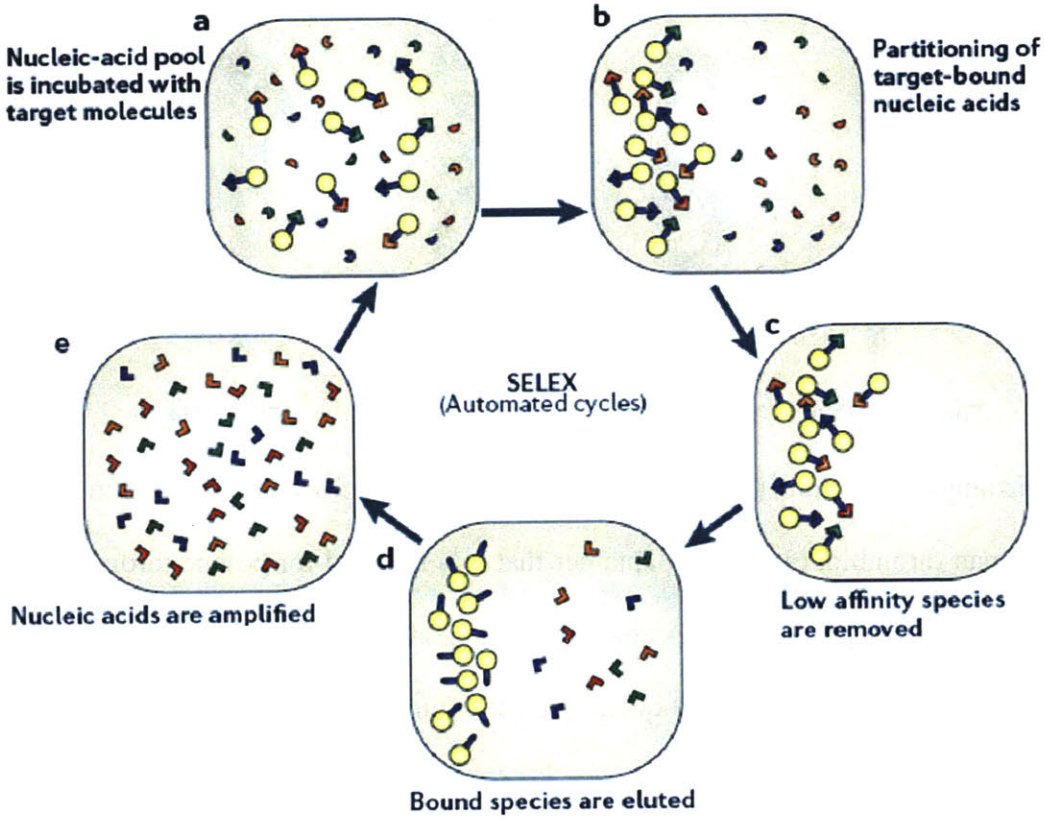

6.2.1b Aptamer Arrays

A company called SomaLogic has already commercialized multiplexed photoaptamer (for photoaptamer explanation, see below) arrays with limits of detection as low as 10 fM for some of the protein analytes such as interleukin-16, vascular endothelial growth factor, and endostatin. *[21]* Here however, I would like to summarize the efforts to fabricate aptamer arrays in the lab-scale. Ellington group is one of research labs working extensively on aptamers. They first set up the basics of aptamer arrays by using tools for DNA arrays *[22]* then gave a more educated road map on how to produce and process aptamer microarrays (selection process for aptamers, modifying selected aptamers, arraying procedure, blocking the spotted substrate, labeling the targets and data analysis etc.). *[23]* They immobilized biotinylated RNA-aptamers

which bind to hen egg white lysozyme on streptavidin slides via spotting. The detection was carried out by fluorescently labeled target proteins (Scheme 6.2). They also underlined that some aptamer clones may have a fluorescent dye preference such that a good clone exhibited 42-fold preference for Cy3 labeled targets than Cy5 labeled ones; hence extra attention should be paid to reagents to be used in the detection process. *[23]*

Scheme 6.2. Schematic comparison of immobilization analyte capture methods of cDNA (on polylysine slides) and aptamer (on streptavidin coated slides) microarrays *[23]*

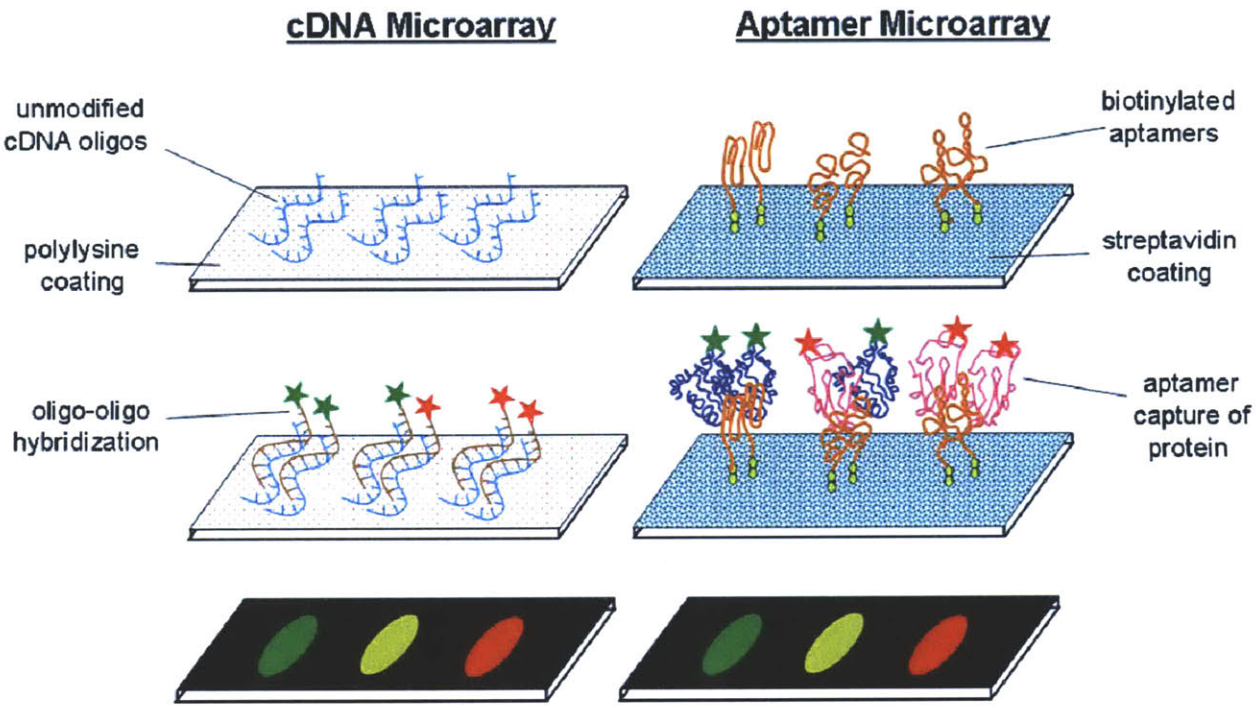

The same group also presented an aptamer array for detection of multiple proteins. *[24]* They have immobilized RNA aptamers (anti-lysozyme and anti-ricin) and two DNA aptamers (anti-IgE and anti-thrombin) on streptavidin or neutravidin coated slides via a manual arrayer. They have optimized the buffer solution, the procedure for washing and drying, and evaluated

the surface coating effects. Their result underlines the multiplexing capacity of aptamer arrays leading to their possible use in proteomics. *[24]*

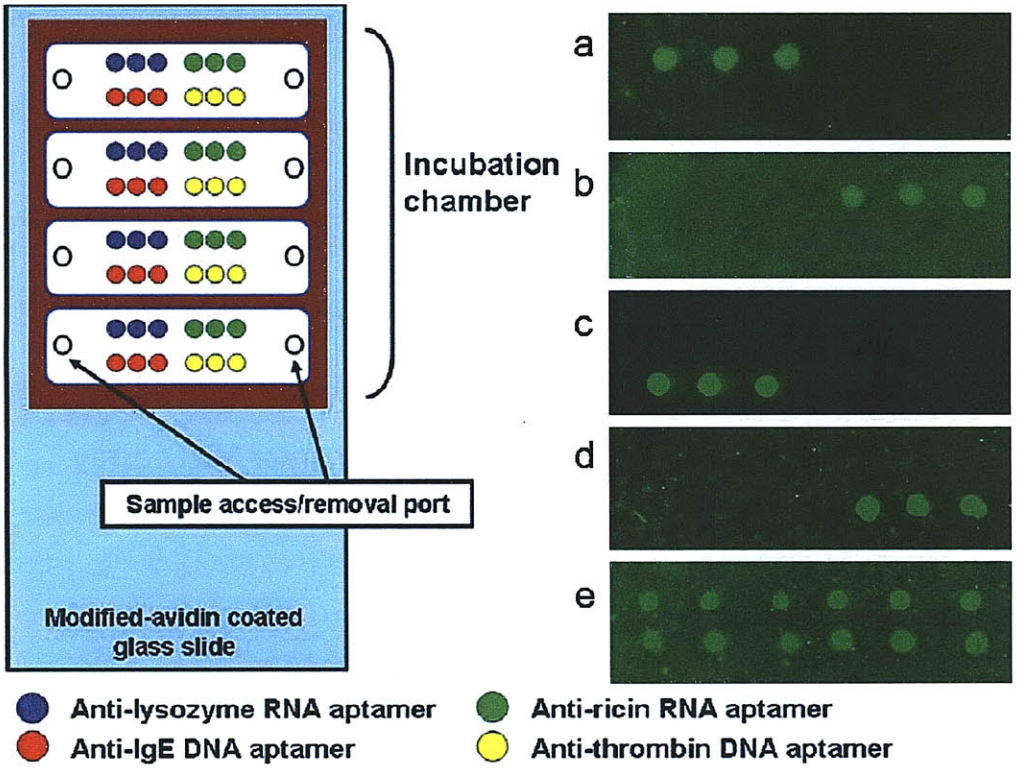

Figure 6.2: (Left) Schematic illustration for the multiplex aptamer microarray. Sample access/removal port indicates the introduction points for buffers and target proteins (Right) Fluorescence images of aptamer microarrays, targets are Cy3 labeled a) 1 nM Cy3–lysozyme, b) 10nM Cy3–ricin, c) 1 nM Cy3–IgE, d) 10nM Cy3–thrombin, e) an aptamer microarray stained with SYBR555 (a stain for oligonucleotides) as a positive control. *[24]*

Yamamoto-Fujita and Kumar introduced analyte dependent oligonucleotide modulation assay (ADONMA) involving an aptamer which is splited into two nonfunctional units (1st unit is immobilized in an array format, and 2nd unit is fluorescently labeled and used for detection) instead of a full length aptamer. These two nonfunctional units fold into a hairpin structure in the

presence of its target protein resulting in the immobilization of the 2nd unit bearing the fluorescence label. The detection is carried out via fluorescence microscopy. This technique (tested for HIV 1 Tat in this report) offers a plausible way to detect complex formation without labeling the analyte and for aptamer immobilization only one of the units needs to be modified. *[25]*

Scheme 6.3. Schematic illustration of ADONMA process *[25]*

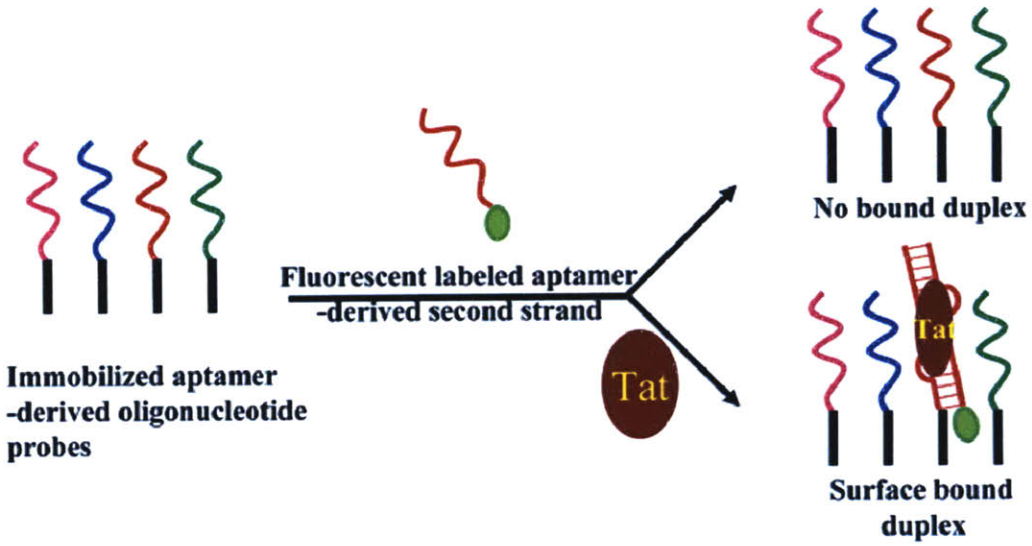

Balamurgan *et al.* investigated the effects of the linker and coadsorbant of aptamer arrays on gold surfaces. *[26]* As a model system they used a thrombin binding aptamer with two different modifications; one with a six unit long methylene and another with methylene tethered to an oligo(ethylene oxide chain). The candidate coadsorbants were an oligo(ethylene oxide) based one and 6-mercapta-1-hexanol, which removed some of the aptamer from the surface. The best aptamer and coadsorbant combination was the ones with oligo(ethylene oxide) groups. *[26]* Leo *et al.* also looked into the effect of the linker (spacer) composition on sensitivity of aptamer arrays. *[27]* They have compared oligodeoxythymidine and dodecyl linkers with two different lengths each and although all linkers gave enhanced sensitivity, the oligo-linkers exhibited better

performance. In the same work, they have investigated the avidity effects, namely synergistic binding which is larger than the sum of individual bonds, in the array as well. By coprinting two distinct aptamers onto the same spot, they have observed the avidity effect in the presence of an oligo-linker and speculated that it is due to the negative charge and flexibility of the oligo-linker which are lacked by the dodecyl linkers. They reported 100-1000 fold increase in the sensitivity compared to unmodified aptamers. *[27]* Walter *et al.* investigated the effect of surface charge and spacer length. The authors concluded that the optimization of an aptamer array mostly depends on assuring the aptamer can fold correctly; hence utilization of a long spacer to minimize steric hindrance and a negative surface to push the immobilized aptamer away from the surface to prevent unfolding were critical in array performance. *[28]*

There is also a modified class of aptamers, photoaptamers, containing photoreactive 5-bromodeoxyuridine which covalently crosslinks to the target protein when irradiated by 308 nm light. Golden *et al.* reported utilization of two photoaptamers targeting basic fibroblast growth factor with comparable affinities to commercially available ELISA antibodies. *[29]* Bock *et al.* demonstrated that these crosslinked structures (bound aptamer-protein) can withstand subsequent harsh washing steps to remove the unbound protein resulting in higher sensitivity. *[21]* Smith e*t al.* surveyed three photoaptamers against their target and non-target proteins to assess the sensitivity of the photoaptamers and reported more than 10^4-fold difference between the target and non-target binding. *[30]* They have also put photoaptamers in a microarray format and detected subnanomolar quantities of the target protein. *[30]* Meisenheimer and Koch's review on photocrosslinking of nucleic acids and proteins gives more detailed information about chromophores, aminoacids which can be modified to bear a chromophore and reaction mechanisms of the photocrosslinking process. *[31]*

As mentioned earlier, since aptamers are oligonucleotides, fabricating aptamer microarrays can be carried out by tools borrowed from DNA microarray technology such as pin-based spotting. In addition, the vast knowledge on surface chemistry for DNA can alleviate the whole technology. So far, the most common surface for aptamer (biotinylated) arrays is avidin/streptavidin coated surfaces. *[22, 23, 32]* Silanized glass *[28, 33]* and gold substrates *[15, 26, 34]* have also been utilized as immobilization platforms for aptamers. A comprehensive review on chemical mechanisms of aptamer immobilization was compiled by Balamurgan *et al.* *[35]*

Considering the specificity aptamers exhibit against their targets and theoretical unlimited number of combinations makes aptamers ideal candidates for protein arrays. Unlike antibodies, they can be obtained synthetically with minimum batch to batch variation lowering the cost associated with fabricating such arrays as well. *[7]* In addition, aptamer arrays have been shown to be used several times without losing its properties after washing such as in regeneration of an aptamer based quartz crystal microbalance biosensor *[36]* and capture-regeneration cycle of a molecular aptamer beacon targeting thrombin. *[37]* The latter case involves an aptamer folding into a quadruplex structure in the presence of the target analyte and the regeneration is carried out by disturbing this aptamer fold by hydrochloric acid. *[37]* As another example to aptamer stability, Sultan *et al.* incorporated aptamers into the layer-by-layer assembly as the polyanion layer with poly(diallyldimethylammonium chloride) as the polycation. The aptamer layer retained its ability to bind its target (specificity) albeit with a slight loss in affinity (binding power). *[38]*

6.2.1c Detection Methods

Conceivably, this molecular recognition between aptamers and proteins should be coupled with feasible detection methods. Once again, the technology for assessing DNA microarrays, fluorescence microscopy, can be readily utilized for aptamer arrays by employing fluorescently labeled protein targets. *[22, 23]* For aptamer immobilized on metallic surfaces, Surface Plasmon Resonance (SPR) was proven to be a viable detection technique. *[34]* Li *et al.* utilized a sandwich type method, through attaching the related antibody onto the bound aptamer-protein complex the authors demonstrated the amplification of the signal one would conventionally get from an SPR measurement of plain aptamer-protein binding. *[15]* SPR has also been utilized to enrich an aptamer which was found to bind to human influenza virus; namely SPR was used as a biosensor to detect highest binding affinity aptamer among a pool of aptamers which are slightly modified versions of a known aptamer. *[39]* Recently, Kelvin probe force microscopy has been shown to detect binding down to a size scale of 30 nm; however only in the edges of the immobilized protein pattern (feature size 1.5-2 μm). *[40]* Fluorescence resonance energy transfer (FRET) *[41]* is also a common method which requires labeling of the aptamer, target protein or both. Fluorescence polarization anisotropy utilizes immobilized and labeled aptamers and detects the change in the fluorescence polarization due to the rotation of the aptamer upon binding with the target protein. *[32, 42]* On the other hand, Jhaveri *et al.* reported a procedure to select aptamers accommodating fluorophores during SELEX to remedy the problems associated with decreasing in binding energy due to the introduction of the fluorophore. *[43]* This SELEX process included addition of fluorophore labeled oligonucleotides in a random pool of sequences, selecting the ligand binding aptamers and further trimming those which exhibit change in fluorescence intensity due to molecular recognition. *[43]* In addition,

aptamers have found many applications in biosensors, comprehensive literature surveys regarding to aptamer biosensors can be found in reviews by Navani and Li, *[44]* and Cho *et al.* *[10]*

6.2.1d Problems Associated with Aptamers

As one can imagine, in the early days of aptamers the bottleneck of aptamer arrays was actually finding the best aptamer which binds to the target protein. The possibility of finding the best aptamer scales with the starting library of sequences; namely larger the library, higher the likelihood of figuring out the best combination. In addition, SELEX procedure is composed of several iterations (5-20 rounds) for best results. *[45]* In 1998, Ellington Lab has automated the selection process hence decreasing the time required from months/weeks to days. *[45]* However, despite this progress a table compiled by Collett *et al.* listing the known aptamers in 2005 contains ~20 entries. *[23]* After this date, new aptamers such as an HIV 1 (a new version), *[46]* an anti-leukemia *[47]*, anti-prion, *[48, 49]* have also emerged; yet this number is still well below the predictions. *[11]*

One drawback of RNA aptamers is their susceptibility to degradation with ribonucleases which are frequently found in physical fluids. However, considerable remedies were suggested to overcome this issue such as modifications on the ribozyme backbone *[50]* or the side groups susceptible to hydrolysis, *[51]* and selecting a polymerase (the enzyme which synthesizes DNA and RNA) which can incorporate modified oligonucleotides (more stable than natural ones) while transcripting DNA or RNA. *[52]*

6.2.1e Applicability to (Li)SuNS

Aptamers are oligonucleotides with a specific 3-D shape. Unlike antibodies they can go through reversible denaturation; namely they can lose their shape intermittently but their shape can be regenerated resulting in robustness which is an advantage in any fabrication technique. Besides, SELEX is a versatile process to select aptamers in such a way that various aptamers targeting different proteins can be picked up to works in same environmental conditions such as pH and temperature which is critical in an array application. In other words, during SELEX some limitations can be introduced to the system and for instance the initial library can be for instance screened to select aptamers which works in pH 7. *[7]* In addition, functional groups or fluorescent molecules can be attached to precise locations in aptamers leading to an ease in immobilization and detection.

I believe (Li)SuNS can be an ideal platform to replicate aptamer arrays due to the vast experience in printing oligonucleotides. In my opinion, Crook's 'zip-code' approach *[53]* (Chapter 2) would be a versatile tool to fabricate/replicate aptamer arrays. 'Zip-code' approach suggest an innovative way to immobilize aptamers on a master surface: since aptamers are synthetically synthesized nucleic acid sequences, they can bear an end-sequence which can bind to the zip-code on the master surface. A single zip-code master can be utilized to bind several different aptamer array configurations without the need to fabricate a separate master for each array. In addition, aptamers can contain biotin moieties that can be captured by streptavidin coated substrates.

6.2.2 Affibody Molecules

6.2.2a Structure and Synthesis

Another class of protein binding agents is 'engineered scaffold proteins' which include anticalins modeled on lipocalin structures, *[54]* trinectins derived from a fibronectin III domain, *[55]* designed repeat polypeptides such as ankyrin *[56]* and leucine, *[57]* and Affibody molecules, which are engineered from the Z domain of protein A. *[58, 59]* Here, I will only focus on Affibody molecules, which is a trademark, since it is one of the most widely investigated scaffolds. As the name implies, these are 'scaffolds' (polypeptide folds) that host a novel binding element. The 'scaffold' (host) is supposed be robust to bear various substitutions/insertions; namely an affinity function is introduced into the framework of a stably folded protein. The variations in the protein structure are carried out by a combinatorial protein engineering approach which changes the information (i.e. aminoacids) on the peptide in a stable manner; hence creating a library. *[58, 60]* Expectedly, the most important property of a protein scaffold is to retain its stability even after the introduced changes in its structure such that enough aminoacids should be replaced to make a good ligand binding interface but not that many to avoid instability of the host protein. *[58, 61]* The advantages against antibodies include good thermal stability, lack of disulfide bonds (i.e. free of cysteines, disulfide bonds are formed by between the thiol groups of cysteines, it plays an important role in protein folding but inherently unstable) and easy to synthesize (modify an existing scaffold). *[59]*

Affibodies are constructed from α–helical structure of bacterial cell surface receptors (staphylococcal surface Protein A, SPA). Native Protein A can bind to immunoglobulin and is known to extremely stable with good solubility in physiological fluids. *[62]* The Z-domain is derived from Protein A, containing 58 aminoacids (~6 kDa) and forming a three anti-parallel

helices *[62, 63]*. 13 surface exposed aminoacids in the helices one and two of the Z-domain was genetically randomized to construct a combinatorial library. *[62, 64]* This randomization is an innovative way to create different affinities. *[58]* The Z-domain does not contain disulfide bonds; hence can be utilized in reducing environments and synthetic modifications can be carried out without disrupting the initial fold. *[65, 66]* In addition, due to the lack of cysteine residues, fluorophores, which are important tools for detection, can be incorporated in this structure without disturbing the stability. *[67]* Up until now, there has been many works reporting different affibody constructs against protein targets such as human epidermal growth factor receptor 2 (HER2) in picomolar range, *[68]* human serum albumin in femtomolar range, *[69]* human epidermal growth factor receptor (EGFR) *[70]* and interleukin-2 (a protein playing a major role in regulation of cellular immune responses) *[71]* in 0.1 micromolar range, c-jun (an oncogenic transcription factor) in micromolar range. *[72]*

Scheme 6.4. Schematic illustration of a) the three-helix bundle Z-domain (13 randomized positions during affibody protein library constructions highlighted in yellow, b) side view, c) top view *[73]*

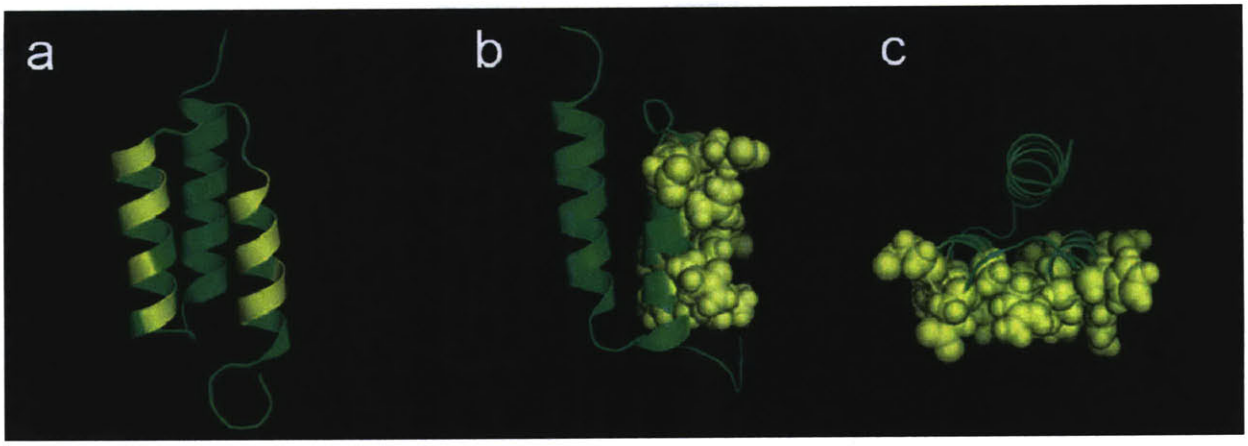

Affibody molecules, unlike oligonucleotide based designed sequences (aptamers), cannot amplify themselves. Hence, their selection is carried out through the genes encoding them by phage display method. *[62, 70, 74, 75]* In phage display method, the gene (DNA fragment) which encodes a specific protein is fused into the genes of a certain bacteriophage (a virus) synthesizing the coat proteins of the virus. Thereafter, the target coat proteins (now encoded by the fused DNA) on the surface can be harnessed by an immobilized receptor *in vitro*. *[76]* In one of the earlier reports, Nord et al. reported selection of affibodies against, insulin and a human alipoprotein by using phage display; the reported affinity for the *Taq* DNA polymerase were on the micromolar range which was lower than the one between the polymerase and the original domain. *[62]* However, it was possible to enhance the affinity for *Taq* DNA polymerase (30-50 nM) with selectively directing the re-randomization of aminoacids (helix shuffling) to one of the two helices constituting the binding surface for *Taq* DNA polymerase; namely forming a second library. *[77]* On the other hand, it is also possible to obtain affinities in nanomolar to 0.1 micromolar range depending on the affibody-protein pair via phage display method. *[70]* In addition, solid phase peptide synthesis has been also employed to generate affibody molecules; through this method certain molecules (i.e.fluorophores or biotin) can be introduced to the specific locations of the affibody molecules during synthesis. *[78]*

6.2.2b Affibody Arrays

Renberg *et al.* fabricated an affibody microarray containing two affibodies, Z_{taq} and Z_{IgA}, targeting *Taq* DNA polymerase and human IgA respectively via spotting. *[78]* The authors reported their best detection limit as 30 pM for *Taq* DNA polymerase and 3 pM for human IgA. They have examined two different oriented immobilization chemistries: streptavidin-biotin and

cysteine-thiol-dextran as well as random immobilization on carboxymethyl-dextran slides. Cysteine or biotin was coupled to the sidechain of the last aminoacid of the Z-domain. Both dextran slides exhibited good signal-to-noise ratio whereas streptavidin slides had a high background and low signal intensity. *[78]* The effect of multidomain binding (up to four identical binding domains) between Affibody and target analyte was also investigated in a microarray format via fluorescently labeled target proteins as well as sandwich assays involving a secondary detection agent (antibodies). *[79]* Multimeric Affibody ligands exhibited good sensitivity and no cross-reactivity (among six dimeric ligands) and the signal intensity difference between monomeric and dimeric ligands was reported to be the highest. *[79]* Utilization of Affibody ligands in combination with antibodies in ELISA type assays has also been studied. Affibody ligand targeting immunoglobulin A (IgA) was incubated on ELISA plates and after treating the plates with target protein in human sera, detection was carried out by an antibody targeting the same protein. *[80]* The authors also tried first incubating the antibody and using Affibody ligand as the detection agent as well. They reported comparable results to ELISA involving two antibodies for capturing and detection in the case of Affibody ligand as the capture and antibody for the detection agent. *[80]* Apart from microarrays, the applications of affibody molecules include affinity chromatography for purification of biomolecules; *[74]* radiolabeled Affibody molecules are utilized in tumor imaging *in vivo* as well. *[68, 70, 81]*

6.2.2c Detection Methods

Detection strategies for affibody arrays include fluorescence microscopy, *[78, 79]* FRET by introduction of donor/acceptor pair to the affibody, *[66]* and another FRET-based method involving two fluorophore labeled affibodies one of which competes with the target analyte for

the binding region. *[82]* In both FRET-based strategies, the detection is carried out by monitoring the shift in the relative fluorescence of the two fluorophores. *[66, 82]* Surface Plasmon Resonance (SPR) is a viable technique when the whole surface of the immobilization slide is composed of Affibody molecules. *[72, 83]*

6.2.2d Applicability to (Li)SuNS

As presented in Chapter 4, we have reported the replication of peptide features via LiSuNS while keeping their functionality and specificity. This peptide system was of coiled-coil motif which is also composed of α-helices like Affibody molecules. In addition, for selective immobilization (such as on gold squares), specific chemical groups can also be introduced to affibody molecules as explained by Renberg *et al* during solid state synthesis. *[78]*

It is my optimist prediction that LiSuNS can be employed to transfer target analytes bound to Affibody molecules onto a secondary surface (and vice versa) which can lead the way for more extensive studies of Affibody molecules and their target proteins considering the complexation of Affibody molecules and target proteins is reversible. On the other hand, some of the engineered scaffold proteins interact with their target by forming a locus inside them (like a hole), I believe the application of (Li)SuNS will be more towards the surface bound structures rather than those. Also, one should keep in mind that Affibody molecules, although more robust than antibodies, are still proteins and by nature more fragile than their oligonucleotide counterparts.

6.3 References

[1] H. Zhu, M. Snyder, *Current Opinion in Chemical Biology* **2003**, *7*, 55.
[2] M. F. Templin, D. Stoll, J. M. Schwenk, O. Pötz, S. Kramer, T. O. Joos, *Proteomics* **2003**, *3*, 2155.
[3] R. Barry, M. Soloviev, *Proteomics* **2004**, *4*, 3717.
[4] A. Bradbury, N. Velappan, V. Verzillo, M. Ovecka, L. Chasteen, D. Sblattero, R. Marzari, J. Lou, R. Siegel, P. Pavlik, *Trends in Biotechnology* **2003**, *21*, 275.
[5] C. A. K. Borrebaeck, *Immunology Today* **2000**, *21*, 379.
[6] B. B. Haab, M. J. Dunham, P. O. Brown, *Genome Biology* **2001**, *2*, 1.
[7] S. D. Jayasena, *Clinical Chemistry* **1999**, *45*, 1628.
[8] P. Holliger, P. J. Hudson, *Nature Biotechnology* **2005**, *23*, 1126.
[9] D. S.Wilson, J. W. Szostak, *Annual Review of Biochemistry* **1999**, *68*, 611.
[10] E. J. Cho, J.-W. Lee, A. D. Ellington, *Annual Reviews of Analytical Chemistry* **2009**, *2*, 241.
[11] W. Rowe, M. Platt, P. J. R. Day, *Integrative Biology* **2009**, *1*, 53.
[12] E. W. M. Ng, D. T. Shima, P. Calias, J. Emmett T. Cunningham, D. R. Guyer, A. P. Adamis, *Nature Reviews Drug Discovery* **2006**, *5*, 123.
[13] N. S. Que-Gewirth, B. A. Sullenger, *Gene Theraphy* **2007**, *14*, 283.
[14] S. M. Nimjee, C. P. Rusconi, B. A. Sullenger, *Annual Review of Medicine* **2005**, *56*, 555.
[15] Y. Li, H. J. Lee, R. M. Corn, *Analytical Chemistry* **2007**, *79*, 1082.
[16] A. D. Ellington, J. W. Szostak, *Nature* **1990**, *346*, 818.
[17] C. Tuerk, L. Gold, *Science* **1990**, *249*, 505.
[18] A. D. Ellington, J. W. Szostak, *Nature* **1992**, *355*, 850.
[19] T. Mairal, V. C. Özalp, P. L. Sánchez, M. Mir, I. Katakis, C. K. O'Sullivan, *Analytical and Bioanalytical Chemistry* **2008**, *390*, 989.
[20] D. H. J. Bunka, P. G. Stockley, *Nature Reviews* **2006**, *4*, 588.
[21] C. Bock, M. Coleman, B. Collins, J. Davis, G. Foulds, L. Gold, C. Greef, J. Heil, J. S. Heilig, B. Hicke, M. N. Hurst, G. M. Husar, D. Miller, R. Ostroff, H. Petach, D. Schneider, B. Vant-Hull, S. Waugh, A. Weiss, S. K. Wilcox, D. Zichi, *Proteomics* **2004**, *4*, 609.
[22] J. R. Collett, E. J. Cho, J. F. Lee, M. Levy, A. J. Hood, C. Wan, A. D. Ellington, *Analytical Biochemistry* **2005**, *338*, 113.
[23] J. R. Collett, E. J. Cho, A. D. Ellington, *Methods* **2005**, *37*, 4.
[24] E. J. Cho, J. R. Collett, A. E. Szafranska, A. D. Ellington, *Analytica Chimica Acta* **2006**, *504*, 82.
[25] R. Yamamoto-Fujita, P. K. R. Kumar, *Analytical Chemistry* **2005**, *77*, 5460.
[26] S. Balamurugan, A. Obubuafo, S. A. Soper, R. L. McCarley, D. A. Spivak, *Langmuir* **2006**, *22*, 6446.
[27] Y.-H. Lao, K. Peck, L.-C. Chen, *Analytical Chemistry* **2009**, *81*, 1747.
[28] J.-G. Walter, O. Kokpinar, K. Friehs, F. Stahl, T. Scheper, *Analytical Chemistry* **2008**, *80*, 7372.
[29] M. C. Golden, B. D. Collins, M. C. Willis, T. H. Koch, *Journal of Biotechnology* **2000**, *81*, 167.
[30] D. Smith, B. D. Collins, J. Heil, T. H. Koch, *Molecular and Cellular Proteomics* **2003**, *2*, 11.

[31] K. M. Meisenheimer, T. H. Koch, *Critical Reviews in Biochemistry and Molecular Biology* **1997**, *32*, 101 — 140.
[32] T. G. McCauley, N. Hamaguchi, M. Stanton, *Analytical Biochemistry* **2003**, *319*, 244.
[33] K. Stadtherr, H. Wolf, P. Lindner, *Analytical Chemistry* **2005**, *77*, 3437.
[34] Y. Li, H. J. Lee, R. M. Corn, *Nucleic Acids Research* **2006**, *34*, 6416.
[35] S. Balamurugan, A. Obubuafo, S. A. Soper, D. A. Spivak, *Analytical and Bioanalytical Chemistry* **2008**, *390*, 1009.
[36] M. Liss, B. Petersen, H. Wolf, E. Prohaska, *Analytical Chemistry* **2002**, *74*, 4488.
[37] A.-E. Radi, J. L. A. Sanchez, E. Baldrich, C. K. O'Sullivan, *Journal of American Chemical Society* **2006**, *128*, 117.
[38] Y. Sultan, R. Walsh, C. Monreal, M. C. DeRosa, *Biomacromolecules* **2009**, *10*, 1149.
[39] T. S. Misono, P. K. R. Kumar, *Analytical Biochemistry* **2005**, *342*, 312.
[40] P. Gao, Y. Cai, *Analytical and Bioanalytical Chemistry* **2009**, *394*, 207.
[41] G.-I. Kim, K.-W. Kim, Min-KyuOh, Y.-M. Sung, *Nanotechnology* **2009**, *20*.
[42] R. A. Potyrailo, R. C. Conrad, A. D. Ellington, G. M. Hieftje, *Analytical Chemistry* **1998**, *70*, 3419.
[43] S. Jhaveri, M. Rajendran, A. D. Ellington, *Nature Biotechnology* **2000**, *18*, 1293.
[44] N. K. Navani, Y. Li, *Current Opinion in Chemical Biology* **2006**, *10*, 272.
[45] J. C. Cox, P. Rudolph, A. D. Ellington, *Biotechnology Progress* **1998**, *14*, 845.
[46] T. M. A. Gronewold, A. Baumgartner, J. Hierer, S. Sierra, M. Blind, F. Schafer, J. Blumer, T. Tillmann, A. Kiwitz, R. Kaiser, M. Zabe-Kuhn, E. Quandt, M. Famulok, *Journal of Proteome Research* **2009**, *8*, 3568.
[47] K. Sefah, Z. Tang, D. Shangguan, H. Chen, D. Lopez-Colon, Y. Li, P. Parekh, J. Martin, L. Meng, J. Phillips, Y. Kim, W. Tan, *Leukemia* **2009**, *23*, 235.
[48] D. Ogasawara, H. Hasegawa, K. Kaneko, K. Sode, K. Ikebukuro, *Prion* **2007**, *1*, 248.
[49] S. Gilch, H. M. Schatzl, *Cellular and Molecular Life Sciences* **2009**, *66*, 2445.
[50] W. A. Pieken, D. B. Olsen, F. Benseler, H. Aurup, F. Eckstein, *Science* **1991**, *253*, 314.
[51] L. Beigelman, J. A. McSwiggen, K. G. Draper, C. Gonzalez, K. Jensen, A. M. Karpeisky, A. S. Modak, J. Matulic-Adamic, A. B. DiRenzo, P. Haeberli, D. Sweedler, D. Tracz, S. Grimm, Francine E. Wincott, V. G. Thackray, N. Usman, *Journal of Biological Chemistry* **1995**, *270*.
[52] J. Chelliserrykattil, A. D. Ellington, *Nature Biotechnology* **2004**, *22*, 1155.
[53] H. Lin, J. Kim, L. Sun, R. M. Crooks, *Journal of American Chemical Society* **2006**, *128*, 3268.
[54] D. R. Flower, *Biochemical Journal* **1996**, *318*, 1.
[55] A. Koide, C. W. Bailey, X. Huang, S. Koide, *Journal of Molecular Biology* **1998**, *284*, 1141.
[56] H. K. Binz, P. Amstutz, A. Kohl, M. T. Stumpp, C. Briand, P. Forrer, M. G. Grutter, A. Pluckthun, *Nature Biotechnology* **2004**, *22*, 575.
[57] M. T. Stumpp, P. Forrer, H. K. Binz, A. Pluckthun, *Journal of Molecular Biology* **2003**, *332*, 471.
[58] P.-A. Nygren, A. Skerra, *Journal of Immunological Methods* **2004**, *290*, 3.
[59] H. K. Binz, P. Amstutz, A. Pluckthun, *Nature Biotechnology* **2005**, *23*, 1257
[60] P. Amstutz, P. Forrer, C. Zahnd, A. Pluckthun, *Current Opinion in Biotechnology* **2001**, *12*, 400.
[61] M. Friedman, S. Stahl, *Biotechnology and Applied Biochemistry* **2009**, *53*, 1.

[62] K. Nord, E. Gunneriusson, J. Ringdahl, S. Stahl, M. Uhlen, P.-A. Nygren, *Nature Biotechnology* **1997**, *15*, 772.
[63] R. J. Hosse, A. Rothe, B. E. Power, *Protein Science* **2005**, *15*, 14.
[64] K. Nord, J. Nilsson, B. Nilsson, M. Uhlen, P.-A. Nygren, *Protein Engineering* **1995**, *8*, 601.
[65] K. Nord, O. Nord, M. Uhlen, B. Kelley, C. Ljungqvist, P.-A. Nygren, *European Journal of Biochemistry* **2001**, *268*, 4269.
[66] T. Engfeldt, B. Renberg, H. Brumer, P.-A. Nygren, A. E. Karlstrom, *ChemBioChem* **2005**, *6*, 1043
[67] A. Karlstrom, P.-A. Nygren, *Analytical Biochemistry* **2001**, *295*, 22.
[68] A. Orlova, M. Magnusson, T. L. J. Eriksson, M. Nilsson, B. Larsson, I. Hoiden-Guthenberg, C. Widstrom, J. Carlsson, V. Tolmachev, S. Stahl, F. Y. Nilsson, *Cancer Research* **2006**, *66*, 4339.
[69] A. Jonsson, J. Dogan, N. Herne, L. Abrahmsen, P.-A. Nygren, *Protein Engineering, Design & Selection* **2008**, *21*, 515.
[70] M. Friedman, E. Nordberg, I. Hoiden-Guthenberg, H. Brismar, G. P. Adams, F. Y. Nilsson, J. Carlsson, a. S. Stahl, *Protein Engineering, Design & Selection* **2007**, *20*, 189.
[71] C. Gronwall, E. Snelders, A. J. Palm, F. Eriksson, N. Herne, S. Stahl, *Biotechnology and Applied Biochemistry* **2008**, *50*, 97.
[72] E. Lundberg, H. Brismar, T. Graslund, *Biotechnology and Applied Biochemistry* **2009**, *52*, 17.
[73] P.-A. Nygren, *FEBS Journal* **2008**, *275*, 2668.
[74] K. Nord, E. Gunneriusson, M. Uhlen, P.-A. Nygren, *Journal of Biotechnology* **2000**, *80*, 45.
[75] J. Ronnmark, H. Gronlund, M. Uhlen, P.-A. Nygren, *European Journal of Biochemistry* **2002**, *269*, 2647.
[76] S. S. Sidhu, *Current Opinion in Biotechnology* **2000**, *11*, 610.
[77] E. Gunneriusson, K. Nord, M. Uhlen, P.-A. Nygren, *Protein Engineering* **1999**, *12*, 873.
[78] B. Renberg, I. Shiroyama, T. Engfeldt, P.-A. Nygren, A. E. Karlstrom, *Analytical Biochemistry* **2005**, *341*, 334.
[79] B. Renberg, J. Nordin, A. Merca, M. Uhlen, J. Feldwisch, P.-A. Nygren, A. E. Karlstrom, *Journal of Proteome Research* **2007**, *6*, 171.
[80] M. Andersson, J. Ronnmark, I. Arestrom, P.-A. Nygren, N. Ahlborg, *Journal of Immunological Methods* **2003**, *283*, 225.
[81] F. Y. Nilsson, V. Tolmachev, *Current Opinion in Drug Discovery & Development* **2007**, *10*, 167.
[82] B. Renberg, P.-A. Nygren, M. Eklund, A. E. Karlstrom, *Analytical Biochemistry* **2004**, *334*, 72.
[83] M. Wikman, E. Rowcliffe, M. Friedman, P. Henning, L. Lindholm, S. Olofsson, S. Stahl, *Biotechnology and Applied Biochemistry* **2006**, *45*, 93.

Chapter 7 Experimental Section

7.1 Experimental Methods for the Replication of DNA Nanoarrays

Silicon wafers were cleaned with Piranha solution (Sulfuric acid/ hydrogen peroxide: 3/1) and a ~5 nm thick chromium adhesive layer was deposited onto silicon via e-beam evaporation, (Piranha solution is extremely dangerous and should be handled with care). Gold nanoparticles were prepared as explained in the reference (Lu, JQ. & Yu, S., *Langmuir*, **2006**, 22, 3951) with Au to pyridine ratio of 0.35. $PS_{(780)}$-*b*-$P2VP_{(200)}$ was purchased from Polymer Source, Inc., gold(III) chloride trihydrate was obtained from Aldrich and toluene was purchased from EMD.

7.1.1 Substrate Preparation

Gold-on-glass: Mica substrates were purchased from Molecular Imaging Corp., and 200 nm thick gold (111) was evaporated on freshly cleaved mica via e-beam evaporation. The gold layer was transferred from mica to a glass substrate using epoxy (377, Epoxy Technology) as an adhesion layer according to the method described in the reference (Gupta, P.; Loos, K.; Korniakov, A.; Spagnoli, C.; Cowman, M.; Ulman, A. *Angew. Chem.-Int. Edit.* 43, 520-523 (2004)).

7.1.2 Experimental Steps for the SuNS Cycle

All modified DNA strands were purchased from Integrated DNA Technologies. Phosphate buffered saline (PBS) and saline sodium citrate (SSC) were obtained from VWR. 6-mercapto-1-hexanol (MH) was purchased from Sigma-Aldrich. Dithiothreitol (DTT) was purchased from Biochem. All other chemicals were purchased from Sigma-Aldrich, Fluka, or BioChem and used as received. Millipore water (18.2MΩcm) was used to clean samples and

make all required buffer solutions. The following sequences are employed in this thesis (hexyl thiol is abbreviated as 'HS'):

HS-A (50 mer): 5'- /5ThioMC6-D/ CCA GGA TTT TCA TGA GGG GCC GTA GCT TGA GCC ACC ACT GTT CTT TGG GA - 3'

HS-A' (50mer): 5'- /5ThioMC6-D/ TCC CAA AGA ACA GTG GTG GCT CAA GCT ACG GCC CCT CAT GAA AAT CCT GG - 3'

A' (50 mer): 5' - /5RhoR-XN/ CCA GGA TTT TCA TGA GGG GCC GTA GCT TGA GCC ACC ACT GTT CTT TGG GA –3'

A' (100 mer): 5' - /5AmMC6/ TTT TTT TTT TTT CCA GGA TTT TCA TGA GGG GCC GTA GCT TGA GCC ACC ACT GTT CTT TGG GAC TCT ACA CTG CCC TCT GGA AAG CCA AAC CTC TTC TGA A - 3'

Thiol modified DNA molecules (purchased as disulfides) were reduced before use. Dithiolated oligonucleotides were reduced by dissolving ~10 nmole of DNA in 1 ml of a 0.1M phosphate buffer (pH 7) aqueous solution containing solid phase dithiothreitol (DTT), followed by filtering the solution through a syringe filter of pore size 0.2 μm (Life Sciences, poly(tetrafluoroethylene) membrane) . To reach the targeted ionic strength, 1M potassium phosphate buffer solution (pH 3.8) was added to the filtered solution to reach a 5 μM DNA concentration. For hybridization, 1M NaCl in TE buffer (10 mM Tris buffer pH 7.2 and 1 mM ethylenediamine tetraacetic acid (EDTA)) was added to the solution instead of 1M potassium phosphate buffer solution. In the case of hybridization of printed DNA with amine terminated 100-mer DNA or rhodamine terminated 50-mer DNA, there was no reduction step, only 1M NaCl in TE buffer was added to reach 5 μM DNA concentration.

To allow DNA immobilization on gold nanoparticles, a few drops of 5 μM solution of thiolated single-stranded DNA (HS-A) (50 mer) were placed onto the substrate, and allowed to react under a cover slip in a humidified chamber for 1 day. After rinsing with water, the substrates were treated with a 1mM 6-mercapto-1-hexanol (MH) aqueous solution for 30 min to minimize nonspecific adsorption of single-stranded DNA, rinsed with deionized water and blown dry with air. For hybridization, the single-stranded DNA immobilized master was treated with 1 M NaCl in TE buffer/phosphate buffer (1/1) containing 5 μM complementary DNA molecules (HS-A') under a cover slip for 1 day in a humidified chamber. The substrates were washed with 4X standard sodium citrate (SSC), 2X SSC and water consecutively. After drying, the hybridized master was brought into contact with a gold-on-glass surface in a vise and stored in a desiccator for 1 day to achieve bond formation between the HS-A' and the gold surface. For dehybridization, the vise was placed in the oven at the temperature of 90 °C. After 30 min, the vise was released, a small amount of dehybridization buffer (0.1 M NaCl/TE buffer) was dropped onto the substrates and the substrates were separated.

7.1.3 AFM, STM and TEM

Tapping Mode AFM (TM-AFM) images were obtained using a Digital Instrument Nanoscope IIIa. All experiments presented in the paper were performed using Veeco

NanoprobeTM tips (Model #: RTESP; Length: 125 μm, Resonance Frequency ~ 30 kHz). STM measurements were carried out on a Veeco Multimode STM with mechanically cut Pt/Ir tips. TEM was performed on a JEOL 200CX operating at 200 kV (Courtesy of Dr. Ryan D. Bennett).

X-ray photoelectron spectroscopy experiments were performed on a Kratos Axis Ultra X-ray photoelectron spectrometer (Kratos Analytical, Manchester, UK) employing a

monochromatic Al Kα source (1486.7 eV) and an electron takeoff angle of 90° relative to the sample plane. A survey scan (0–1100 eV binding energy range, 160 eV pass energy), and high-resolution scans of the P 2p peak (139-127 eV) and Au 4f (91.5-80 eV) were conducted with 10 eV pass energy (10 sweeps each). The relative values of P and Au were calculated with the default relative surface factor (RSF) values of 0.486 and 6.25, respectively.

7.1.4 The Radial Distribution Function (RDF) Calculations

The RDF calculations were performed over 2 μm × 2 μm tapping-mode (TM-AFM) height images of the master and the printed pattern. ImageJ was used to process the images. The bright spots in the images were marked by the 'Threshold' function and the coordinates of the dots were recorded. The RDF was calculated by a custom written code using Matlab 7.1.

7.2 Experimental Methods for the Supramolecular Replication of Peptide and Peptide/DNA Features

7.2.1 Coiled-coil Peptide Synthesis (Courtesy of Dr. Muthu Murugesan)

Peptides were synthesized by standard 9*H*-(f)luoren-9-yl(m)eth(o)xy(c)arbonyl (Fmoc) solid phase techniques. Amino acids and resin were purchased from Novabiochem (UK) and all other reagents for solid phase synthesis were obtained from AGTC Bioproducts (UK). Peptides were dried in a vacuum and purified by reverse-phase HPLC (Gilson) using a 20%- 65% water/acetonitrile gradient containing of 0.1% TFA. The identities of each coiled-coil were confirmed by Mass Spectrometry (Micromass Ltd., Altrincham, UK).

Peptide sequences were designed based on the work described by Litowski & Hodges. (Litowski, J.R. & Hodges, R.S. Designing Heterodimeric Two-stranded α-Helical Coiled-coils Effects of Hydrophobicity and α-helical Propensity on Protein Folding, Stability, and Specificity. The Journal of Biological Chemistry 2002, 277 (40), 37272-37279). The sequences used in this thesis are:

E: Ac- E VSALEKE VSALEKE VSALEKE VSALEK GGGC $CONH_2$

K: Ac- CGGG K VSALKEK VSALKEK VSALKEK VSALKE $CONH_2$

Three glycines (G) were introduced into the sequence design to space the coiling domain from the cysteine residue (C) that acts as an anchor to the surfaces.

The secondary structure of the peptides was evaluated by Circular Dichroism Spectroscopy (CD). (Figure 4.3b) CD Spectra were recorded on a Dichroism Spectropolarimeter Jasco 715 (by Dr. Anna Laromaine) The temperature was maintained a 20 °C by a water bath. CD spectra were the average of four scans obtained by collecting data at 0.1 nm intervals from 290 nm to 190 nm. The results were expressed as mean residue molar ellipticity [θ] with units of deg cm^2/ dmol and calculated from the following equation:

$$[\theta] = ([\theta]_{obs} \times MRW) / (10lc) \qquad \text{Equation 1}$$

Where '$[\theta]_{obs}$' is the ellipticity measured in millidegrees, 'MRW' is the mean residue molecular weight (molecular weight of the peptide divided by the number of amino acid residues), 'c' is the peptide concentration in mg/mL (1 mg/mL), and 'l' is the optical path length of the cell in cm. Peptide solutions were prepared in PBS buffer (50 mM PO_4, 100 mM KCl, pH 7.0).

Both **E** and **K** exhibit a random coil spectrum with a broad minimum around 200 nm, but when mixed (**E/K**) form heterodimers that exhibit a typical α-helical spectra with minima at 208 and 222 nm characteristic of the coiled-coil structure.[1] The ratio of $[\theta]_{222}/[\theta]_{208}$ has been found to be 0.93.

7.2.2 Substrate Preparation

10μm × 10μm gold square array: A silicon wafer coated with a commercially available photoresist (OCG 825) was exposed to UV light using an optical mask containing 10μm × 10μm square shaped holes, followed by the development of the exposed regions. Onto this substrate, a 5 nm chromium layer (adhesion layer) and subsequently 30 nm gold layer were evaporated. Lift-off was carried on in *N*-methyl-2-pyrrolidone.

Poly(dimethylsiloxane) (PDMS) prepolymer kit was purchased from Dow Corning (Sylgard 184). The silicon elastomer and the curing agent were mixed with a weight ratio of 10:1. This mixture was allowed to settle down to spontaneously remove the trapped air bubbles for 1 hour. Following this, it was poured into the Petri dish containing a hybridized master.

7.2.3 Experimental Steps for the LiSuNS Cycle

N-hydroxysuccinimide Fluorescein (NHS-Fluorescein) was received from Pierce Biotechnology Inc. The rest of the chemicals are the same as in Section 6.2.2.

DNA sequences (Hexyl thiol is abbreviated as 'HS', acrylic phosphoramidite is abbreviated as 'Acry', and rhodamine red is abbreviated as 'RhoR'. All were attached to the 5' end):

HS-A (or RhoR-A): 5'- /5ThioMC6-D/ (or - /5RhoR-XN/) TCC CAA AGA ACA GTG GTG GCT CAA GCT ACG GCC CCT CAT GAA AAT CCT GG-3'

Acry-A': 5'-TTT TTT TTT TTT CCA GGA TTT TCA TGA GGG GCC GTA GCT TGA GCC ACC ACT GTT CTT TGG GA-3'

Preparation of peptide masters on gold features: Peptides and DNA sequences were kept with excess dithiothreitol (DTT) to disrupt any disulfide group for 30 min. The substrates were treated with 0.15 mM aqueous solution of **K** for 12 hours. After cleaning with DI water and drying, the master was backfilled with 1mM mercaptohexanol (MH) for 30 min. Again, after washing with PBS and DI water, and drying, the master was treated with 0.15 mM aqueous solution of **E.** Before printing, the **K**-functionalized master was washed briefly with PBS and water, and blow dried. PDMS prepolymer was prepared as mentioned above and poured into the Petri dish containing a hybridized master. After curing at 60 °C for 1.5 hours, the solidified polymer was separated from the master.

Preparation of peptide/DNA master on a gold slide: Gold slides were purchased from Sigma-Aldrich (100 nm thickness with titanium adhesion layer, product code: 643246) and used as received. A microfluidic channel made of PDMS was placed onto this substrate. Thiol modified DNA molecules (purchased as disulfides) were reduced before use by dissolving 1 nmole of DNA in 100 μl of a 0.1M phosphate buffer (pH 7) containing solid phase dithiothreitol (DTT). The mixture was shaken at room temperature for 20 minutes and filtered through a syringe filter of pore size 0.2 μm (Life Sciences, poly(tetrafluoroethylene) membrane). After reduction, to reach the targeted ionic strength and concentration (5 μM), 1 M potassium phosphate buffer solution (pH 3.8) was added. This solution was injected into the outer channels and a 0.15 mM peptide **K** in PBS solution was injected into the single inner channel. After 24 hours, the PDMS mold was removed; the master was washed with DI water and placed into 1 mM MH solution for 30 minutes. After thorough washing with DI water, the master was first

treated with 0.15 mM complementary peptide **E** in aqueous solution for 3 hours under a cover slip, and then washed with PBS and DI water. After blow drying, a 10 μM solution Acry-A' in 1 M NaCl/TE buffer (10 mM Tris buffer pH 7.2 and 1 mM ethylenediamine tetraacetic acid (EDTA)) was dropped to the surface and left for hybridization under a cover slip. The coiled/hybridized master was washed with 4×SSC, 2×SSC and DI water briefly, and dried before printing. PDMS prepolymer was prepared as mentioned above and poured into the Petri dish containing a hybridized master. After curing at 60 °C for 1.5 hours, the solidified polymer was separated from the master.

Post-printing Treatments on PDMS (secondary substrate) after Peptide Printing: The printed PDMS substrate was peeled from the master, washed with DI water and treated with 0.15 mM of complementary fluorescent peptide in 10 mM PBS. After 3 hours, it was washed with PBS and DI water, and then imaged with a fluorescent microscope.

Post-printing Treatments on PDMS (secondary substrate) after DNA/Peptide Printing: After separation from the master, the PDMS substrate was washed with water and treated with 1 μM RhoR-A (the complementary to the cDNA:Acry-A') in 1 M NaCl/TE buffer. After 3 hours, the substrate was washed with 4×SSC, 2×SSC, and DI water briefly, and treated with NHS-Fluorescein (1 mg/ml) in PBS for 3 hours. The substrate was washed with PBS and water and then imaged via fluorescent microscopy.

7.2.4 Fluorescence Microscopy

Fluorescence microscopy images were obtained by a Zeiss Axioplan 2 with a mercury lamp. To image RhoR-A (fluorescently tagged DNA), a filter with excitation and collection at

470 and 515 nm, respectively was used. To image NHS-Fluorescein, the respective wavelengths were 456 and 590 nm.

7.3 Experimental Methods for Printing onto Polyelectrolyte Multilayers

7.3.1 Substrate Preparation

Polyelectrolyte Multilayers (PEMs) *(Courtesy of Dr. Jennifer Lichter)* Polyelectrolyte multilayers (PEMs) were constructed as follows: 0.01 M solutions in 18 M-Ohm Milli-Q water of poly(acrylic acid) (PAA) (Mw = 200 000 g/mol; 25% aqueous solution; Polysciences) or poly(allylamine hydrochloride) (PAH) (Mw = 70 000 g/mol; Polysciences) were pH adjusted using 1M HCl and NaOH. Using an automated dipper, glass substrates were dipped alternately into polymer baths for 15 minutes followed by 3 rinse steps (2 min, 1 min, 1 min). Cationic PAH was the first layer adsorbed. Notation refers to the assembly conditions with the PAA pH followed by the PAH pH i.e., a (7.5/3.5) PEM was assembled using PAH at pH 7.5 and PAA at pH 3.5.

7.3.2 Experimental Steps for the SuNS Cycle

10 μm × 10 μm gold square array was prepared as mentioned above. In addition to DNA sequence listed above, this sequence was also used:

NH2-A: 5'- /5AmMC6/ TCC CAA AGA ACA GTG GTG GCT CAA GCT ACG GCC CCT CAT GAA AAT CCT GG - 3'

NH2-A'-RhoG: 5' - /5AmMC6/CCA GGA TTT TCA TGA GGG GCC GTA GCT TGA GCC ACC ACT GTT CTT /36-FAM/ - 3'

To allow DNA immobilization on 10 μm × 10 μm gold master, a few drops of 5 μM solution of thiolated single-stranded DNA (HS-A) (50 mer) were placed onto the substrate, and allowed to react under a cover slip in a humidified chamber for 2 days. After rinsing with water, the substrates were treated with a 1mM 6-mercapto-1-hexanol (MCH) aqueous solution for 1 hour to minimize nonspecific adsorption of single-stranded DNA, rinsed with deionized water and blown dry with air. For hybridization, the single-stranded DNA immobilized master was treated with 1 M NaCl in TE buffer/phosphate buffer (1/1) containing 5 μM complementary DNA molecules (NH_2-A'-RhoG, 45 bases) under a cover slip for 2 days in a humidified chamber. The substrates were washed with 4X standard sodium citrate (SSC), 2X SSC and water consecutively. The substrates were washed with 4X standard sodium citrate (SSC), 2X SSC and water consecutively. After drying, the hybridized master was brought into contact with PEM surface which was kept in pH 7 DI water for 30 seconds and dried with air immediately before the contact. The printing carried out in a home-built stamping machine. The stamping machines is composed of two stainless steel chunks which have holes to apply vacuum to hold the substrates in place; also the temperature of the chunks can be controlled with circulating water of desired temperature. The stamping period for these substrates is between 15-20 hours, 4 hours of this time the substrates are kept at 45 °C. For dehybridization, the temperature of the chunks was raised to 90 °C. After 15 min, the chunks were separated vertically and the substrates were washed with DI water and subsequently imaged with fluorescence microscopy.

The reactive ion ethed silicon substrate (with 10 μm × 10 μm square features) was treated with triethoxysilylbutyraldehyde (TESA) in vacuum for 1 hour. The substrate was then baked in an oven at 130 ° C. An amine-terminated strand was used immobilized in this surface in pH 7

phosphate buffer at 5 μM concentration. The rest of the process (hybridization and contact) was the same as describe above.